LIBRARY – AIR RESOURCES BOARD

DEVELOPMENT OF A SURROGATE KINETIC MECHANISM FOR PHOTOCHEMICAL SMOG

Joseph A. Leone and John H. Seinfeld
Department of Chemical Engineering
California Institute of Technology
Pasadena, California 91125

FINAL REPORT

to

Air Resources Board
State of California

in completion of research under
ARB Contract No. A2-042-32

Disclaimer

The statements and conclusions in this report are those of the contractor and not necessarily those of the California Air Resources Board. The mention of commercial products, their source or their use in connection with material reported herein is not to be construed as either an actual or implied endorsement of such products.

TD
884.3
L465

TABLE OF CONTENTS

	Page
INTRODUCTION	ii
DEVELOPMENT AND TESTING OF THE EXPLICIT MECHANISM	1
DEVELOPMENT OF A FIRST GENERATION SURROGATE MECHANISM	10
Inorganic Reactions	10
Alkene Reactions	10
Aromatic Reactions	10
Alkane Reactions	11
Carbonyl Reactions	11
QUANTITATIVE COMPARISON OF THE EXPLICIT AND SUR1 MECHANISMS	12
DEVELOPMENT OF A SECOND GENERATION SURROGATE MECHANISM	25
QUANTITATIVE COMPARISON OF THE EXPLICIT AND SUR2 MECHANISMS	27
EVALUATION OF THE SUR2 MECHANISM	36
APPLICATION TO THE ATMOSPHERE	38
CONCLUSIONS	40
REFERENCES	42
APPENDIX	45

DEVELOPMENT OF A SURROGATE KINETIC MECHANISM FOR PHOTOCHEMICAL SMOG

INTRODUCTION

There currently exist several reaction mechanisms that describe the organic chemistry of the urban atmosphere, and, at the same time, maintain a balance between chemical detail and mechanism length (1-6). These reaction mechanisms can be classified into two general categories, surrogate mechanisms and lumped mechanisms. In surrogate mechanisms the organic species in a particular class are represented by one or more members of that class, while in lumped mechanisms a generalized species is used to represent compounds of similar structure or reactivity. In general, lumped reaction mechanisms contain fewer non-steady-state species, making them more attractive from a computational point of view. An example of a generalized species lumped mechanism is the mechanism of Falls and Seinfeld (1), hereafter called the Caltech mechanism.

These condensed kinetic mechanisms are used in urban air quality models to determine how changes in emission levels will affect ambient air quality. Although each of the existing kinetic mechanisms for photochemical smog has been evaluated using the same body of experimental data, several investigators have shown that different mechanisms predict substantially different degrees of emission controls to achieve the same desired air quality under identical conditions (7-9). In a recent study, Leone and Seinfeld (10,11) have identified many of the reasons for these discrepancies in predictions. In that study, two major problems found with the Caltech mechanism are an inadequate treatment of atmospheric aromatic

chemistry, and the use of out-of-date rate constants and photolysis rates (particularly out-of-date aldehyde photolysis rates). When modifications were made to these reactions, the predictions of the Caltech mechanism were found to be in much closer agreement with those of a detailed explicit reaction mechanism for photochemical smog (10,11). Unfortunately, it is not possible to make use of this modified Caltech mechanism until a complete re-analysis of the entire mechanism with respect to experimental data has been performed.

The goal of this work is to develop a new condensed chemical reaction mechanism for photochemical smog that can replace the Caltech mechanism in the Caltech urban airshed model. Since condensed reaction mechanisms either lumped or surrogate, are derived from detailed, explicit chemistry, an effective approach to form a condensed mechanism for photochemical smog is by using surrogate species to eliminate or condense many of the least important species and reactions contained in the explicit mechanisms. This approach leads to the class of condensed mechanisms referred to as surrogate mechanisms which, because of their very nature, are easier to modify than lumped mechanisms when new experimental kinetic and mechanistic information become available. As noted earlier, the disadvantage of surrogate mechanisms in the past has been the large number of species that they contained. However, the recent work of Leone and Seinfeld (10,11) provides evidence that many of the species contained in surrogate mechanisms are not important from an ozone production point of view. That work also presents a counter species method of evaluating the contribution of individual species to the overall ozone production predicted by the mechanism. With this technique one can identify non-steady-state species that can be

eliminated with only minor effects on the predictive ability of the mechanism. Thus, it now appears possible to formulate a surrogate mechanism for photochemical smog that is suitable for use in air quality simulation models and could be easily updated when new kinetic or mechanistic data become available.

The approach taken in this study is therefore to first formulate a detailed explicit reaction mechanism for photochemical smog containing the chemistry of the important atmospheric organics. The formation of this explicit mechanism is summarized in the next section. After evaluating this explicit mechanism using smog chamber data, a surrogate condensed mechanism is formed by eliminating many of the fast reacting and less important species from the explicit mechanism. The resulting surrogate mechanism is similar in structure to the mechanism of Atkinson et al. (2). Next, the predictions of the explicit and surrogate condensed mechanisms are compared to determine if any significant loss of predictive ability has occurred. Following this, the counter species analysis technique mentioned above is applied to both the explicit and surrogate mechanisms to determine which additional non-steady-state species can be safely eliminated from the surrogate mechanism. The final version of the surrogate mechanism is then extensively evaluated against a variety of experimental data from both indoor and outdoor smog chamber facilities.

Table 1. Organic Composition of Ambient Los Angeles Air (29) and Smog Chamber Experiment SUR-119J (12).

Compound	Ambient Air Concentration Range (ppbv)	SUR-119J Concentration (ppbv)
Alkynes		
acetylene	26-94	46.4
Alkanes		
methane	-	2740.0
ethane	32-221	76.8
propane	11-99	17.0
isobutane	10-33	0.2
n-butane	21-70	166.0
isopentane	23-83	-
n-pentane	9-34	97.6
2,3-dimethylbutane	2-8	-
2-methylpentane	8-28	-
3-methylpentane	4-15	-
n-hexane	5-20	-
2,2,3-trimethylbutane	0-9	-
2,4-dimethylpentane	2-6	-
2,3-dimethylpentane	2-9	-
3-methylhexane	3-24	-
2,2,4-trimethylpentane	3-15	-
n-heptane	3-11	-
2,5-dimethylhexane	1-3	-
2,3,4-trimethylpentane	2-5	-
3-methylheptane	2-5	-
2,2,5-trimethylhexane	1-4	-
n-octane	1-5	-
n-nonane	1-3	-
n-decane	1-9	-
Cycloalkanes		
methylcyclopentane	4-16	-
cyclohexane	7-31	-
dimethylcyclopentane	1-19	-
methylcyclohexane	3-14	-
dimethylcyclohexane	0-1	-
Alkenes		
ethylene	32-91	43.2
propene	7-32	10.6
1-pentene	1-8	-
2-methyl-1-pentene	0-4	-

Table 1. Organic Composition of Ambient Los Angeles Air (29) and Smog Chamber Experiment SUR-119J (12) (Continued)

Compound	Ambient Air Concentration Range (ppbv)	SUR-119J Concentration (ppbv)
Alkenes (Continued)		
2-butene	-	13.7
2-methyl-2-butene	-	14.8
Aromatics		
benzene	12-29	1.6
toluene	20-68	16.8
ethylbenzene	3-12	6.4
m- and p-xylene	11-45	42.4
o-xylene	4-13	-
n-propylbenzene	1-3	0.1
p-ethyltoluene	4-12	-
o-ethyltoluene	1-3	-
1,3,5-trimethylbenzene	4-12	-
1,2,4-trimethylbenzene	4-12	-
1,2,3-trimethylbenzene	1-4	1.6
n-butylbenzene	0-2	-
isopropyl benzene	-	0.4
m-ethyltoluene	-	1.0
Carbonyls		
formaldehyde	4-86	38.0
acetaldehyde	2-39	20.0
propionaldehyde	-	3.2
propanal+acetone+acrolein	1-54	-
n-butanal	0-5	-
benzaldehyde	0-2	-

Alkanes:	Aromatics:
propane	toluene
n-butane	m-xylene
2,3-dimethylbutane	
Alkenes:	Carbonyls:
ethene	formaldehyde
propene	acetaldehyde
trans-2-butene	propionaldehyde
	acetone

Excluding methane, acetylene, and ethane, 529.8 ppb of initial organics are present in SUR-119J. Of these, 503.7 ppb, or 95 percent is represented by the 12 organics included in the explicit mechanism. In the case of ambient Los Angeles air, these 12 species account for 538 ppb, or 49 per cent of the 1103 ppb of total reactive organics contained in the 50 major species*. Thus, we conclude that the explicit mechanism should provide a reasonable description of the chemistry occurring in a typical urban atmosphere. Since the reactions of species such as methane, ethane, acetylene, etc., are not included, the explicit mechanism is not suitable for use under clean tropospheric conditions.

The reactions and rate constants comprising the explicit mechanism were taken almost exclusively from four sources. The inorganic reactions were compiled using the recent reviews of Baulch et al. (13) and DeMore et al. (14). The aromatic reactions were taken mostly from the recent studies of Leone and Seinfeld (15) and Leone et al. (16). The vast majority of

*This calculation is based on the maximum concentrations measured by Grosjean and Fung (29).

the reactions and rate constants used in the explicit mechanism were taken from the review of Atkinson and Lloyd (17).

Even though the explicit mechanism represents the state of current understanding of atmospheric organic chemistry, there is still considerable uncertainty in many of the reactions and rate constants. In addition, we have only included in the explicit mechanism the reactions of a small number of the many organic species present in the typical urban troposphere. For these reasons, it is necessary to evaluate the explicit mechanism against experimental smog chamber data. The ability to model chamber data does not in any way guarantee that a mechanism is correct, especially with the uncertainty that exists in the magnitude of chamber radical sources. However, it does provide some evidence that the most important species and reactions are accounted for in the reaction mechanism.

We have chosen to test the explicit mechanism using series of 11 hydrocarbon-NO_x experiments performed at SAPRC (EC-231, EC-232, EC-233, EC-235, EC-237, EC-238, EC-241, EC-242, EC-243, EC-245, EC-246, and SUR-119J). These are multiple hydrocarbon-NO_x experiments in which both the initial hydrocarbon distribution and the $[RHC]_0/[NO_x]_0$ are varied. The initial conditions for each of these experiments are given in Table A.2. The chamber dependent reactions added to the explicit mechanism to adopt it for modeling chamber experiments are (18,19):

O_3 wall loss: $k = 1.65 \times 10^{-3}$ min^{-1}

NO wall source: $k = 1.0 \times 10^{-4}$ min^{-1}

OH radical source: $k = k_1\ (0.39 + 1.37[NO_2])$ ppb-min^{-1}

heterogeneous HNO_3 formation: $k = 4.4 \times 10^{-6}$ ppm^{-1}-min^{-1}

The results of simulating most of the above experiments with the explicit mechanism are shown in the Appendix (Figures A.1 through A.9). In nearly every case there is good agreement between the predictions of the explicit mechanism and the experimental data. In general, the O_3 and PAN peak heights are slightly over-predicted, while the NO_2 peak height is predicted very well. Both the timing of the NO_2 and O_3 peaks, and the hydrocarbon decay rates are predicted very well, indicating that the radical initiation and termination processes are represented adequately in the explicit mechanism. When examining the results in Figures A.1 through A.9, one should keep in mind that the explicit mechanism contains no adjustable parameters. Similarly, the chamber dependent terms are held constant and not varied as the initial conditions of the experiments change.

In summary, the explicit mechanism contains the reactions of the most important organic species found in the typical polluted urban atmosphere. Because there is considerable uncertainty in portions of this mechanism (particularly in the aromatic chemistry), the explicit mechanism should not be thought of as an exact description of atmospheric organic chemistry. In spite of this shortcoming, the explicit mechanism represents the state of the art in our understanding of atmospheric organic chemistry, and therefore provides a necessary starting point for the development of a surrogate condensed mechanism and for assessing the performance of this surrogate mechanism.

DEVELOPMENT OF A FIRST GENERATION SURROGATE MECHANISM

The explicit mechanism shown in Table A.1 serves as the starting point for the development of a new surrogate mechanism. The chemistry of each class of species (inorganics, alkanes, alkenes, aromatics, and carbonyls) is simplified by combining reactions and eliminating fast reacting or unimportant species. This simplification process is similar to that used by Atkinson et al. (2). The resulting mechanism, hereafter called SUR1, is shown in Table A.3. Many of the details regarding the formulation of the SUR1 mechanism can be found in the footnotes to Table A.3.

Inorganic Reactions

The only changes from the inorganic reactions appearing in the explicit mechanism are the elimination of $O(^3P)$, the combining of reactions 16-18 (2), and the elimination of reactions 21 and 22.

Alkene Reactions

The reactions of three alkenes are included in SUR1, ethene, propene, and trans-2-butene. Ethene is treated separately because of its relatively slow rate of reaction with both OH and O_3(10,11,17). The reactions of propene and trans-2-butene are used to represent the chemistry of the terminal and internal alkenes, respectively. By eliminating many of the free radical intermediates, the reactions of these three alkenes are reduced to those shown in Table A.3, section B.

Aromatic Reactions

Three aromatic hydrocarbons are included in SUR1, benzene, toluene, and xylene. Benzene is treated separately, while toluene represents the mono-alkylbenzenes and xylene represents the higher alkylbenzenes. The resulting reactions are shown in section C of Table A.3.

Alkane Reactions

The alkane chemistry contained in SUR1 has been taken directly from Atkinson et al. (2). Methane and ethane are neglected, while propane is treated explicitly. The C_4 and higher alkanes are represented by a lumped average alkane whose chemistry represents an average for the butanes, n- and isopentanes, n-hexane, and n-heptane (2).

Carbonyl Reactions

Formaldehyde, acetaldehyde, acetone, and methylethylketone are treated explicitly. Propionaldehyde is used to represent the C_3 and higher aldehydes. The resulting reactions are listed in part E of Table A.3.

QUANTITATIVE COMPARISON OF THE EXPLICIT AND SUR1 MECHANISMS

The SUR1 mechanism shown in Table A.3 is formulated in a straightforward manner from the explicit mechanism, and we therefore anticipate that these two mechanisms would perform similarly. Unfortunately, the SUR1 mechanism is still too large for use in multidimensional grid models, since it contains 31 non-steady-state species and 83 reactions. We could proceed by eliminating additional species from SUR1, creating a more condensed mechanism (SUR2), whose performance could then be compared to that of the explicit mechanism. However, if the predictions of the SUR2 and explicit mechanisms did not agree, we would not know which portion of the species elimination process was responsible for the error. Instead, we choose to first evaluate the performance of the SUR1 mechanism to insure that it is an adequate representation of the explicit mechanism. Included in this evaluation is a counter species analysis of both the explicit and SUR1 mechanisms. The results of this counter species analysis will be very useful in determining which species of the SUR1 mechanism can be eliminated without significantly affecting the performance of the mechanism. This is exactly the information that we would like to possess before beginning our formulation of a more condensed surrogate mechanism (SUR2).

Figures 1-4 illustrate how the explicit and SUR1 mechanisms compare in their predictions of maximum O_3, NO_2, and PAN concentrations, and the time of the ozone maximum. The same chamber-dependent terms (shown in Table A.6) were used with both reaction mechanisms to obtain these results. The initial conditions for these simulations correspond to the 10 multi-hydrocarbon-NO_x smog chamber experiments performed at SAPRC that were used to evaluate the explicit mechanism (EC-231 through EC-246). One can see

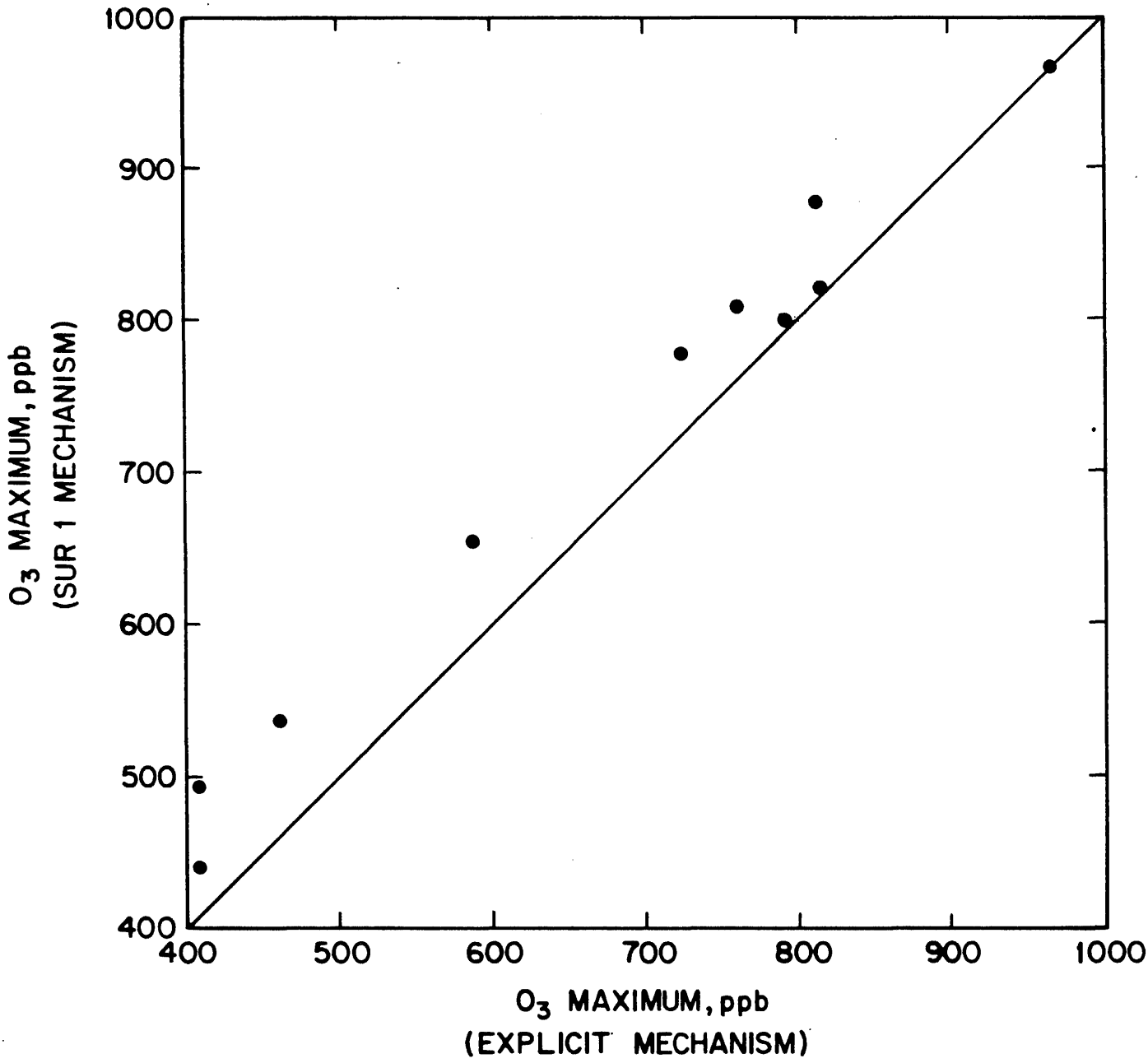

Figure 1. Comparison of peak O_3 concentrations predicted by the explicit and SUR1 mechanisms. Each point corresponds to one of the SAPRC multi-hydrocarbon-NO_x experiments EC-231 through EC-246.

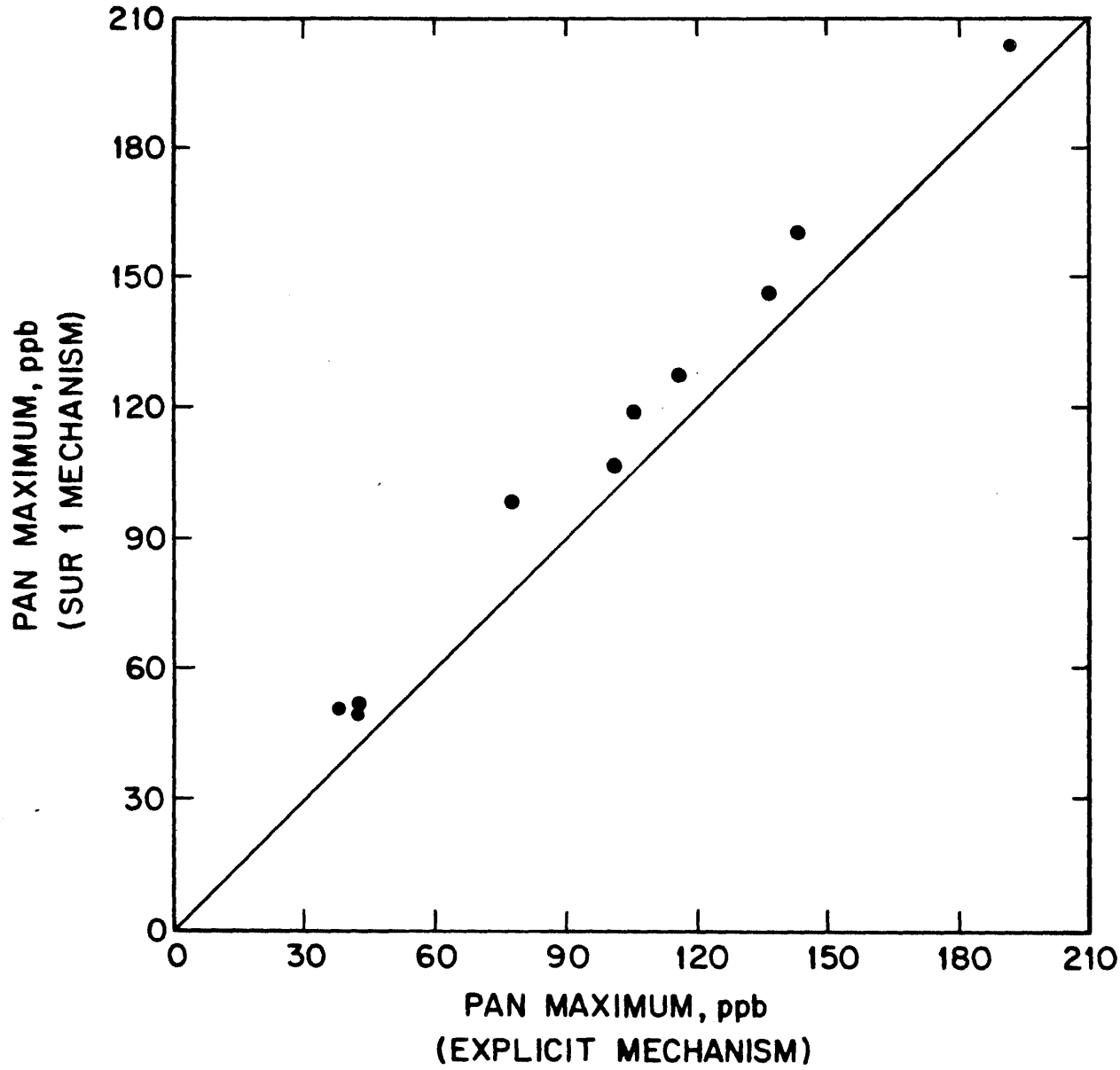

Figure 2. Comparison of peak PAN concentrations predicted by the explicit and SUR1 mechanisms. Each point corresponds to one of the SAPRC multi-hydrocarbon-NO_x experiments EC-231 through EC-246.

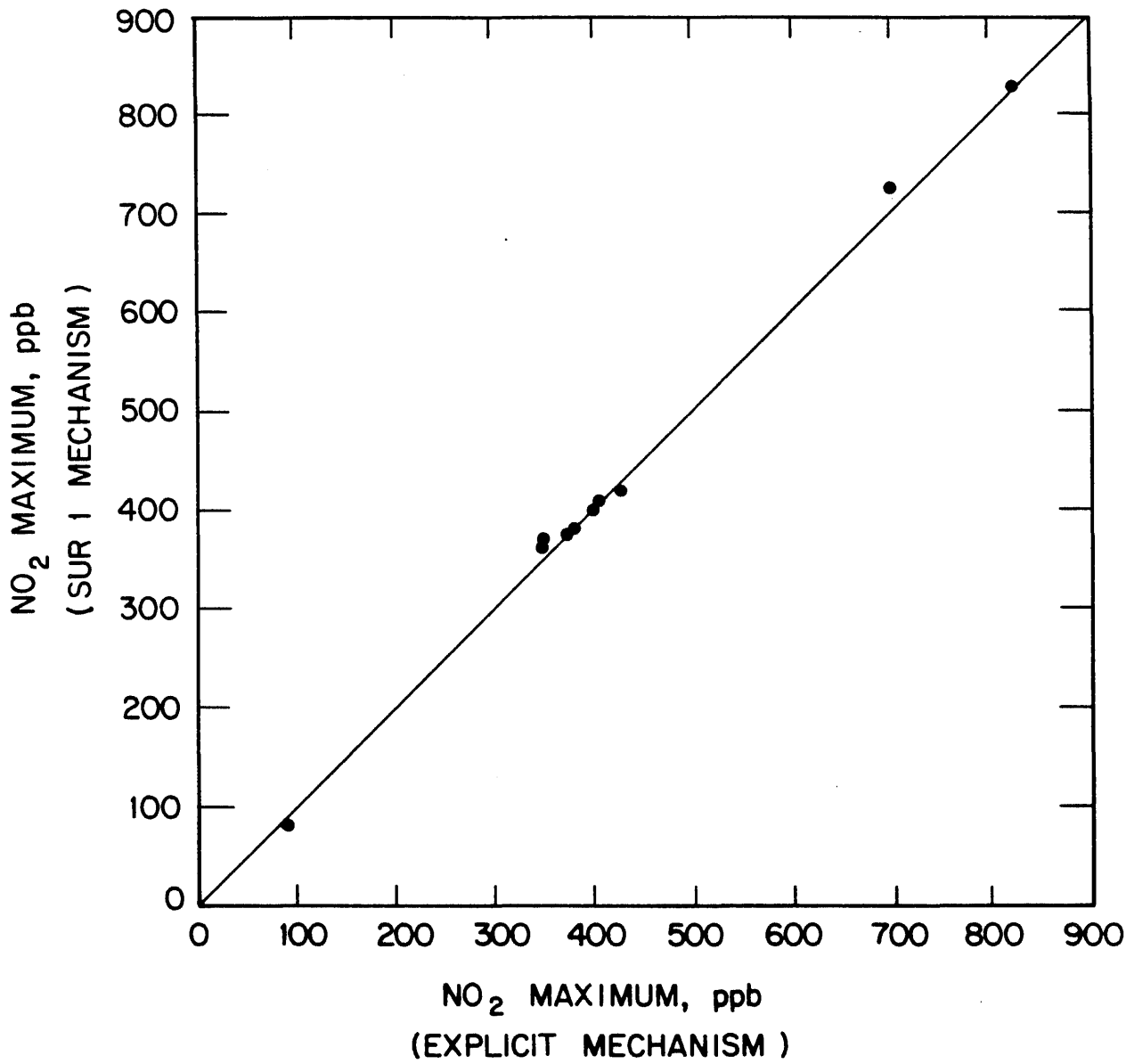

Figure 3. Comparison of peak NO_2 concentrations predicted by the explicit and SUR1 mechanisms. Each point corresponds to one of the SAPRC multi-hydrocarbon-NO_x experiments EC-231 through EC-246.

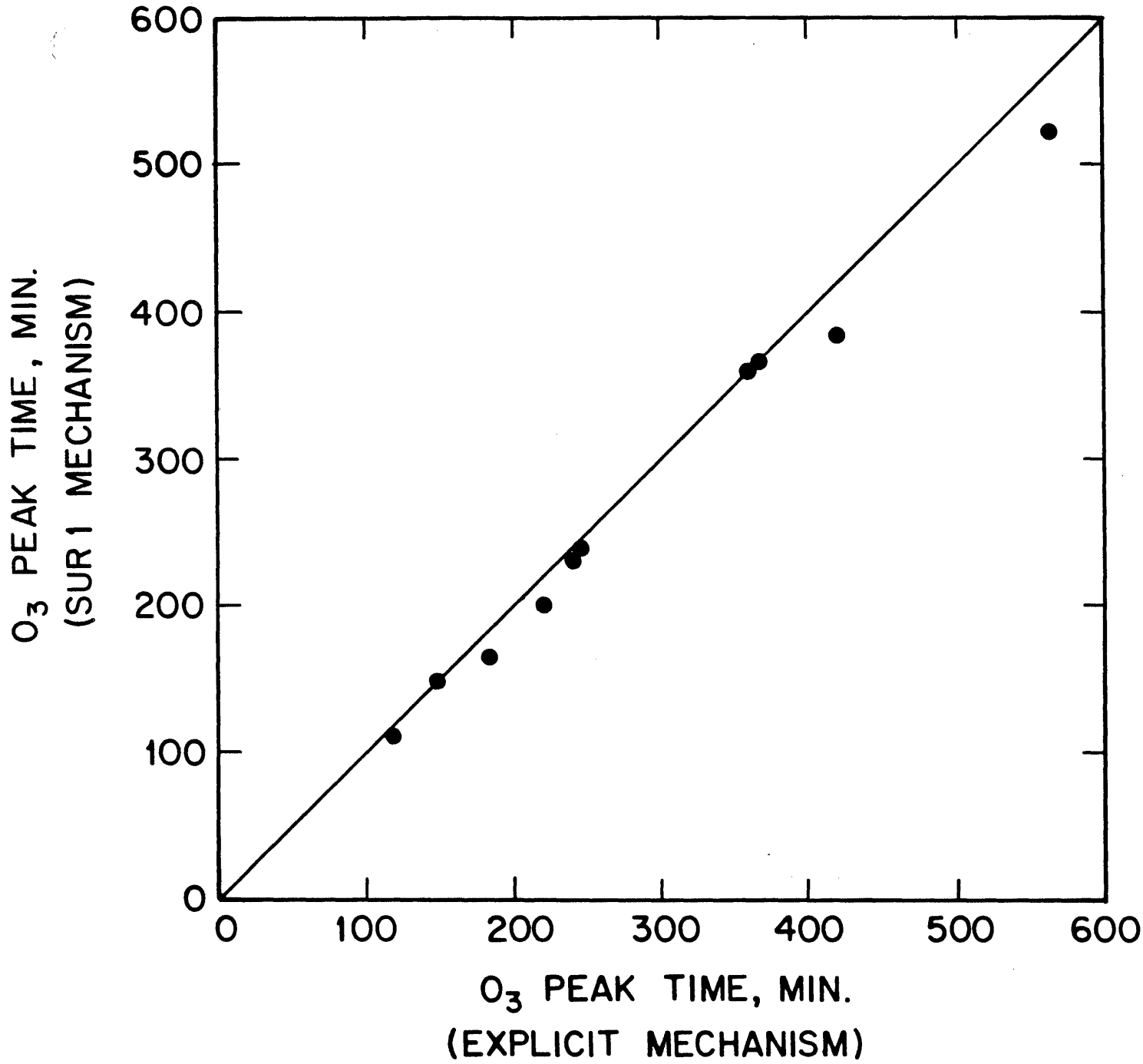

Figure 4. Comparison of peak O_3 times predicted by the explicit and SUR1 mechanisms. Each point corresponds to one of the SAPRC multi-hydrocarbon-NO_x experiments EC-231 through EC-246.

that the predictions of the SUR1 mechanism lie close to those of the explicit mechanism. These results illustrate that the overall performance of the SUR1 mechanism compares well with the explicit mechanism; however, they tell us nothing of how the individual portions of the SUR1 mechanism correspond to their counterparts in the explicit mechanism. In order to gain this information we must use a counter species analysis.

The details of the counter species analysis technique are presented elsewhere (10,20), and are therefore not discussed here. The information provided by this analysis is the amount of NO to NO_2 conversions attributable to each of the important species appearing in a reaction mechanism. Since O_3 production is related to the amount of NO being converted to NO_2, this analysis provides us with an indirect way of assessing the amount of ozone production for which each of the initially present organics is responsible. By applying this analysis to both the explicit and SUR1 mechanisms, we can determine how well the simplified chemistry in SUR1 represents the explicit chemistry found in the explicit mechanism.

Some typical results of the counter species analysis are shown in Table 2 and Figures 5-8. Figure 5 shows that the total amount of NO to NO_2 conversions predicted by the two mechanisms agree very well. This agreement is expected, since we saw in Figure 1 that the two mechanisms predicted similar peak ozone levels. Table 2 shows the detailed counter species results for the simulations of experiments EC-231, EC-233, and EC-242. The results for the remaining seven simulations are very similar. Examination of these results shows that each portion of the SUR1 mechanism represents the NO to NO_2 conversion behavior of the explicit mechanism very well. In particular, the NO to NO_2 conversions attributable to the alkenes are very

Table 2. Comparison of Counter Species Results for the Explicit and SUR1 Mechanisms Using Initial Conditions from SAPRC Experiments EC-231, EC-233, and EC-242.

Experiment	EC-231		EC-233		EC-242	
Mechanism	Explicit	SUR1	Explicit	SUR1	Explicit	SUR1
I) AROMATICS						
toluene abstraction	3	4	1	1	7	7
toluene addition	44	59	10	14	85	103
m-xylene+OH	155	149	44	42	358	320
methyl glyoxal+hν	65	57	20	16	139	117
methyl glyoxal+OH	8	7	2	2	13	7
glyoxal	1	0	0	0	1	0
benzaldehyde	0	0	0	0	0	0
o-cresol	1	6	0	2	1	11
dimethyl phenol	3		1		5	
pyruvic acid	0	0	0	0	0	0
2-butene-1,4-dial	3	20	1	6	6	22
4-oxo-2-pentenal	10		3		20	
other γ-dicarbonyls	14		4		29	
TOTAL AROMATIC	202	212	55	57	450	430
II) ALKANES						
propane+OH	0	0	0	0	0	0
butane+OH	253	686	204	525	98	195
2,3-dimethylbutane+OH	378		293		88	
butane+O(^{3}P)	0	-	0	-	0	-
2,3-dimethylbutane+O(^{3}P)	2	-	0	-	0	-
TOTAL ALKANE	631	686	497	525	186	195
III) ALKENES						
ethene+OH	544	554	117	116	807	803
ethene+O_3	169	162	24	21	267	244
propene+OH	87	85	41	39	75	72
propene+O_3	43	45	17	18	38	41

Table 2. Comparison of Counter Species Results for the Explicit and SUR1 Mechanisms Using Initial Conditions from SAPRC Experiments EC-231, EC-233, and EC-242 (Continued)

Experiment	EC-231		EC-233		EC-242	
Mechanism	Explicit	SUR1	Explicit	SUR1	Explicit	SUR1
III) ALKENES (cont)						
butene+OH	41	40	18	17	71	66
butene+O_3	35	38	17	17	62	69
$\dot{C}H_2O\dot{O}$	74	72	6	5	86	81
$CH_3\dot{C}HO\dot{O}$	15	16	4	4	23	23
TOTAL ALKENE	919	924	234	228	1320	1295
IV) CARBONYLS						
initial HCHO	8	7	2	2	9	8
initial CH_3CHO	0	0	0	0	0	0
initial C_2H_5CHO	0	0	0	0	0	0
initial $CH_3C(O)CH_3$	0	0	0	0	0	0
created HCHO	235	267	51	59	328	343
created CH_3CHO	49	48	28	25	44	27
created C_2H_5CHO	0	4	0	4	0	1
created C_3H_7CHO	9		8		3	
created $CH_3C(O)CH_3$	10	2	7	2	1	1
TOTAL ALDEHYDE	8	7	2	2	9	8
V) INITIAL CO	15	15	8	8	7	7
TOTAL	1775	1844	796	820	1972	1935

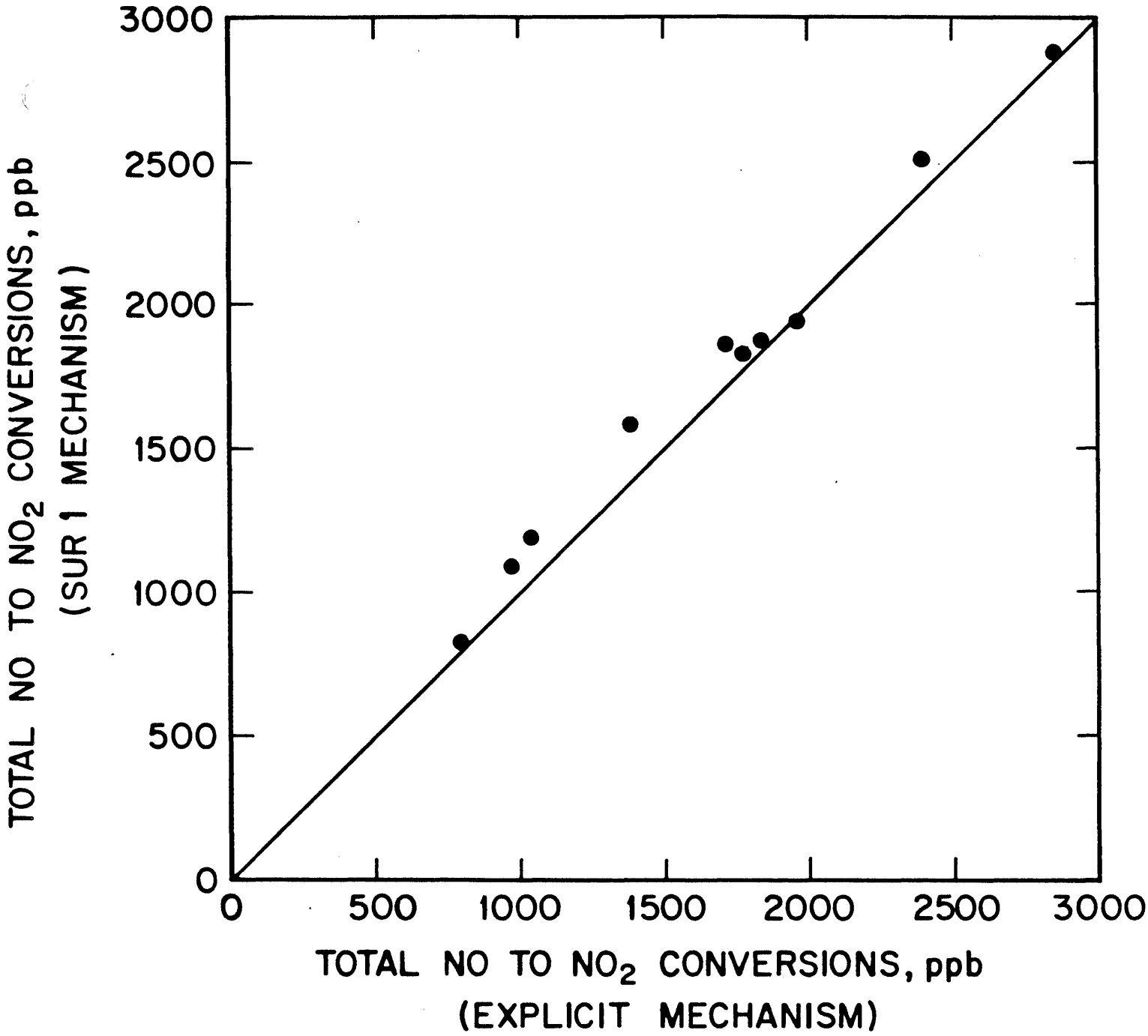

Figure 5. Comparison of the total amount of NO to NO_2 conversions predicted by the explicit and SUR1 mechanisms. Each point corresponds to one of the SAPRC multi-hydrocarbon-NO_x experiments EC-231 through EC-246.

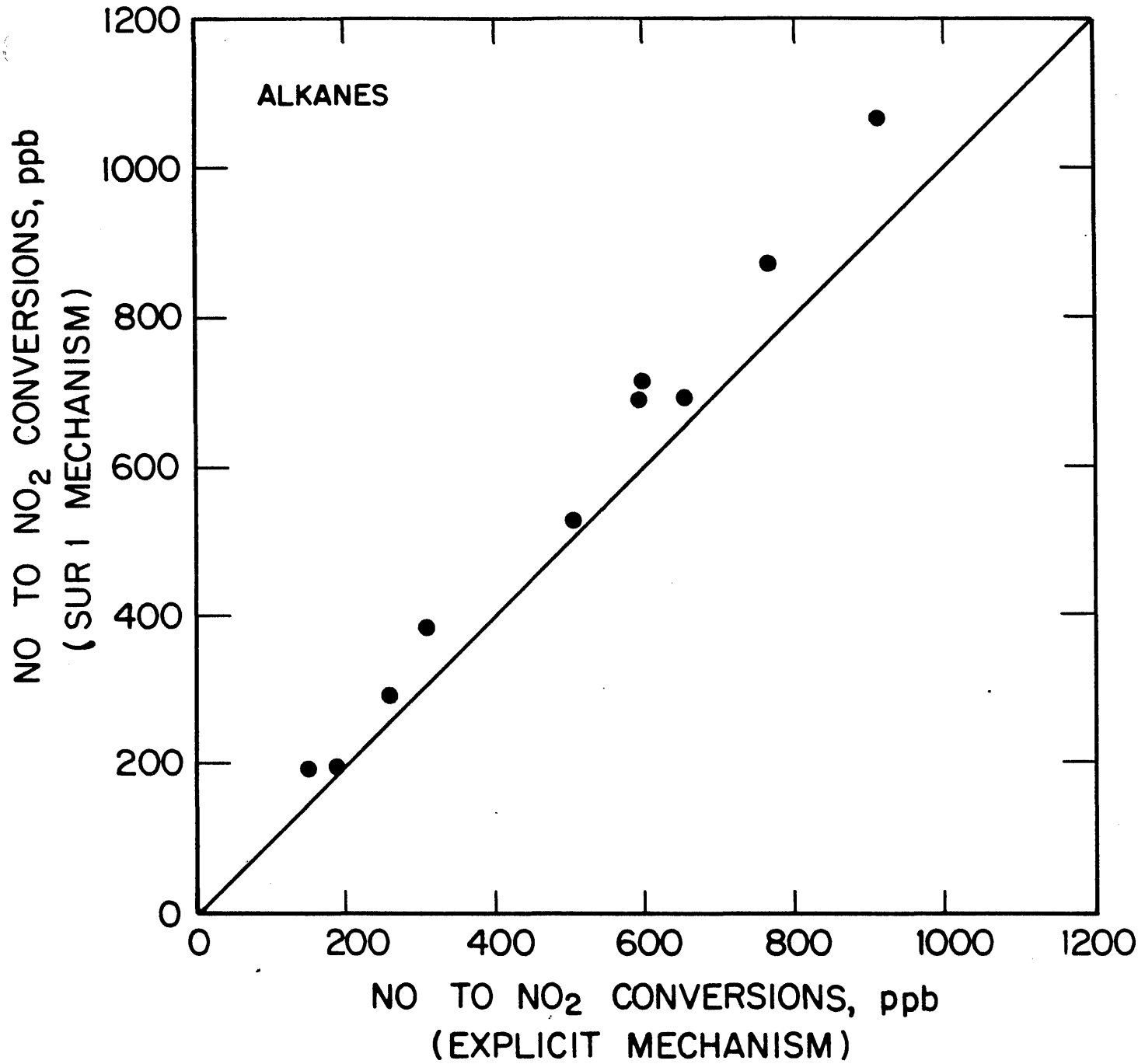

Figure 6. Comparison of the counter species results for the alkanes between the explicit and SUR1 mechanisms. Each point corresponds to one of the SAPRC multi-hydrocarbon-NO_x experiments EC-231 through EC-246.

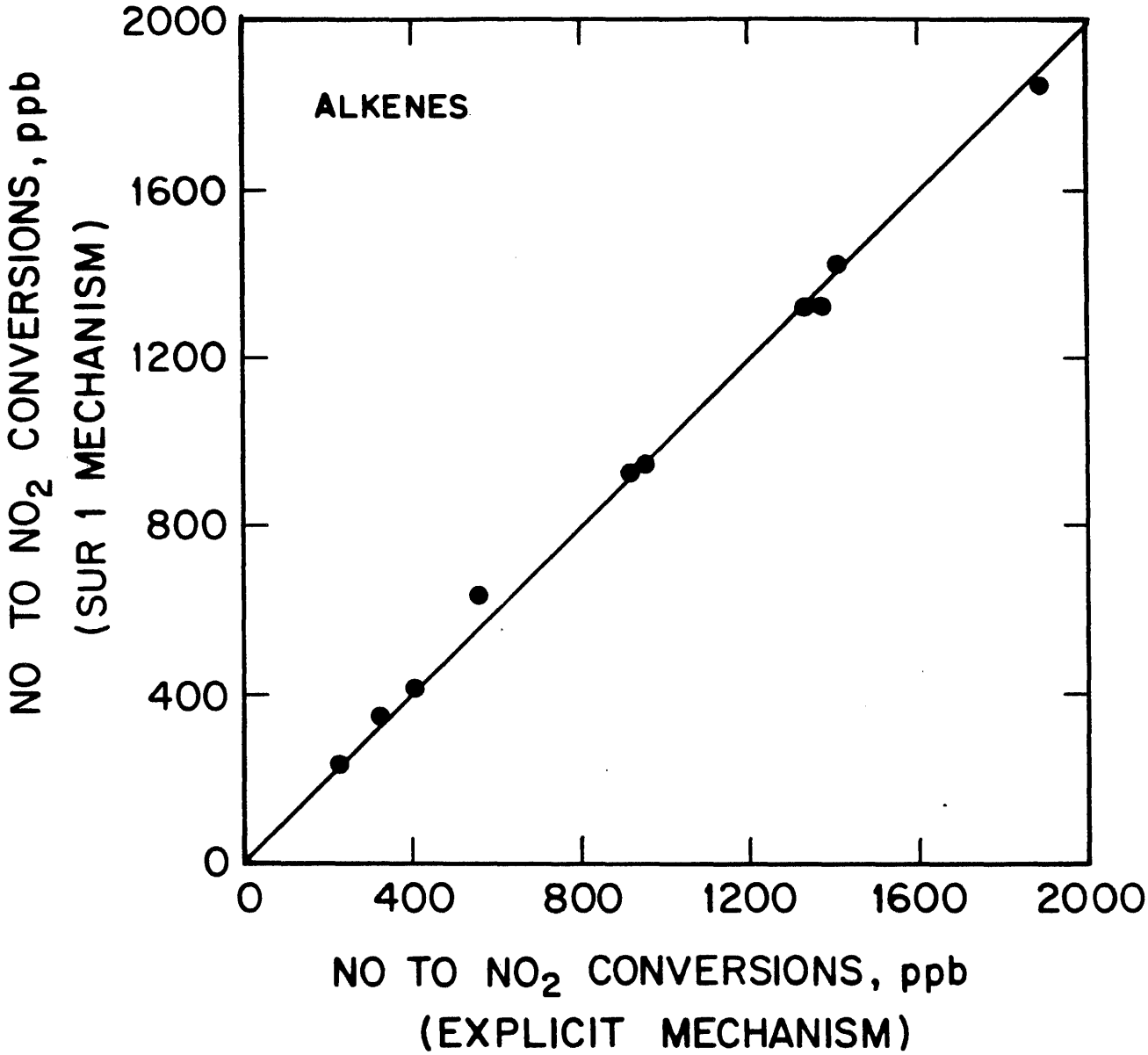

Figure 7. Comparison of the counter species results for the alkenes between the explicit and SUR1 mechanisms. Each point corresponds to one of the SAPRC multi-hydrocarbon-NO_x experiments EC-231 through EC-246.

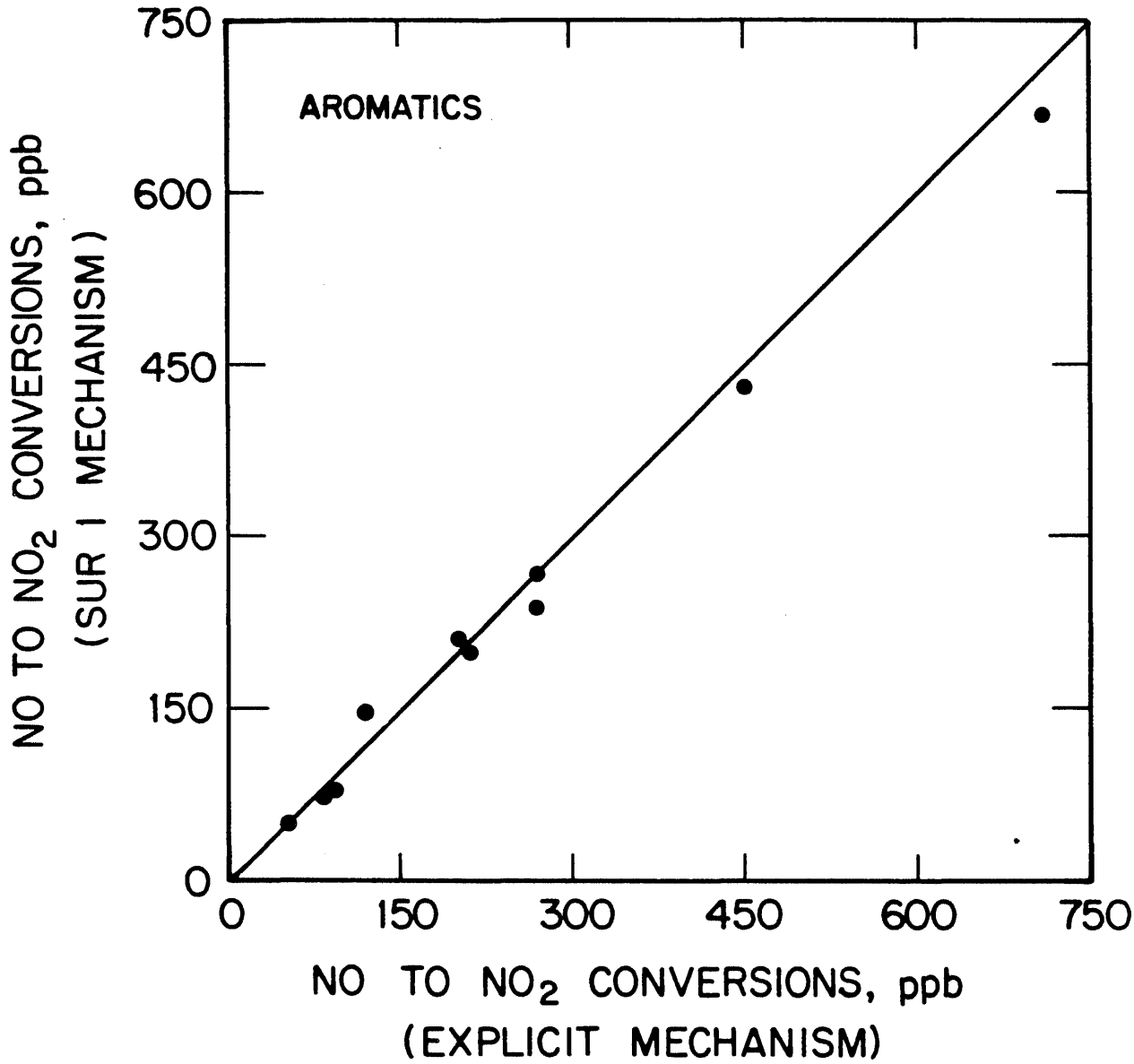

Figure 8. Comparison of the counter species results for the aromatics between the explicit and SUR1 mechanisms. Each point corresponds to one of the SAPRC multi-hydrocarbon-NO_x experiments EC-231 through EC-246.

similar for the two mechanisms. The agreement for the aromatics and alkanes is not quite as close, but the amount of simplification in going from the explicit to condensed treatments is much greater for these species. Figures 6-8 show the counter species results for each of the 10 simulations in an alternate form. Once again, we see that each portion of the surrogate mechanism represents the explicit chemistry very well.

The above results are important because they show that the overall performance of the SUR1 mechanism, as shown in Figures 1-4, is not fortuitous. Accurate overall results can be obtained even if individual portions of the surrogate mechanism contain inaccurate representations of the chemistry. For example, an over-reactive surrogate treatment of alkane chemistry could be hidden by an under-reactive representation of aromatic chemistry. Such compensating errors could cause serious problems when the mechanism is applied under a different set of conditions. The counter species results show that this type of error is not occurring under the conditions in which we have evaluated SUR1.

DEVELOPMENT OF A SECOND GENERATION SURROGATE MECHANISM

The number of non-steady-state species contained in the SUR1 mechanism must be reduced if it is to be practical for use in multidimensional urban air quality models. The results of the counter species analysis, such as those shown in Table 2, provide the information needed to determine which species can be safely eliminated. Examining these results shows that acetone, methyl ethyl ketone, benzaldehyde, peroxybenzoyl nitrate, glyoxal, pyruvic acid, propane*, propionaldehyde, and peroxypropionyl nitrate ($C_2H_5CO_3NO_2$) can be eliminated with only minor effects on mechanism predictions. In addition, we can eliminate two species by lumping together propene and butene, and toluene and xylene, as shown below.

Alkenes: Reactions 25 and 27 of the SUR1 mechanism become,

$$(25)\quad OLE + OH \rightarrow 0.95\gamma HCHO + (1.8-0.85\gamma)CH_3CHO + (0.9 + 0.05\gamma)(HO_2\cdot + NO_2) - NO$$

$$k_{25} = 3.7\times10^{4}\gamma + 1.0\times10^{5}(1-\gamma)$$

where,

$$\gamma = \frac{[propene]_o}{[propene]_o+[butene]_o}$$

Reactions 26 and 28 of the SUR1 mechanism become,

$$(26)\quad OLE + O_3 \rightarrow (1-0.5\gamma)CH_3CHO + (0.4-0.2\gamma)CH_3\dot{C}H\dot{O}O + (0.24+0.09\gamma)CO + (0.29-0.09\gamma)HO_2\cdot + (0.19-0.09\gamma)OH + (0.43-0.21\gamma)CH_3O_2\cdot + (0.05-0.03\gamma)CH_3O\cdot + 0.2\gamma\dot{C}H_2O\dot{O}$$

$$k_{26} = 1.6\times10^{-2}\gamma + 2.7\times10^{-1}(1-\gamma)$$

*Propane should not be eliminated in cases where long range transport is being studied.

Aromatics: Reactions 36 and 37 of the SUR1 mechanism become,

(34) ARO + OH → (0.25-0.05β) 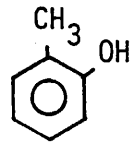 + (1-0.1β)HO_2·
(lumped xylene)

+ (0.75-0.05β)(NO_2 - NO + CH(O)CH=CHCHO)

+ (0.68 + 0.02β)$CH_3C(O)CH_0$ + (0.08-0.08β)$(CHO)_2$ + 0.1β 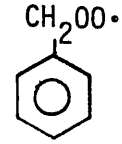

ARO + OH → (0.25-0.05β) 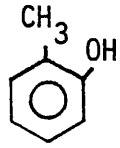 + (1-0.1β)HO_2·
(m-xylene)

+ (0.75-0.05β)(NO_2-NO + CH(O)CH=CHCHO)

+ (0.75-0.05β)$CH_3C(O)CHO$ + 0.1β 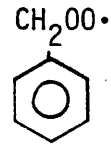

$$k_{34} = 9.4\times10^3\beta + 2.7\times10^4(1-\beta) \quad \text{for lumped xylene}$$

$$k_{34} = 9.4\times10^3\beta + 3.4\times10^4(1-\beta) \quad \text{for m-xylene}$$

$$\beta = \frac{[\text{toluene}]_0}{[\text{toluene}]_0+[\text{xylene}]_0}$$

Since the molar weighted average rate constants shown above are based on initial conditions, they strictly apply only at the start of a simulation. The use of these rate constants introduces some error into the mechanism; however, tests indicate that the magnitude of these errors is small as long as the species that are lumped together do not have large differences in rate constants or concentrations (10). For this reason, we choose not to lump benzene together with toluene and xylene, i.e., benzene reacts at a much slower rate in the atmosphere.

The mechanism that results after the above changes are made is shown in Table A.4. This new mechanism, which we call SUR2, contains 58 reactions and 20 non-steady-state species* and is therefore compact enough for use in grid models of urban air pollution. A list of the non-steady-state species appearing in SUR2 is shown in Table A.5. Since propionaldehyde is not treated in the SUR2 mechanism, acetaldehyde now represents all $\geq$C2 aldehydes. However, even though propane has been removed, the lumped group ALK still represents $\geq$C4 alkanes.

QUANTITATIVE COMPARISON OF THE EXPLICIT AND SUR2 MECHANISMS

The performance of the SUR2 mechanism is compared to that of the explicit mechanism in Figures 9-16. Figures 9-11 compare the two mechanisms in their predictions of O_3, PAN, and NO_2 maxima, while Figure 12 compares the timing of the O_3 peak. The initial conditions for these simulations correspond once again to those of SAPRC experiments EC-231 through EC-246. Examination of Figures 9-12 shows that the predictions of the SUR2 mechanism are in good agreement with those of the explicit mechanism. In fact, comparing Figures 9-12 with Figures 1-4 shows that the predictions of the SUR2 mechanism actually differ only slightly from those of the SUR1 mechanism. This is not surprising since the counter species analysis showed that the species that were eliminated from SUR1 were not important from an ozone production point of view.

The counter species results for the SUR2 and explicit mechanisms are compared in Figures 13-16. Once again the best agreement between the

*See the footnote to Table A.5.

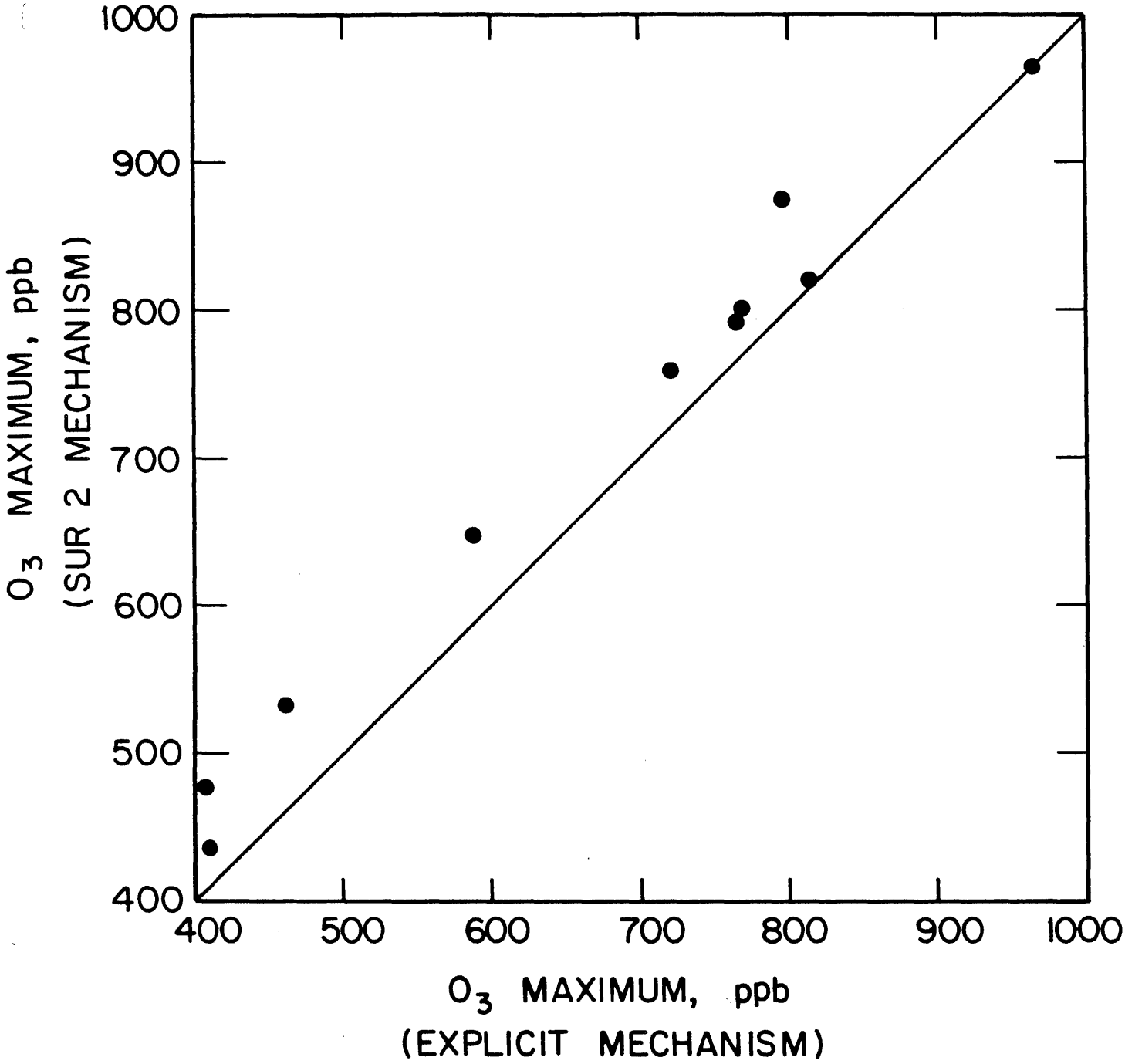

Figure 9. Comparison of peak O_3 concentrations predicted by the explicit and SUR2 mechanisms. Each point corresponds to one of the SAPRC multi-hydrocarbon-NO_x experiments EC-231 through EC-246.

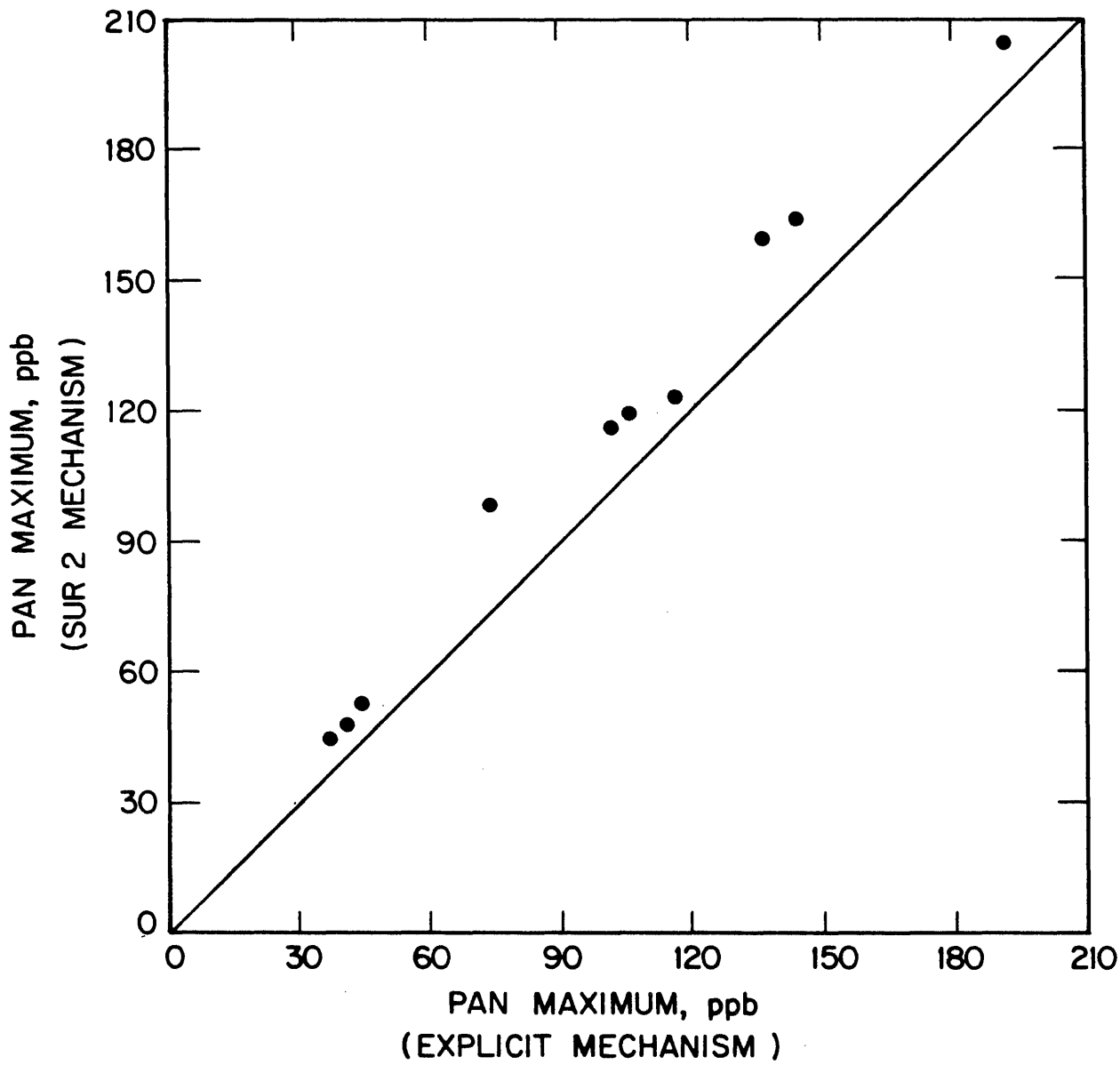

Figure 10. Comparison of peak PAN concentrations predicted by the explicit and SUR2 mechanisms. Each point corresponds to one of the SAPRC multi-hydrocarbon-NO_x experiments EC-231 through EC-246.

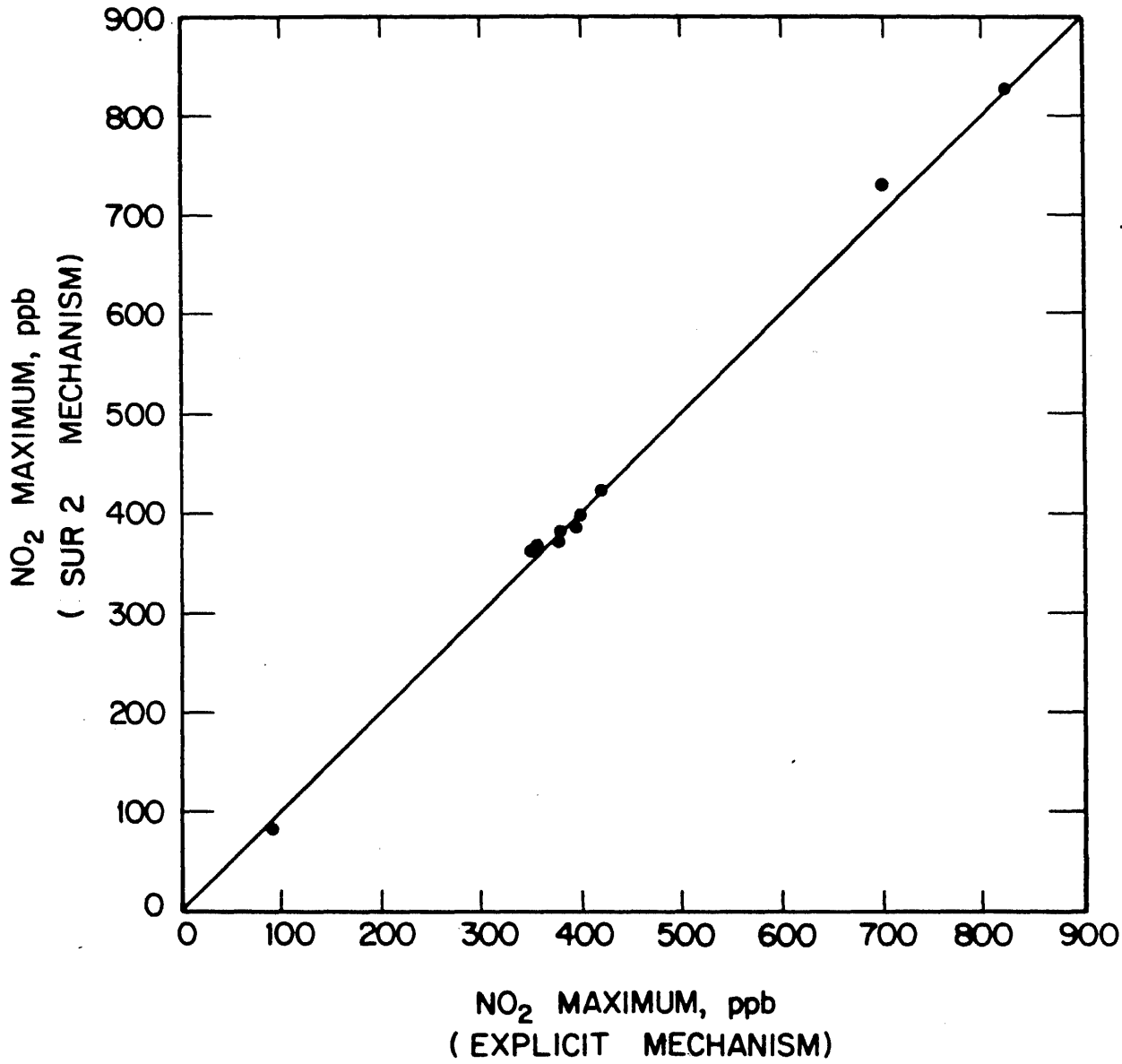

Figure 11. Comparison of peak NO_x concentrations predicted by the explicit and SUR2 mechanisms. Each point corresponds to one of the SAPRC multi-hydrocarbon-NO_x experiments EC-231 through EC-246.

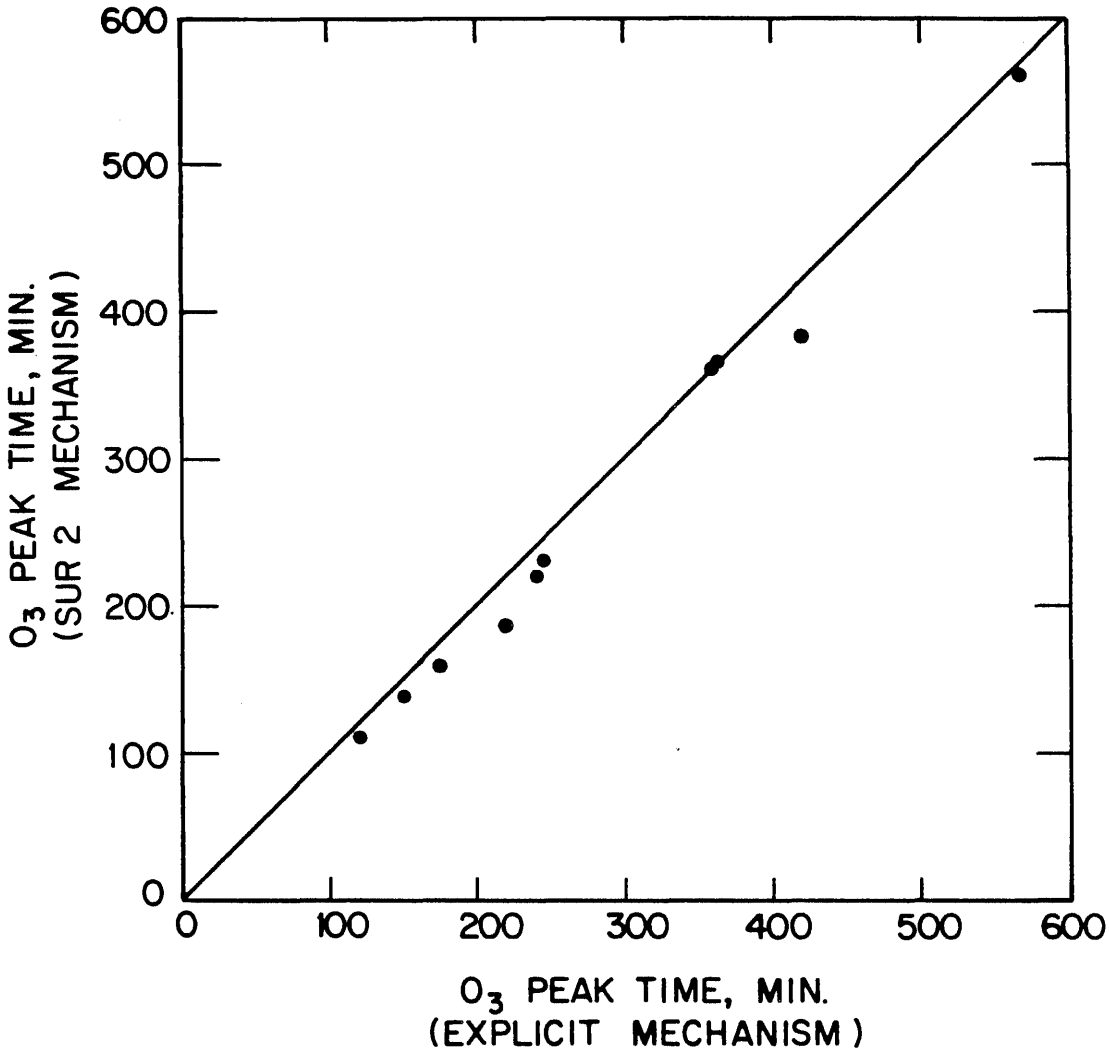

Figure 12. Comparison of peak O_3 times predicted by the explicit and SUR2 mechanisms. Each point corresponds to one of the SAPRC multi-hydrocarbon-NO_x experiments EC-231 through EC-246.

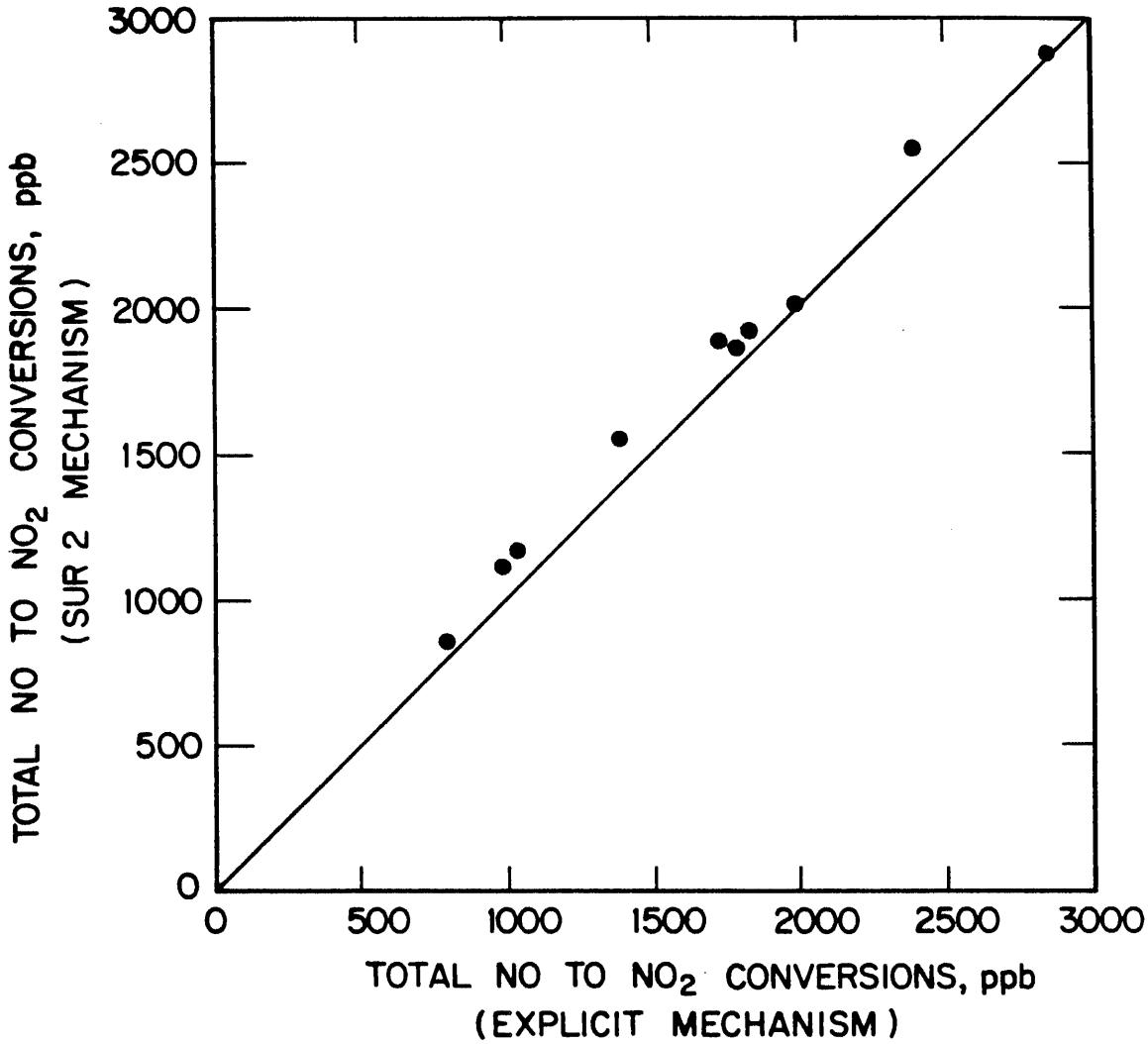

Figure 13. Comparison of the total amount of NO to NO_2 conversions predicted by the explicit and SUR2 mechanisms. Each point corresponds to one of the SAPRC multi-hydrocarbon-NO_x experiments EC-231 through EC-246.

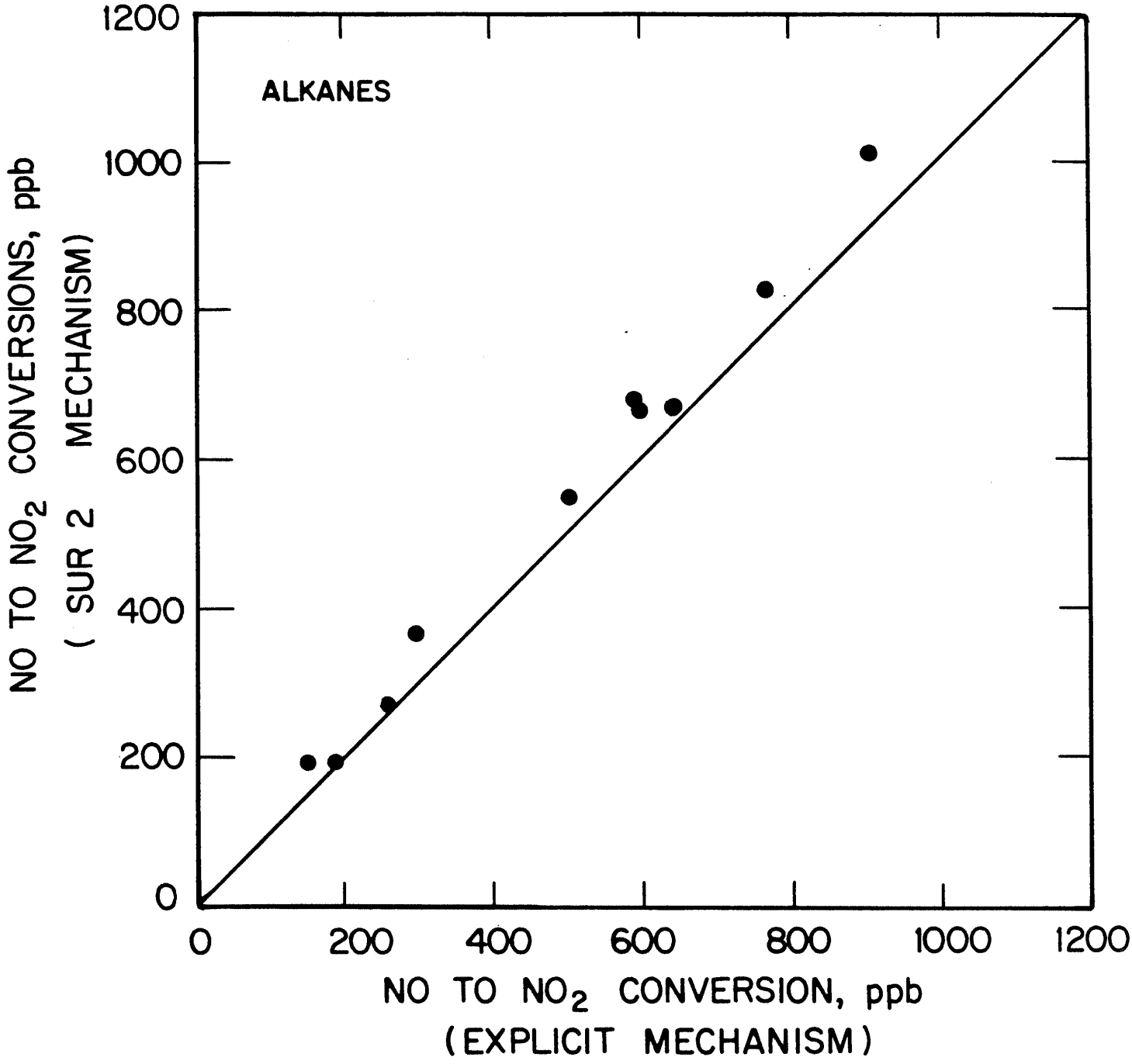

Figure 14. Comparison of the counter species results for the alkanes between the explicit and SUR2 mechanisms. Each point corresponds to one of the SAPRC multi-hydrocarbon-NO_x experiments EC-231 through EC-246.

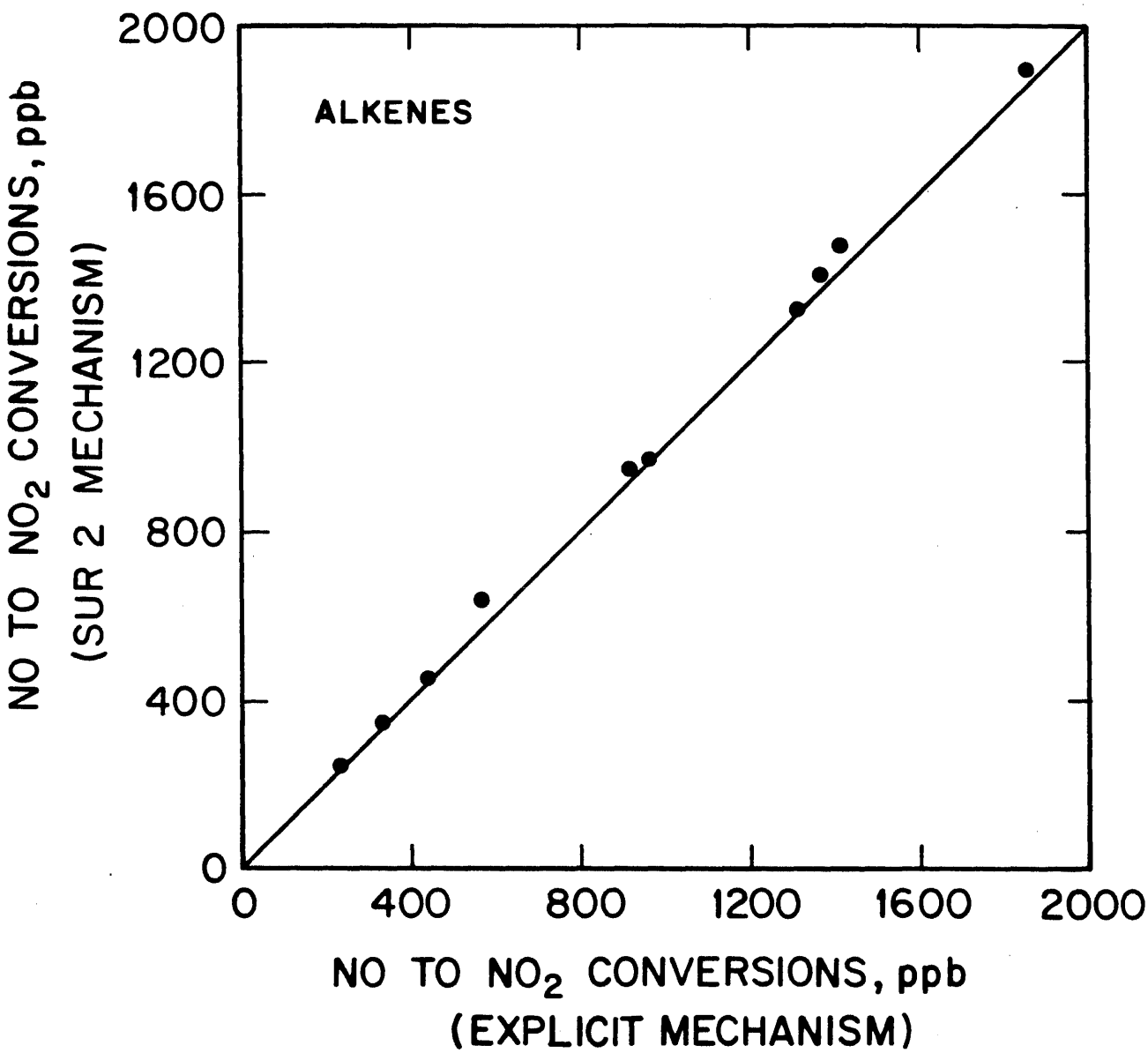

Figure 15. Comparison of the counter species results for the alkenes between the explicit and SUR2 mechanisms. Each point corresponds to one of the SAPRC multi-hydrocarbon-NO_x experiments EC-231 through EC-246.

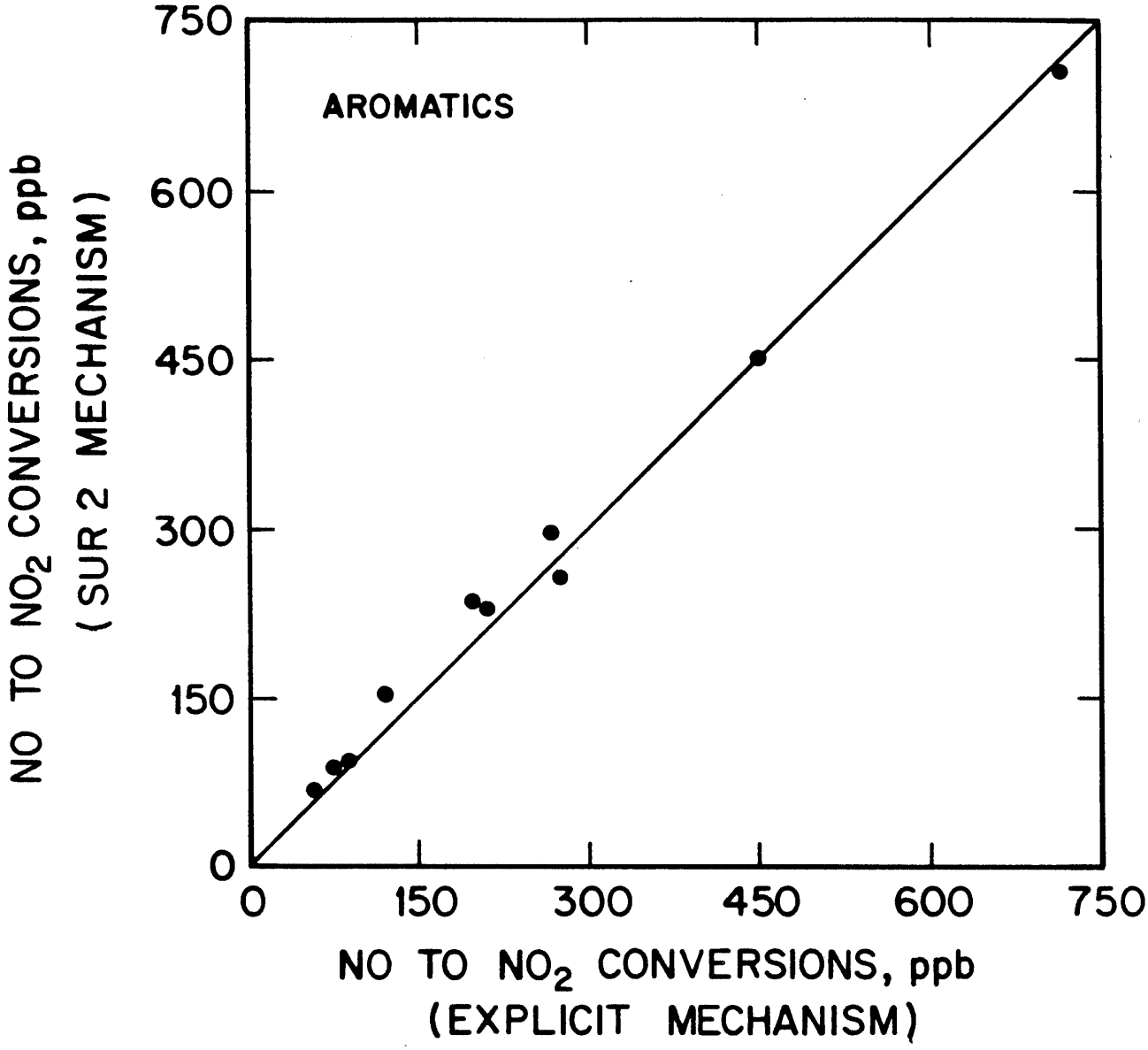

Figure 16. Comparison of the counter species results for the aromatics between the explicit and SUR2 mechanisms. Each point corresponds to one of the SAPRC multi-hydrocarbon-NO_x experiments EC-231 through EC-246.

surrogate and explicit mechanisms is obtained with the alkenes, but very good agreement is also found for the alkanes and aromatics. This type of agreement for each class of organic indicates that the SUR2 mechanism represents the chemistry found in the explicit mechanism very well.

Tests with the SUR2 mechanism indicate that one additional non-steady-state species, o-cresol, can be eliminated with less than a five percent effect on the predictions of the mechanism. This elimination would reduce the number of non-steady-state species from 20 to 19. However, with recently developed solution techniques, the amount of CPU time required for solution increases approximately linearly with the number of non-steady-state species (21,22). Thus, it is no longer crucial that the number of species be kept to an absolute minimum. With this in mind, we have decided not to remove o-cresol from the SUR2 mechanism.

EVALUATION OF THE SUR2 MECHANISM

The first step in evaluating the SUR2 mechanism for use in urban air quality models is to evaluate the performance of the mechanism against smog chamber data. In addition to testing the ozone formation aspect of the SUR2 mechanism, these evaluations will indicate how well the mechanism can predict important characteristics such as organic decay rates. In evaluating mechanisms with experimental data, it is very important to make use of data from more than one smog chamber facility, especially because of the different magnitudes of chamber specific radical sources in different facilities. We have chosen therefore to model experiments from two quite different smog chamber facilities, the evacuable chamber at SAPRC, and the outdoor chamber at the University of North

Carolina (UNC). The indoor chamber at SAPRC is relatively small ($5.8m^3$), makes use of artificial solar radiation, operates under conditions of constant temperature and light intensity, and appears to supply a relatively large source of free radicals to the chamber contents (18). In contrast, the UNC chamber is very large ($\sim 100m^3$ per side of a dual chamber), uses natural sunlight, operates near ambient temperature, and apparently has a considerably smaller wall radical source than the SAPRC chamber (27).

In order to adapt the SUR2 mechanism for modeling chamber experiments it is necessary to add several reactions to the mechanism, which are summarized in Table A.6. The SAPRC experiments we have chosen to model are once again the 10 multi-hydrocarbon-NO_x experiments EC-231 through EC-246. The initial conditions and physical parameters for these experiments have been given in Table A.2. Six experiments from the outdoor UNC chamber will also be simulated. These experiments are also multi-hydrocarbon-NO_x runs in which both the initial hydrocarbon distribution and the $[RHC]_o/[NO_x]_o$ ratio are varied. The initial conditions for these six experiments are given in Table A.7.

Many of the results of modeling these 16 experiments with the SUR2 mechanism are shown in Figures A.10 through A.23. The agreement between experiment and prediction is good with both sets of experimental data. The results for the SAPRC experiments (Figures A.10 through A.17) are very close to those obtained with the explicit mechanism (Figures A.1 through A.9), a further indication that the SUR2 mechanism is a good representation of the explicit chemistry in the explicit mechanism. In the experiments at SAPRC, the SUR2 mechanism, like the explicit mechanism, tends to over-predict the O_3 peak heights and slightly over-predict the PAN peak

height. The time of the NO_2 and O_3 peaks, the height of the NO_2 peak, and the hydrocarbon decay rates are all predicted very well. In the experiments performed at UNC*, the SUR2 mechanism does very well in predicting O_3 and PAN peak heights, with the typical O_3 peak being slightly under-predicted. Once again, the time of the ozone peak and the hydrocarbon decay rates lie very close to the experimental data. We repeat that, while chamber effects are used in these simulations, each chamber dependent term is set at the value recommended by either SAPRC or UNC, and not varied as the initial conditions of the experiments changed.

APPLICATION TO THE ATMOSPHERE

Up to this point, the SUR2 mechanism has only been applied under conditions, such as a smog chamber experiment, where the initial organic distribution is known exactly. In the atmosphere the organic distribution is not well defined, and fresh emissions are continuously being added. In this case, one needs a way of formulating a set of initial conditions that will accurately represent the complicated atmospheric mix. Although relatively few studies of ambient organic concentrations have been performed to date, many major cities now have some information available on both ambient organic distributions and emissions inventories. When ambient organic data are available for the city of interest, these data should be used with measurements of total NMHC and the information in Table 3 to obtain the initial conditions for use with the SUR2 mechanism. This is the standard method of obtaining initial conditions for atmospheric applications of lumped

*PAN was not measured in some of the UNC experiments, so the experimental NO_2 data actually correspond to the sum of NO_2 and PAN.

Table 3. Surrogate Species Used with the SUR2 Mechanism and the Compounds They Represent[1]

Surrogate Species	Compounds Represented
ALK	All C_4 and greater alkanes
propene	All C_3 and greater terminal alkenes
trans-2-butene	All C_4 and greater internal alkenes
toluene	All mono-alkylbenzenes
xylene	All di- and tri-alkylbenzenes
acetaldehyde	All C_2 and greater aldehydes
formaldehyde	formaldehyde
benzene	benzene
ethene	ethene

[1] In the SUR2 mechanism, propene and butene are lumped into the OLE group, and toluene and xylene are lumped into the ARO group. However, the individual concentrations of the surrogate species (propene, butene, toluene, and xylene) must be calculated in order to determine the stoichiometric coefficients and rate constants for the reactions involving the OLE and ARO groups.

mechanisms. If no detailed organic composition data are available for the city of interest, a distribution of organics must be assumed. Experimental studies of organics in urban air, such as the investigation of Grosjean and Fung (29), should be helpful in this matter. Obviously, more work is needed in order to both better characterize the distribution of ambient organics and to understand the effects of varying this distribution on the predictions of chemical mechanisms.

CONCLUSIONS

A surrogate condensed chemical reaction mechanism for photochemical smog containing the latest available kinetic and mechanistic data is developed here and is extensively tested against experimental data from two smog chamber facilities. In addition, a counter species analysis has shown that the predictions of the individual portions of the surrogate mechanism are in good agreement with those of a detailed explicit mechanism for photochemical smog. The new mechanism contains 20 non-steady-state species, making it compact enough for use in multidimensional grid models of urban air pollution. A major advantage of the new mechanism is the ease with which it can be modified to incorporate new kinetic or mechanistic information because of the straightforward manner in which the mechanism was formulated from the detailed explicit chemistry.

Future work should concentrate on the atmospheric application of the new mechanism. Ozone isopleths generated with the new mechanism should be compared to those obtained using the existing mechanisms for photochemical smog. The effects of dilution, hydrocarbons aloft, and aldehydes aloft on the predictions of the new mechanism should be studied. In addition, more

attention should be directed toward the specification of initial conditions using measurements of atmospheric hydrocarbon distributions and emission inventories.

REFERENCES

(1) Falls, A.H. and Seinfeld, J. H. (1978), "Continued Development of a Kinetic Mechanism for Photochemical Smog," Environmental Science and Technology, 12, 1398-1406.

(2) Atkinson, R., Lloyd, A.C. and Winges, L. (1982), "An Updated Chemical Mechanism for Hydrocarbons/NO_x/SO_2 Photooxidations Suitable for Inclusion in Atmospheric Simulation Models," Atmospheric Environment, 16, 1341-1355.

(3) Killus, J.P. and Whitten, G.Z. (1982), A New Carbon-Bond Mechanism for Air Quality Modeling, U.S. Environmental Protection Agency Report No. EPA-600/3-82-041.

(4) Dodge, M.C. (1977), Combined Use of Modeling Techniques and Smog Chamber Data to Derive Ozone-Precursor Relationships, U.S. Environmental Protection Agency Report, EPA-600/3-77-001a, 881-889.

(5) Demerjian, K.L. (1982), "Personal Communication."

(6) Penner, J.E. and Walton, J.J. (1982) Air Quality Model Update, Lawrence Livermore Laboratory Report UCID - 19300, Lawrence Livermore National Laboratory, University of California, Livermore, California, 55 pp.

(7) Jeffries, H.E., Sexton, K.G. and Salmi, C.N. (1981), Effects of Chemistry and Meteorology on Ozone Control Calculations Using Simple Trajectory Models and the EKMA Procedure, Final Report to the U.S. Environmental Protection Agency Under Contract No. 68-02-3523, School of Public Health, University of North Carolina, Chapel Hill, North Carolina, 373 pp.

(8) Whitten, G.Z. (1981) Comments at U.S. Environmental Protection Agency Workshop on the Empirical Kinetic Modeling Approach, December 15-16, Research Triangle Park, NC.

(9) Carter, W.P.L., Winer, A.M. and Pitts, J.N., Jr. (1982) "Effect of Kinetic Mechanisms and Hydrocarbon Composition on Oxidant-Precursor Relationships Predicted by the EKMA Isopleth Technique," Atmospheric Environment 16, 113-120.

(10) Leone, J.A. and Seinfeld, J.H. (1983) Evaluation of Chemical Reaction Mechanisms for Photochemical Smog - Part II. Quantitative Evaluation of the Mechanisms, U.S. Environmental Protection Agency Report (in press).

(11) Leone, J.A. and Seinfeld, J.H. (1984) "Comparative Analysis of Chemical Reaction Mechanisms for Photochemical Smog," Atmospheric Environment (in press).

(12) Pitts, J.N., Winer, A.M., Darnall, K.R. et al. (1976), Chemical Consequences of Air Quality Standards and of Control Implementation Programs: Roles of Hydrocarbons, Oxides of Nitrogen, and Aged Smog in the Production of Photochemical Oxidant, Final Report to the California Air Resources Board under Contract Number 4-212, Statewide Air Pollution Research Center, University of California Riverside, California, 444 pp.

(13) Baulch, D.L., Cox, R.A., Crutzen, P.J., Hampson, R.F., Kerr, J.A., Troe, J. and Watson, R.T. (1982), "Evaluated Kinetic and Photochemical Data for Atmospheric Chemistry: Supplement 1. CODATA Task Group on Chemical Kinetics," J. Physical and Chemical Reference Data, 11, 327-496.

(14) DeMore, W.B., Watson, R.T., Howard, C.J., Golden, D.M., Molina, M.J., Hampson, R.F., Kurylo, M. and Ravishankara, A.R. (1982), Chemical Kinetics and Photochemical Data for Use in Stratospheric Modeling, Jet Propulsion Laboratory Publication 82-57, California Institute of Technology, Pasadena, California.

(15) Leone, J.A. and Seinfeld, J.H. (1983), "An Updated Chemical Mechanism for the Atmospheric Photooxidation of Toluene," International Journal of Chemical Kinetics, 16, 159-193.

(16) Leone, J.A., Flagan, R.C., Grosjean, D. and Seinfeld, J.H. (1984), "An Outdoor Smog Chamber and Modeling Study of Toluene-NO_x Photooxidation," International Journal of Chemical Kinetics, (in press).

(17) Atkinson, R. and Lloyd, A.C. (1984), "Evaluation of Kinetic and Mechanistic Data for Modeling of Photochemical Smog," J. Phys. Chem. Ref. Data, 13 (2), in press.

(18) Carter, W.P.L., Atkinson, R., Winer, A.M. and Pitts, J.N. Jr., (1982) "Experimental Investigation of Chamber-Dependent Radical Sources," International Journal of Chemical Kinetics, 14, 1071-1103.

(19) Atkinson, R., Carter, W.P.L., Darnall, K.R., Winer, A.M., and Pitts, J.N. Jr. (1980), "A Smog Chamber and Modeling Study of the Gas Phase NO_x-Air Photooxidation of Toluene and the Cresols," International Journal of Chemical Kinetics, 12, 779-837.

(20) Leone, J.A. and Seinfeld, J.H. (1983), "Analysis of the Characteristics of Complex Chemical Reaction Mechanisms - Application to Photochemical Smog Chemistry," Environmental Science & Technology, 18, 280-287.

(21) Russell, A. (1984), "Personal Communication."

(22) Young, T.R. and Boris, J.P. (1977), "A Numerical Technique for Solving Stiff Ordinary Differential Equations Associated with the Chemical Kinetics of Reactive-Flow Problems," Journal of Physical Chemistry, 81, 2423-2427.

(23) Pitts, J.N., Jr., Darnall, K., Carter, W.P.L., Winer, A.M. and Atkinson, R. (1979), Mechanisms of Photochemical Reactions in Urban Air - Final Report, U.S. Environmental Protection Agency Report No. EPA-600/3-79-110.

(24) Demerjian, K.L., Schere, K.L. and Peterson, J.T. (1980), "Theoretical Estimates of Actinic (Spherically Integrated) Flux and Photolytic Rate Constants of Atmospheric Species in the Lower Troposphere," Advances in Environmental Science and Technology, 10, 369-459.

(25) Grosjean, D. (1983), "Atmospheric Reactions of Pyruvic Acid," Atmospheric Environment, 17, 2379-2382.

(26) Horowitz, A. and Calvert, J.G. (1982), "Wavelength Dependence of the Primary Processes in Acetaldehyde Photolysis," J. Physical Chemistry, 86, 3105-3114.

(27) Jeffries, H.E., Kamens, R.M., Sexton, K.G. and Gerhardt, A.A. (1982), Outdoor Smog Chamber Experiment to Test Photochemical Models, U.S. Environmental Protection Agency Report.

(28) Plum, C.N., Sanhueza, E., Atkinson, R., Carter, W.P.L. and Pitts, J.N., Jr., "OH Radical Rate Constants and Photolysis Rates of α-Dicarbonyls," Environmental Science and Technology, 17, 479.

(29) Grosjean, D. and Fung, K. (1984), "Hydrocarbons and Carbonyls in Los Angeles Air," Journal Air Pollution Control Association, 34, 537-543.

APPENDIX

Table A.1. Explicit Reaction Mechanism

Reaction[1,2]	Rate Constant[3]	Activation Energy (K)	Note
Inorganic Reactions (13,14,17):			
1) $NO_2 + h\nu \rightarrow NO + O(^3P)$	0.30	-	1
2) $O(^3P) + O_2 \rightarrow O_3$	2.6×10^1	-5.1×10^2	
3) $O_3 + NO \rightarrow NO_2 + O_2$	2.7×10^1	1.5×10^3	
4) $O(^3P) + NO_2 \rightarrow NO + O_2$	1.4×10^4	-	
5) $O_3 + NO_2 \rightarrow NO_3 + O_2$	4.7×10^{-2}	2.45×10^3	
6) $NO_3 + NO \rightarrow 2NO_2$	3.0×10^4	-	
7) $HO_2 + NO_2 \rightarrow HO_2NO_2$	1.6×10^3	-	
8) $NO_2 + OH \rightarrow HNO_3$	1.6×10^4	-	
9) $O_3 + OH \rightarrow HO_2 + O_2$	9.9×10^1	9.7×10^2	
10) $O_3 + HO_2 \rightarrow OH + 2O_2$	3.0×10^0	5.8×10^2	
11) $HO_2NO_2 \rightarrow HO_2 + NO_2$	5.1×10^0	1.042×10^4	
12) $HO_2 + NO \rightarrow NO_2 + OH$	1.2×10^4	-2.4×10^2	
13) $HO_2 + HO_2 \rightarrow H_2O_2 + O_2$	3.9×10^3	-1.2×10^3	
14) $HO_2 + HO_2 + H_2O \rightarrow H_2O_2 + O_2 + H_2O$	2.2×10^{-1}	-5.8×10^3	
15) $O_3 + h\nu \rightarrow O(^3P) + O_2$	$6.5 \times 10^{-2}\ k_{NO_2}$	-	2
16) $O_3 + h\nu \rightarrow O(^1D) + O_2$	$2.8 \times 10^{-3}\ K_{NO_2}$	-	2
17) $O(^1D) \rightarrow O(^3P)$	4.3×10^{10}	-	
18) $O(^1D) + H_2O \rightarrow 2OH$	3.2×10^5	-	
19) $NO + OH \rightarrow HONO$	9.7×10^3	-	
20) $HONO + h\nu \rightarrow NO + OH$	$1.8 \times 10^{-1}\ k_{NO_2}$	-	2
21) $NO + NO + O_2 \rightarrow 2NO_2$	7.2×10^{-10}	-5.3×10^2	
22) $NO_3 + NO_2 \rightarrow NO + NO_2 + O_2$	5.9×10^{-1}	1.23×10^3	

Table A.1 (continued)

Reaction [1,2]	Rate Constant[3]	Activation Energy (K)	Note
23) $NO_3 + NO_2 \rightarrow N_2O_5$	1.6×10^3	-	
24) $N_2O_5 \rightarrow NO_2 + NO_3$	3.1×10^0	1.108×10^4	
25) $N_2O_5 + H_2O \rightarrow 2HNO_3$	4.4×10^{-6}	-	1
26) $H_2O_2 + OH \rightarrow HO_2 + H_2O$	2.5×10^3	-	
27) $H_2O_2 + h\nu \rightarrow 2OH$	$8.4 \times 10^{-4}\ k_{NO_2}$	-	2
28) $CO + OH \xrightarrow{O_2} HO_2 + CO_2$	4.0×10^2	-	
29) $NO_3 + h\nu \rightarrow 0.3NO + 0.7NO_2 + 0.70(^3P)$	$1.55 \times 10^1\ k_{NO_2}$	-	3

Aldehyde Reactions and PAN Formation (17):

30) $CH_3CHO + h\nu \xrightarrow{2O_2} CH_3O_2\cdot + HO_2 + CO$	$2.58 \times 10^{-4}\ k_{NO_2}$	-	4
31) $CH_3CHO + OH \xrightarrow{O_2} CH_3C(O)O_2\cdot + H_2O$	2.4×10^4	-2.6×10^2	
32) $CH_3O_2\cdot + NO \rightarrow NO_2 + CH_3O\cdot$	1.1×10^4	-	
33) $CH_3O\cdot + O_2 \rightarrow HCHO + HO_2\cdot$	2.1×10^0	1.35×10^3	
34) $CH_3O\cdot + NO_2 \rightarrow CH_3ONO_2$	2.2×10^4	-	
35) $CH_3O_2\cdot + HO_2 \rightarrow CH_3OOH + O_2$	9.2×10^3	-1.3×10^3	
36) $CH_3C(O)O_2\cdot + NO \xrightarrow{2O_2} NO_2 + CH_3O_2\cdot + CO_2$	1.1×10^4	-	
37) $CH_3C(O)O_2\cdot + NO_2 \rightarrow PAN$	6.9×10^3	-	
38) $CH_3C(O)O_2\cdot + HO_2 \rightarrow CH_3C(O)O_2H + O_2$	4.4×10^3	-	
39) $PAN \rightarrow CH_3C(O)O_2\cdot + NO_2$	2.2×10^{-2}	1.354×10^4	
40) $HCHO + h\nu \rightarrow H_2 + CO$	$3.3 \times 10^{-3}\ k_{NO_2}$	-	4
41) $HCHO + h\nu \xrightarrow{2O_2} 2HO_2 + CO$	$2.35 \times 10^{-3}\ k_{NO_2}$	-	4

Table A.1 (continued)

Reaction[1,2]	Rate Constant[3]	Activation Energy (K)	Note
42) $HCHO + OH \xrightarrow{O_2} HO_2 + CO + H_2O$	1.6×10^4	-	
α-Dicarbonyl Chemistry (17,28):			
43) $CH_3C(O)CHO + OH \xrightarrow{O_2} CH_3C(O)O_2\cdot + CO + H_2O$	2.5×10^4	-	
44) $CH_3C(O)CHO + h\nu \xrightarrow{2O_2} CH_3C(O)O_2\cdot + + HO_2 + CO$	$1.3\times10^{-2}\ k_{NO_2}$	-	
45) $CH_3C(O)CHO + h\nu \xrightarrow{2O_2} CH_3O_2\cdot + HO_2 + 2CO$	$6.0\times10^{-3}\ k_{NO_2}$	-	
46) $(CHO)_2 + OH \xrightarrow{O_2} HO_2 + 2CO + H_2O$	1.7×10^4	-	
47) $(CHO)_2 + h\nu \rightarrow 0.13HCHO + 0.87H_2 + 1.87CO$	$8.0\times10^{-3}\ k_{NO_2}$	-	
Toluene Abstraction Pathway (15,16)			
48) $C_6H_5\text{-}CH_3 + OH \xrightarrow{O_2} C_6H_5\text{-}CH_2O_2\cdot + H_2O$	7.5×10^2	-	
49) $C_6H_5\text{-}CH_2O_2\cdot + NO \rightarrow NO_2 + C_6H_5\text{-}CH_2O\cdot$	9.0×10^3	-	
50) $C_6H_5\text{-}CH_2O_2\cdot + NO \rightarrow C_6H_5\text{-}CH_2ONO_2$	1.0×10^3	-	
51) $C_6H_5\text{-}CH_2O\cdot + O_2 \rightarrow C_6H_5\text{-}CHO + HO_2$	1.0×10^1	6.9×10^2	
52) $C_6H_5\text{-}CH_2O\cdot + NO_2 \rightarrow C_6H_5\text{-}CH_2ONO_2$	1.9×10^4	-	
53) $C_6H_5\text{-}CHO + h\nu \rightarrow$ stable products	1.6×10^{-3}	-	
54) $C_6H_5\text{-}CHO + OH \xrightarrow{O_2} C_6H_5\text{-}C(O)O_2\cdot + H_2O$	1.9×10^4	-	
55) $C_6H_5\text{-}C(O)O_2\cdot + NO \xrightarrow{O_2} NO_2 + C_6H_5\text{-}O_2\cdot + CO_2$	1.0×10^4	-	

Table A.1 (continued)

Reaction[1,2]	Rate Constant[3]	Activation Energy (K)	Note
56) $C_6H_5\text{-}C(O)O_2\cdot + NO_2 \rightarrow C_6H_5\text{-}C(O)O_2NO_2$	6.9×10^3	-	
57) $C_6H_5\text{-}C(O)O_2NO_2 \rightarrow C_6H_5\text{-}C(O)O_2\cdot + NO_2$	9.6×10^{-3}	1.304×10^4	
58) $C_6H_5\text{-}O_2\cdot + NO \rightarrow NO_2 + C_6H_5\text{-}O\cdot$	9.0×10^3	-	
59) $C_6H_5\text{-}O_2\cdot + NO_2 \rightarrow NO_3 + C_6H_5\text{-}O\cdot$	1.0×10^4	-	
60) $C_6H_5\text{-}O\cdot + NO_2 \rightarrow$ 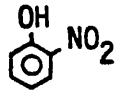	2.2×10^4	-	
61) 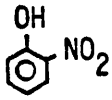 $+ NO_3 \rightarrow$ 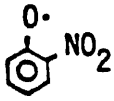 $+ HNO_3$	3.0×10^3	-	
62) 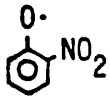 $+ NO_2 \rightarrow$ 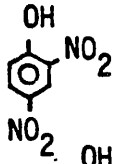	2.2×10^4	-	
63) $+ HO_2 \rightarrow$ $+ O_2$	7.4×10^3	-	

Toluene Addition Pathway (15,16):

64) 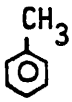 $+ OH \rightarrow$ 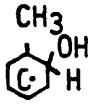	8.7×10^3	-	
65) 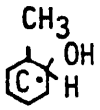 $+ O_2 \rightarrow$ 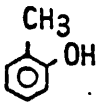 $+ HO_2$	1.0×10^1	6.9×10^2	
66) 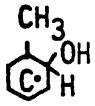 $+ NO_2 \rightarrow$ 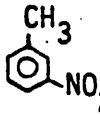 $+ H_2O$	4.4×10^4	-	
67) 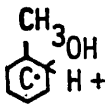 $+ O_2 \rightarrow$ 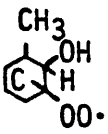	4.9×10^1	-	
68) 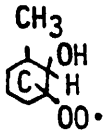 $+ NO \xrightarrow{2O_2} NO_2 + HO_2$ $+ CH_3C(O)CHO + CH(O)CH{=}CHCHO$	1.0×10^4	-	

Table A.1 (continued)

Reaction[1,2]	Rate Constant[3]	Activation Energy (K)	Note
Toluene addition path (continued)			
69) 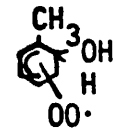 + NO $\xrightarrow{2O_2}$ NO_2 + HO_2 + $(CHO)_2$ + $CH_3C(O)CH{=}CHCHO$	0.0	-	
70) 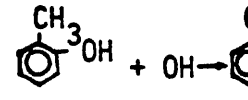 + OH → 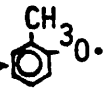 + H_2O	4.9×10^3	9.0×10^2	
71) 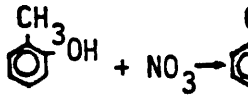 + NO_3 → 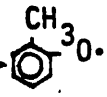 + HNO_3	1.5×10^4	-	
72) 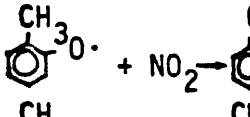 + NO_2 → 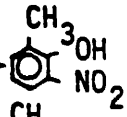	2.2×10^4	-	
73) 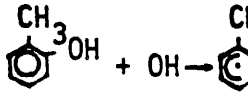 + OH → 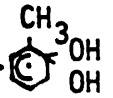	5.6×10^4	-	
74) 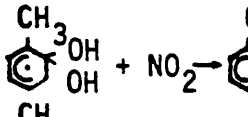 + NO_2 → 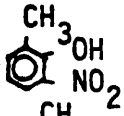 + H_2O	4.4×10^4	-	
75) 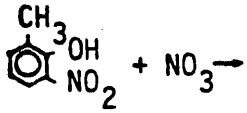 + NO_3 → 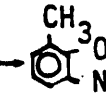 + HNO_3	1.5×10^4	-	
76) 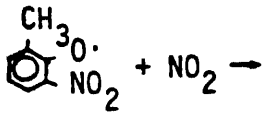 + NO_2 → 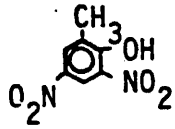	2.2×10^4	-	
77) 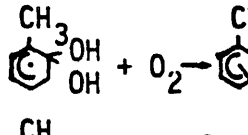 + O_2 → 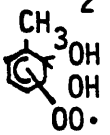	4.9×10^1	-	
78) 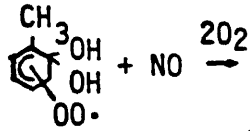 + NO $\xrightarrow{2O_2}$ NO_2 + HO_2 + $CH(O)CH{=}CHCHO$ + $CH_3C(O)COOH$	1.0×10^4	-	
79) 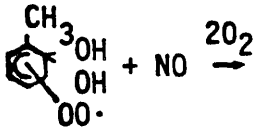 + NO $\xrightarrow{2O_2}$ NO_2 + HO_2 + $CH_3C(O)CH{=}CHCHO$ + $CH(O)COOH$	0.0	-	

Table A.1 (continued)

Reaction[1,2]	Rate Constant[3]	Activation Energy(K)	Note
80) $CH(O)COOH + OH \xrightarrow{O_2} HO_2 + H_2O + CO + CO_2$	2.2×10^{4}	-	
81) $CH_3C(O)COOH + h\nu \rightarrow CH_3CHO + CO_2$	$3.6\times10^{-2}\ k_{NO_2}$	-	5
Conjugated γ-dicarbonyl chemistry (15-17)			
82) $HC(O)CH{=}CHCHO + OH \xrightarrow{O_2} HC(O)CH{=}CHC(O)O_2\cdot + H_2O$	4.4×10^{4}	-	
83) $HC(O)CH{=}CHC(O)O_2\cdot + NO \xrightarrow{O_2} NO_2 + CO_2 + HC(O)CH{=}CHO_2\cdot$	1.0×10^{4}	-	
84) $HC(O)CH{=}CHO_2\cdot + NO \xrightarrow{O_2} NO_2 + HC(O)CH(O_2\cdot)CHO$	1.0×10^{4}	-	
85) $HC(O)CH(O_2\cdot)CHO + NO \rightarrow HC(O)CH(ONO_2)CHO$	4.0×10^{2}	-	
86) $HC(O)CH{=}CHC(O)O_2\cdot + NO_2 \rightarrow HC(O)CH{=}CHCO_3NO_2$	6.9×10^{3}	-	
87) $HC(O)CH{=}CHCO_3NO_2 \rightarrow HC(O)CH{=}CHC(O)O_2\cdot + NO_2$	2.2×10^{-2}	-	
88) $HC(O)CH(O_2\cdot)CHO + NO \xrightarrow{O_2} (CHO)_2 + HO_2 + NO_2 + CO$	1.0×10^{4}	-	
89) $HC(O)CH{=}CHO_2\cdot + NO \rightarrow HC(O)CH{=}CHONO_2$	4.0×10^{2}	-	
90) $HC(O)CH{=}CHO_2\cdot + NO_2 \xrightarrow{O_2} HC(O)CH(O_2\cdot)CHO + NO_3$	1.0×10^{4}	-	
91) $CH_3C(O)CH{=}CHCHO + OH \xrightarrow{O_2} H_2O + CH_3C(O)CH{=}CHC(O)O_2\cdot$	2.2×10^{4}	-	
92) $CH_3C(O)CH{=}CHCHO + OH \xrightarrow{O_2} CH_3C(O)CH(OH)C(O_2\cdot)HCHO$	7.4×10^{3}	-	
93) $CH_3C(O)CH(OH)C(O_2\cdot)HCHO + NO \xrightarrow{O_2} NO_2 + HO_2 + CH_3C(O)CHO + (CHO)_2$	1.0×10^{4}	-	
94) $CH_3C(O)CH{=}CHC(O)O_2\cdot + NO \xrightarrow{O_2} NO_2 + CO_2 + CH_3C(O)CH{=}CHO_2\cdot$	1.0×10^{4}	-	
95) $CH_3C(O)CH{=}CHO_2\cdot + NO \xrightarrow{O_2} NO_2 + CH_3C(O)CH(O_2\cdot)CHO$	1.0×10^{4}	-	
96) $CH_3C(O)CH(O_2\cdot)CHO + NO \rightarrow CH_3C(O)CH(ONO_2)CHO$	8.0×10^{6}	-	
97) $CH_3C(O)CH{=}CHC(O)O_2\cdot + NO \rightarrow CH_3C(O)CH{=}CHCO_3NO_2$	6.9×10^{3}	-	
98) $CH_3C(O)CH{=}CHCO_3NO_2 \rightarrow CH_3C(O)CH{=}CHC(O)O_2\cdot + NO_2$	2.2×10^{-2}	-	
99) $CH_3C(O)CH(O_2\cdot)CHO + NO \xrightarrow{O_2} NO_2 + CH_3C(O)O_2\cdot + (CHO)_2$	5.0×10^{3}	-	

Table A.1 (continued)

Reaction[1,2]	Rate Constant[3]	Activation Energy(K)	Note
Conjugated γ-dicarbonyl chemistry (continued)			
100) $CH_3C(O)CH(O_2\cdot)CHO + NO \xrightarrow{O_2} NO_2 + HO_2 + CH_3C(O)CHO + CO$	5.0×10^3	-	
101) $CH_3C(O)CH{=}CHO_2\cdot + NO \rightarrow CH_3C(O)CH{=}CHONO_2$	8.0×10^2	-	
102) $CH_3C(O)CH{=}CHO_2\cdot + NO_2 \xrightarrow{O_2} NO_3 + CH_3C(O)CH(O_2\cdot)CHO$	1.0×10^4	-	
m-Xylene chemistry (15-17):			
103) 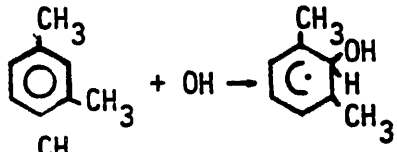	3.4×10^4	-	6
104) 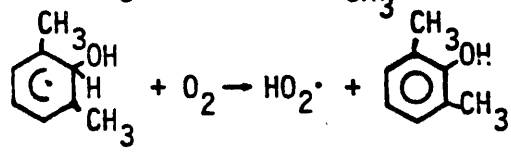	1.0×10^2	6.9×10^2	
105) 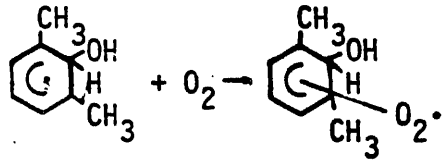	4.7×10^1	-	
106) 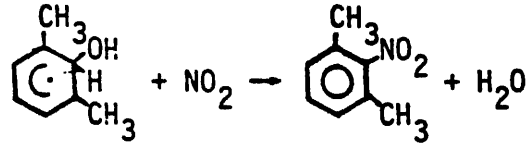	4.4×10^4	-	
107) 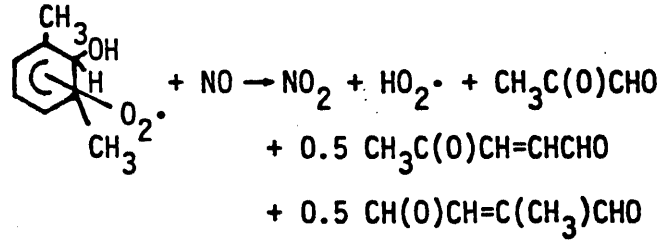	1.0×10^4	-	7
108) 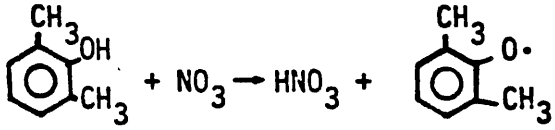	2.2×10^4	-	
109) 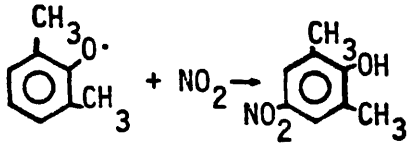	2.2×10^4	-	

Table A.1 (continued)

Reaction[1,2]	Rate Constant[3]	Activation Energy(K)	Note
m-Xylene chemistry (continued)			
110) 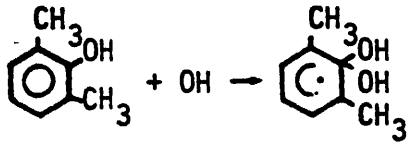	1.1×10^{5}	-	
111) 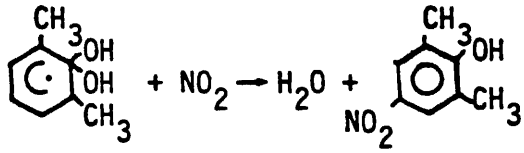	4.4×10^{4}	-	
112) 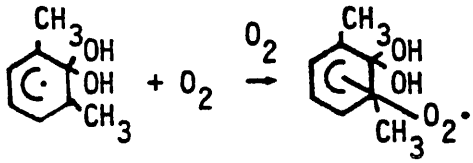	4.7×10^{1}	-	
113) 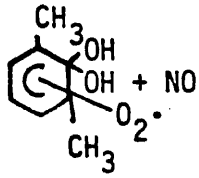 + NO → NO_2 + HO_2 + $CH_3COCOOH$ + 0.5 $CH_3COCH{=}CHCHO$ + 0.5 $CHOCH{=}C(CH_3)CHO$	1.0×10^{4}	-	7
114) $CHOCH{=}C(CH_3)CHO + OH \xrightarrow{O_2} HCOC(OH)H\overset{O_2\cdot}{C}(CH_3)CHO$	7.4×10^{3}	-	
115) $HCOC(OH)H\overset{O_2\cdot}{C}(CH_3)CHO + NO \xrightarrow{O_2} 0.88NO_2 + 0.88(CHO)_2 + 0.88\ HO_2\cdot$	1.0×10^{4}	-	8
116) $CHOCHO{=}C(CH_3)CHO + OH \xrightarrow{O_2} HCOCH{=}\overset{CH_3}{C}CO_3\cdot + H_2O$	4.4×10^{4}		
117) $HCOCH{=}\overset{CH_3}{C}CO_3\cdot + NO \xrightarrow{O_2} NO_2 + HCOCH{=}\overset{CH_3}{C}O_2\cdot + CO_2$			
118) $HCOCH{=}\overset{CH_3}{C}CO_3\cdot + NO_2 \rightarrow HCOCH{=}\overset{CH_3}{C}CO_3\ NO_2$	6.9×10^{3}	-	
119) $HCOCH{=}\overset{CH_3}{C}CO_3NO_2 \rightarrow NO_2 + HCOCH{=}\overset{CH_3}{C}CO_3\cdot$	2.2×10^{-2}	1.354×10^{4}	

Table A.1 (continued)

Reaction[1,2]	Rate Constant[3]	Activation Energy(K)	Note
m-Xylene chemistry (continued)			
120) $HCOCH{=}\overset{CH_3}{C}O_2\cdot + NO \xrightarrow{O_2} NO_2 + CH_3(O)CH(O_2\cdot)CHO$	1.0×10^4	-	
121) $HCOCH{=}\overset{CH_3}{C}O_2\cdot + NO \rightarrow HCOCH{=}\overset{CH_3}{C}CO_2NO_2$	8.0×10^2	-	
122) $HCOCH{=}\overset{CH_3}{C}O_2\cdot + NO_2 \rightarrow NO_3 + CH_3C(O_2\cdot)(CHO)_2$	1×10^4	-	
123) $CH_3C(O_2\cdot)(CHO)_2 + NO \rightarrow CH_3C(ONO_2)(CHO)_2$	8.0×10^2	-	
124) $CH_3C(O_2\cdot)(CHO)_2 + NO \xrightarrow{O_2} 0.75\ HO_2\cdot + 0.75\ CO + 0.75\ CH_3COCHO + 0.25\ (CHO)_2 + 0.25\ CH_3C(O)O_2\cdot + NO_2$	1×10^4	-	
Ethene chemistry (17):			
125) $CH_2{=}CH_2 + OH \xrightarrow{O_2} HOCH_2CH_2O_2\cdot$	1.2×10^4	-3.82×10^2	
126) $HOCH_2CH_2O_2\cdot + NO \rightarrow NO_2 + HOCH_2CH_2O\cdot$	1×10^4		
127) $HOCH_2CH_2O\cdot \rightarrow HCHO + \cdot CH_2OH$	5.6×10^6		
128) $HOCH_2CH_2O\cdot + O_2 \rightarrow HOCH_2CHO + HO_2\cdot$	1.0×10^1	6.9×10^2	9
129) $\cdot CH_2OH + O_2 \rightarrow HCHO + HO_2\cdot$	$k_5=3\times10^3$		
130) $CH_2{=}CH_2 + O_3 \xrightarrow{O_2} HCHO + 0.4\ \dot{C}H_2O\dot{O} + 0.18\ CO_2 + 0.42CO + 0.12\ H_2 + 0.42\ H_2O + 0.12\ HO_2\cdot$	2.5×10^{-3}	2.56×10^3	

Table A.1 (continued)

Reaction [1,2]	Rate Constant [3]	Activation Energy(K)	Note
Propene chemistry (17):			
131) $CH_3CHCH_2 + OH \xrightarrow{O_2} 0.65\ CH_3\overset{O_2\cdot}{\dot{C}}HCH_2OH + 0.35\ CH_3CH(OH)CH_2O_2\cdot$	3.7×10^4	-5.37×10^2	
132) $CH_3\overset{O_2\cdot}{\dot{C}}HCH_2OH + NO \rightarrow NO_2 + CH_3\overset{O\cdot}{\dot{C}}HCH_2OH$	1×10^4	-	
133) $CH_3\overset{O\cdot}{\dot{C}}HCH_2OH \rightarrow CH_3CHO + \cdot CH_2OH$	1×10^5	-	
134) $CH_3CH(OH)CH_2O\cdot \rightarrow HCHO + CH_3\dot{C}HOH$	1×10^2	-	
135) $CH_3\overset{O_2\cdot}{\dot{C}}HCH_2OH + NO \rightarrow CH_3\overset{ONO_2}{\dot{C}}HCH_2OH$	4.0×10^2	-	
136) $CH_3CH(OH)CH_2O_2\cdot + NO \rightarrow NO_2 + CH_3CH(OH)CH_2O\cdot$	1×10^4	-	
137) $CH_3CH(OH)CH_2O_2\cdot + NO \rightarrow CH_3CH(OH)CH_2ONO_2$	400	-	
138) $CH_3\dot{C}HOH + O_2 \rightarrow HO_2\cdot + CH_3CHO$	3×10^3	-	
139) $CH_3CHCH_2 + O_3 \rightarrow 0.5\ CH_3CHO + 0.2\ CH_3\dot{C}HO\dot{O} + 0.06\ CH_4 + 0.27\ CO_2 + 0.33\ CO + 0.20\ HO_2\cdot + 0.1\ OH + 0.22\ CH_3O_2\cdot + 0.03\ CH_3O\cdot + 0.2\ \dot{C}H_2O\dot{O} + 0.06\ H_2 + 0.21\ H_2O$	1.6×10^{-2}	1.897×10^3	
tr-2-butene chemistry (17):			
140) $CH_3CH{=}CH\ CH_3 + OH \xrightarrow{O_2} CH_3CH(OH)\overset{OO\cdot}{\dot{C}}HCH_3$	1.0×10^5	-5.42×10^2	
141) $CH_3CH(OH)\overset{OO\cdot}{\dot{C}}HCH_3 + NO \rightarrow NO_2 + CH_3\overset{OH}{\dot{C}}H\overset{O\cdot}{\dot{C}}HCH_3$	1.0×10^4	-	

Table A.1 (continued)

Reaction[1,2]	Rate Constant[3]	Activation Energy(K)	Note
tr-2-butene chemistry (continued)			
142) $CH_3CH(OH)\overset{OO\cdot}{C}HCH_3 + NO \rightarrow CH_3\overset{OH}{C}H\overset{ONO_2}{C}HCH_3$	8.0×10^{2}	-	
143) $CH_3CH(OH)\overset{O\cdot}{C}HCH_3 \rightarrow CH_3CHO + CH_3\dot{C}HOH$	1.0×10^{4}	-	
144) $CH_3CH_2{=}CH_2CH_3 + O_3 \rightarrow CH_3CHO + 0.4\ CH_3\dot{C}HO\mathring{O}$ $+ 0.12\ CH_4 + 0.36\ CO_2$ $+ 0.24\ CO + 0.29\ HO_2\cdot$ $+ 0.19\ OH + 0.05\ CH_3O\cdot$ $+ 0.43\ CH_3O_2\cdot$	2.7×10^{-1}	1.051×10^{3}	
145) $C\dot{H}_2O\mathring{O} + NO \rightarrow NO_2 + HCHO$	1.0×10^{4}	-	
146) $C\dot{H}_2O\mathring{O} + NO_2 \rightarrow NO_3 + HCHO$	1.0×10^{3}	-	
147) $C\dot{H}_2O\mathring{O} + H_2O \rightarrow HCOOH + H_2O$	6.0×10^{-3}	-	
148) $CH_3\dot{C}HO\mathring{O} + NO \rightarrow NO_2 + CH_3CHO$	1.0×10^{4}	-	
149) $CH_3\dot{C}HO\mathring{O} + NO_2 \rightarrow NO_3 + CH_3CHO$	1.0×10^{3}	-	
150) $CH_3\dot{C}HO\mathring{O} + H_2O \rightarrow CH_3COOH + H_2O$	6.0×10^{-3}	-	
Propane chemistry (17):			
151) $CH_3CH_2CH_3 + OH \rightarrow H_2O + 0.85\ CH_3\overset{OO\cdot}{C}HCH_3$ $+ 0.15\ CH_3CH_2CH_2O_2\cdot$	2.3E3	6.8×10^{2}	
152) $CH_3\overset{OO\cdot}{C}HCH_3 + NO \rightarrow NO_2 + CH_3\overset{O\cdot}{C}HCH_3$	1.1×10^{4}	-	
153) $CH_3CH_2CH_2O_2\cdot + NO \rightarrow NO_2 + CH_3CH_2CHO\cdot$	1.1×10^{4}	-	

Table A.1 (continued)

Reaction[1,2]	Rate Constant[3]	Activation Energy(K)	Note
Propane chemistry (continued)			
154) $CH_3\overset{O\cdot}{C}HCH_3 + O_2 \rightarrow HO_2\cdot + CH_3C(O)CH_3$	4.4×10^{1}	-	
155) $CH_3CH_2CH_2O\cdot + O_2 \rightarrow HO_2\cdot + CH_3CH_2CHO$	1.0×10^{2}	6.9×10^{2}	
n-Butane chemistry (17):			
156) $CH_3CH_2CH_2CH_3 + O(^3P) \xrightarrow{O_2} OH + 0.88\ CH_3CH_2\overset{OO\cdot}{C}HCH_3 + 0.12\ CH_3CH_2CH_2CH_2O_2\cdot$	3.3×10^{1}	2.099×10^{3}	
157) $CH_3CH_2CH_2CH_3 + OH \xrightarrow{O_2} H_2O + 0.86\ CH_3CH_2\overset{OO\cdot}{C}HCH_3 + 0.14\ CH_3CH_2CH_2CH_2O_2\cdot$	3.8×10^{3}	5.59×10^{2}	
158) $CH_3CH_2CH_2CH_2O_2\cdot + NO \rightarrow CH_3CH_2CH_2CH_2O\cdot + NO_2$	1.0×10^{4}	-	
159) $CH_3CH_2CH_2CH_2O_2\cdot + NO \rightarrow CH_3CH_2CH_2CH_2ONO_2$	8.0×10^{2}	8.0×10^{2}	
160) $CH_3CH_2CH_2CH_2O\cdot + O_2 \rightarrow HO_2\cdot + CH_3CH_2CH_2CHO$	1.0×10^{1}	6.90×10^{2}	
161) $CH_3CH_2CH_2CH_2O\cdot \xrightarrow{O_2} \cdot OOCH_2CH_2CH_2CH_2OH$	7.2×10^{6}	4.200×10^{3}	
162) $\cdot OOCH_2CH_2CH_2CH_2OH + NO \rightarrow NO_2 + \cdot OCH_2CH_2CH_2CH_2OH$	1.0×10^{4}	-	
163) $\cdot OOCH_2CH_2CH_2CH_2OH + NO \rightarrow O_2NOCH_2CH_2CH_2CH_2OH$	8.0×10^{2}	-	
164) $\cdot OCH_2CH_2CH_2CH_2OH \rightarrow HOCH_2CH_2CH_2\dot{C}HOH$	3.6×10^{7}	-	
165) $HOCH_2CH_2CH_2\dot{C}HOH + O_2 \rightarrow HO_2\cdot + OHCH_2CH_2CH_2CHO$	1.0×10^{1}	6.90×10^{2}	10
166) $CH_3CH_2\overset{OO\cdot}{C}HCH_3 + NO \rightarrow NO_2 + CH_3CH_2\overset{O\cdot}{C}HCH_3$	1.0×10^{4}	-	

Table A.1 (continued)

Reaction[1,2]	Rate Constant[3]	Activation Energy(K)	Note
n-Butane chemistry (continued)			
167) $CH_3CH_2\overset{OO\cdot}{C}HCH_3 + NO \rightarrow CH_3CH_2\overset{ONO_2}{C}HCH_3$	8.0×10^{2}	-	
168) $CH_3CH_2\overset{O\cdot}{C}HCH_3 + O_2 \rightarrow CH_3CH_2C(O)CH_3 + HO_2\cdot$	4.4×10^{1}	-	
169) $CH_3CH_2\overset{O\cdot}{C}HCH_3 \xrightarrow{O_2} C_2H_5O_2\cdot + CH_3CHO$	4.0×10^{6}	7.0×10^{3}	
170) $C_2H_5O_2\cdot + NO \rightarrow C_2H_5O\cdot + NO_2$	1.1×10^{4}	-	
171) $C_2H_5O\cdot + NO_2 \rightarrow C_2H_5ONO_2$	2.2×10^{4}	-	
172) $C_2H_5O\cdot + NO \rightarrow C_2H_5ONO$	4.4×10^{4}	-	
173) $C_2H_5O\cdot + O_2 \rightarrow CH_3CHO + HO_2\cdot$	1.0×10^{1}	6.90×10^{2}	
2,3-dimethyl butane chemistry (17):			
174) $(CH_3)_2CHCH(CH_3)_2 + O(^3P) \rightarrow (CH_3)_2CHC(O_2\cdot)(CH_3)_2 + OH$	3.1×10^{2}	1.250×10^{3}	
175) $(CH_3)_2CHCH(CH_3)_2 + OH \rightarrow 0.14(CH_3)_2CHCH(CH_3)CH_2O_2\cdot + 0.86\ (CH_3)_2CHC(O_2\cdot)(CH_3)_2$	9.3×10^{3}	-	
176) $(CH_3)_2CHCH(CH_3)CH_2O_2\cdot + NO \rightarrow 0.9\ NO_2 + 0.9\ (CH_3)_2CHCH(CH_3)CH_2O\cdot + 0.1\ (CH_3)_2CHCH(CH_3)CH_2ONO_2$	1.0×10^{4}	-	
177) $(CH_3)_2CHCH(CH_3)CH_2O\cdot + O_2 \rightarrow HO_2\cdot + (CH_3)_2CHCH(CH_3)CHO$	1.0×10^{1}	6.90×10^{2}	
178) $(CH_3)_2CHCH(CH_3)CH_2O\cdot \xrightarrow{O_2} \cdot OOCH_2\overset{CH_3}{C}H\overset{CH_3}{C}HCH_2OH$	1.4×10^{7}	4.20×10^{3}	

Table A.1 (continued)

Reaction[1,2]	Rate Constant[3]	Activation Energy(K)	Note
2,3-dimethyl butane chemistry (continued)			
179) $\cdot OOCH_2\overset{CH_3}{\overset{\vert}{C}}H\overset{CH_3}{\overset{\vert}{C}}HCH_2OH + NO \rightarrow 0.9\ NO_2 + 0.9\ \cdot OCH_2\overset{CH_3}{\overset{\vert}{C}}H\overset{CH_3}{\overset{\vert}{C}}HCH_2OH$ $+ 0.1\ O_2NOCH_2\underset{CH_3}{\underset{\vert}{C}}H\underset{CH_3}{\underset{\vert}{C}}HCH_2OH$	1.0×10^4	-	
180) $\cdot OCH_2\overset{CH_3}{\overset{\vert}{C}}H\overset{CH_3}{\overset{\vert}{C}}HCH_2OH \xrightarrow{O_2} 0.8\ HOCH_2\overset{CH_3}{\overset{\vert}{C}}H\overset{CH_3}{\overset{\vert}{C}}H\cdot OH$ $+ 0.2\ HOCH_2\underset{CH_3}{\underset{\vert}{C}}H\underset{CH_3CH_2OO\cdot}{\underset{\vert}{C}}HCH_2OH$	1.4×10^7	4.200×10^3	
181) $HOCH_2\overset{CH_3}{\overset{\vert}{C}}H\overset{CH_3}{\overset{\vert}{C}}H\cdot OH + O_2 \rightarrow HO_2\cdot + HOCH_2\overset{CH_3}{\overset{\vert}{C}}H\overset{CH_3}{\overset{\vert}{C}}HCHO$	1.0×10^1	6.90×10^2	
182) $HOCH_2\overset{CH_3CH_2OO\cdot}{\overset{\vert}{C}}HCHCH_2OH + NO \rightarrow 0.9\ NO_2 + 0.9\ HOCH_2\overset{CH_3CH_2O\cdot}{\overset{\vert}{C}}HCHCH_2OH$ $+ 0.1\ HOCH_2\overset{CH_3CH_2ONO_2}{\overset{\vert}{C}}HCHCH_2OH$	1.0×10^4	-	
183) $HOCH_2\overset{CH_3CH_2O\cdot}{\overset{\vert}{C}}HCHCH_2OH \xrightarrow{O_2} 0.8\ HO\dot{C}H\overset{CH_3CH_2OH}{\overset{\vert}{C}}HCHCH_2OH$ $+ 0.2\ HOCH_2\underset{\cdot OOH_2C}{\underset{\vert}{C}}H\underset{CH_2OH}{\underset{\vert}{C}}HCH_2OH$	1.4×10^7	4.200×10^3	
184) $HO\dot{C}H\overset{CH_3CH_2OH}{\overset{\vert}{C}}HCH_2OH + O_2 \rightarrow HO_2\cdot + OHC\overset{CH_3CH_2OH}{\overset{\vert}{C}}HCH_2OH$	1.0×10^1	6.90×10^2	
185) $HOCH_2\underset{\cdot OOH_2C}{\underset{\vert}{C}}H\underset{CH_2OH}{\underset{\vert}{C}}HCH_2OH + NO \xrightarrow{O_2} 0.9\ NO_2 + 0.9\ HO_2\cdot$ $+ 0.9\ (HOCH_2)_2CH\underset{CH_2OH}{\underset{\vert}{C}}HCHO$ $+ 0.1\ HOCH_2\underset{O_2NOH_2C}{\underset{\vert}{C}}H\underset{CH_2OH}{\underset{\vert}{C}}HCH_2OH$	1.0×10^4	-	

Table A.1 (continued)

Reaction [1,2]	Rate Constant[3]	Activation Energy	Note
2,3-dimethyl butane chemistry (continued)			
186) $(CH_3)_2CHC(O_2\cdot)(CH_3)_2 + NO \rightarrow 0.9\ NO_2 + 0.9\ (CH_3)_2CHC(O\cdot)(CH_3)_2 + 0.1\ (CH_3)_2CHC(ONO_2)(CH_3)_2$	1.0×10^{4}	-	
187) $(CH_3)_2CHC(O\cdot)(CH_3)_2 \xrightarrow{O_2} CH_3C(O)CH_3 + CH_3CH(O_2\cdot)CH_3$	3.0×10^{7}	6.440×10^{3}	
188) $CH_3CH(O_2\cdot)CH_3 + NO \rightarrow CH_3CH(ONO_2)CH_3$	4.0×10^{2}	-	
189) $CH_3CH(O_2\cdot)CH_3 + NO \rightarrow NO_2 + CH_3CH(O\cdot)CH_3$	1.0×10^{4}	-	
190) $CH_3CH(O\cdot)CH_3 + O_2 \rightarrow CH_3C(O)CH_3 + HO_2\cdot$	4.4×10^{1}	-	
Propionaldehyde chemistry (17):			
191) $C_2H_5CHO + OH \xrightarrow{O_2} H_2O + C_2H_5CO_3\cdot$	2.8×10^{4}	-2.5×10^{2}	
192) $C_2H_5CHO + NO_3 \xrightarrow{O_2} HNO_3 + C_2H_5CO_3\cdot$	2.2×10^{0}	-	
193) $C_2H_5CHO + h\nu \xrightarrow{O_2} C_2H_5O_2\cdot + HO_2\cdot + CO$	$8.4\times10^{-4}k_{NO_2}$	-	11
194) $C_2H_5CO_3\cdot + NO_2 \rightarrow C_2H_5CO_3NO_2$	6.9×10^{3}	-	
195) $C_2H_5CO_3\cdot + NO \xrightarrow{O_2} C_2H_5O_2\cdot + NO_2 + CO$	1.1×10^{4}	-	
196) $C_2H_5CO_3NO_2 \rightarrow C_2H_5CO_3\cdot + NO_2$	2.2×10^{-2}	1.354×10^{4}	
Butyraldehyde chemistry (17):			
197) $C_3H_7CHO + OH \xrightarrow{O_2} H_2O + C_3H_7CO_3\cdot$	3.7×10^{4}	-	
198) $C_3H_7CHO + NO_3 \xrightarrow{O_2} HNO_3 + C_3H_7CO_3\cdot$	2.2×10^{0}	-	

Table A.1 (continued)

Reaction[1,2]	Rate Constant[3]	Activation Energy	Note
Butyraldehyde chemistry (continued)			
199) $C_3H_7CHO + h\nu \xrightarrow{O_2} C_3H_7O_2\cdot + HO_2\cdot + CO$	$8.4\times10^{-4}k_{NO_2}$	-	11
200) $C_3H_7CO_3\cdot + NO_2 \rightarrow C_3H_7CO_3NO_2$	6.9×10^{3}	-	
201) $C_3H_7CO_3\cdot + NO \xrightarrow{O_2} NO_2 + CO_2 + C_3H_7O_2\cdot$	1.1×10^{4}	-	
202) $C_3H_7CO_3NO_2 \rightarrow C_3H_7CO_3\cdot + NO_2$	2.2×10^{-2}	1.354×10^{4}	
203) $C_3H_7O_2\cdot + NO \rightarrow NO_2 + C_3H_7O\cdot$	1.1×10^{4}	-	
204) $C_3H_7O\cdot + NO \rightarrow C_3H_7ONO$	4.4×10^{4}	-	
205) $C_3H_7O\cdot + NO_2 \rightarrow C_3H_7ONO_2$	2.2×10^{4}	-	
206) $C_3H_7O\cdot + O_2 \rightarrow HO_2\cdot + C_2H_5CHO$	1.0×10^{1}	6.90×10^{2}	
Acetone chemistry (17):			
207) $CH_3C(O)CH_3 + OH \xrightarrow{O_2} H_2O + CH_3C(O)CH_2O_2\cdot$	4.1×10^{2}	1.230×10^{3}	
208) $CH_3C(O)CH_3 + h\nu \xrightarrow{O_2} CH_3CO_3\cdot + CH_3O_2\cdot$	$1.7\times10^{-4}k_{NO_2}$		12
209) $CH_3C(O)CH_2O_2\cdot + NO \rightarrow CH_3C(O)CH_2O\cdot + NO_2$	1.0×10^{4}	-	
210) $CH_3C(O)CH_2O_2\cdot + NO \rightarrow CH_3C(O)CH_2ONO_2$	4.0×10^{2}	-	
211) $CH_3C(O)CH_2O\cdot + O_2 \rightarrow HO_2\cdot + CH_3C(O)CHO$	1.0×10^{1}	6.9×10^{2}	

Table A.1 (continued)

Reaction[1,2]	Rate Constant[3]	Activation Energy	Note
MEK chemistry (17):			
212) $C_2H_5C(O)CH_3 + OH \xrightarrow{O_2} H_2O + CH_3\overset{OO\cdot}{C}HC(O)CH_3$	8.1×10^{2}	-	
213) $C_2H_5C(O)CH_3 + h\nu \xrightarrow{O_2} CH_3CO_3\cdot + C_2H_5O_2\cdot$	$1.7\times10^{-3}k_{NO_2}$	-	12
214) $C_2H_5C(O)CH_3 + OH \rightarrow H_2O + C_2H_5C(O)CH_2\cdot$	4.9×10^{2}	-	13
215) $CH_3\overset{OO\cdot}{C}HC(O)CH_3 + NO \rightarrow NO_2 + CH_3\overset{O\cdot}{C}HCOCH_3$	1.0×10^{4}	-	
216) $CH_3\overset{OO\cdot}{C}HC(O)CH_3 + NO \rightarrow CH_3\overset{ONO_2}{C}HC(O)CH_3$	8.0×10^{2}	-	
217) $CH_3\overset{O\cdot}{C}HC(O)CH_3 \xrightarrow{O_2} CH_3CHO + CH_3CO_3\cdot$	7.8×10^{6}	6.440×10^{3}	

[1]Only one isomer is shown, even when several are possible

[2]Reaction formulated from Atkinson and Lloyd (2) unless otherwise noted.

[3]298K, ppm-min units

Notes:

(1) Rate constant is specific for SAPRC smog chamber experiments.

(2) Photolysis rates calculated by averaging over zenith angles between 30° and 60° using the results of Demerjian et al. (24)

(3) Reaction taken from Atkinson et al. (2)

(4) Photolysis rates calculated by averaging over zenith angles between 30° and 60° using the results of Demerjian et al. (24), followed by correction based on the results of Horowitz and Calvert (26).

(5) Rate constant from Grosjean (25).

(6) Abstraction pathway neglected.

Table A.1 (continued)

Notes: (continued)

(7) 50/50 split of the two γ-dicarbonyls is assumed.

(8) 12 percent nitrate formation is assumed.

(9) Reactions of glycolaldehyde are ignored.

(10) Hydroxy substituted aldehydes are assumed to react the same as un-substituted aldehydes.

(11) Photolysis rate assumed to be the same as acetaldehyde.

(12) Photolysis rate from Atkinson et al. (2).

(13) Reactions of the $C_2H_5C(O)CH_2\cdot$ species are neglected.

Table A.2. Initial Conditions and Physical Parameters for the SAPRC Smog Chamber Experiments[1,2]

	Concentration (ppb)									
Experiment	EC-231	EC-232	EC-233	EC-237	EC-238	EC-241	EC-242	EC-243	EC-245	EC-246
NO	440	469	96	377	718	379	377	366	743	386
NO_2	52	24	7	106	234	110	125	115	259	122
ethene	1,051	258	260	875	982	484	2,014	1,939	2,055	253
propene	108	51	51	100	93	45	109	109	104	49
n-butane	1,130	1,102	1,085	1,025	966	464	558	568	534	1,058
trans-2-butene	55	26	25	50	47	24	108	110	102	26
2,3-dimethylbutane	715	612	648	463	420	211	203	84	185	538
toluene	121	32	34	86	83	40	306	155	321	23
m-xylene	108	29	33	91	84	44	306	154	317	23
CO	1,630	1,742	1,299	956	677	1,296	1,021	608	2,510	-
HCHO	20	9	4	1	26	18	28	-	16	-
acetone	1	1	1	3	4	2	4	2	-	2
H_2O (ppm)	$1.621.10^4$	$1.871x10^4$	$2,138x10^4$	$2.348x10^4$	$2.547x10^4$	$2.076x10^4$	$2.4755x10^4$	$1.710x10^4$	$9.217x10^5$	$2.225x10^4$
Temp (K)	302.8	302.5	302.7	303.1	303.6	303.3	303.1	301.8	302.6	303.3
Dilution Rate (min^{-1})	$6.9x10^{-4}$	$3.9x10^{-4}$	$3.9x10^{-4}$	$2.9x10^{-4}$	$2.8x10^{-4}$	$2.9x10^{-4}$	$3.0x10^{-4}$	$2.8x10^{-4}$	$2.9x10^{-4}$	$2.8x10^{-4}$

[1] $k_1 = 0.30\ min^{-1}$ for each experiment

[2] Detailed data tabulations for these experiments can be found in Pitts et al. (23)

Table A.3. SUR1 Reaction Mechanism

	Reaction[1,2]	Rate Constant[3]	Activation Energy (K)	Note
A) Inorganic Reactions:				
1)	$NO_2 + h\nu \rightarrow NO + O_3$	3.0×10^{-1}	-	1
2)	$O_3 + NO \rightarrow NO_2 + O_2$	2.7×10^{1}	1.5×10^{3}	2
3)	$O_3 + NO_2 \rightarrow NO_3 + O_2$	4.7×10^{-2}	2.45×10^{3}	2
4)	$NO_3 + NO \rightarrow 2NO_2$	3.0×10^{4}	-	2
5)	$HO_2 + NO_2 \rightarrow HO_2NO_2$	1.6×10^{3}	-	2
6)	$NO_2 + OH \rightarrow HNO_3$	1.6×10^{4}	-	2
7)	$O_3 + OH \rightarrow HO_2 + O_2$	9.9×10^{1}	9.7×10^{2}	2
8)	$O_3 + HO_2 \rightarrow OH + 2O_2$	3.0×10^{0}	5.8×10^{2}	2
9)	$HO_2NO_2 \rightarrow HO_2 + NO_2$	5.1×10^{0}	1.042×10^{4}	2
10)	$HO_2 + NO \rightarrow NO_2 + OH$	1.2×10^{4}	-2.4×10^{2}	2
11)	$HO_2 + HO_2 \rightarrow H_2O + O_2$	3.9×10^{3}	-1.2×10^{3}	2
12)	$HO_2 + HO_2 + H_2O \rightarrow H_2O_2 + O_2 + H_2O$	2.2×10^{-1}	-5.8×10^{3}	2
13)	$O_3 + H_2O + h\nu \rightarrow 2OH$	$2.8 \times 10^{-3}\ K_{NO_2}$	-	3
14)	$NO + OH \rightarrow HONO$	9.7×10^{3}	-	2
15)	$HONO + h\nu \rightarrow NO + OH$	$1.8 \times 10^{-1}\ k_{NO_2}$	-	4
16)	$NO_3 + NO_2 \rightarrow N_2O_5$	1.6×10^{3}	-	2
17)	$N_2O_5 \quad NO_2 + NO_3$	3.1×10^{0}	1.108×10^{4}	2
18)	$N_2O_5 + H_2O \rightarrow 2HNO_3$	4.4×10^{-6}	-	5
19)	$H_2O_2 + OH \rightarrow HO_2 + H_2O$	2.5×10^{3}	-	2
20)	$H_2O_2 + h\nu \rightarrow 2OH$	$8.4 \times 10^{-4}\ k_{NO_2}$	-	4
21)	$CO + OH \xrightarrow{O_2} HO_2 + CO_2$	4.0×10^{2}	-	2
22)	$NO_3 + h\nu \rightarrow 0.3NO + 0.7NO_2 + 0.70\ O_3$	$1.55 \times 10^{1}\ k_{NO_2}$	-	6

Table A.3 SUR1 Reaction Mechanism (continued)

	Reaction[1,2]	Rate Constant[3]	Activation Energy (K)	Note
B) Alkene Reactions:				
23)	$CH_2{=}CH_2 + OH \rightarrow NO_2\text{-}NO + 2HCHO + HO_2\cdot$	1.2×10^{4}	-3.8×10^{2}	7
24)	$CH_2{=}CH_2 + O_3 \rightarrow HCHO + 0.42CO + 0.12HO_2\cdot + 0.4\dot{C}H_2O\dot{O} + 0.18CO_2 + 0.12H_2 + 0.42H_2O$	2.5×10^{-3}	2.56×10^{3}	2
25)	$CH_3CHCH_2 + OH \rightarrow 0.95(NO_2\cdot + HO_2\cdot + HCHO + CH_3CHO) - NO$	3.7×10^{4}	-5.37×10^{2}	8
26)	$CH_3CHCH_2 + O_3 \rightarrow 0.5CH_3CHO + 0.2CH_3\dot{C}HO\dot{O} + 0.33CO + 0.20HO_2\cdot + 0.10H + 0.2CH_3O_2\cdot + 0.03CH_3O\cdot + 0.2\dot{C}H_2O\dot{O} + 0.06CH_4 + 0.27CO_2 + 0.06H_2 + 0.21H_2O$	1.6×10^{-2}	1.897×10^{3}	2
27)	$CH_3CH{=}CHCH_3 + OH \rightarrow 0.9NO_2 + 0.9HO_2\cdot + 1.8CH_3CHO - NO + 0.1$ Nitrate	1.0×10^{5}	-5.42×10^{2}	9
28)	$CH_3CH{=}CHCH_3 + O_3 \rightarrow CH_3CHO + 0.4CH_3\dot{C}HO\dot{O} + 0.24CO + 0.29HO_2\cdot + 0.19OH + 0.05CH_3O\cdot + 0.43CH_3O_2\cdot + 0.12CH_4 + 0.36CO_2$	2.7×10^{-1}	1.051×10^{3}	2
29)	$\dot{C}H_2O\dot{O} + NO \rightarrow NO_2 + HCHO$	1.0×10^{4}	-	2
30)	$\dot{C}H_2O\dot{O} + NO_2 \rightarrow NO_3 + HCHO$	1.0×10^{3}	-	2

Table A.3. SUR1 Reaction Mechanism (continued)

	Reaction[1,2]	Rate Constant[3]	Activation Energy (K)	Note
31)	$\dot{C}H_2O\dot{O} + H_2O \rightarrow HCOOH + H_2O$	6.0×10^{-3}	-	2
32)	$CH_3\dot{C}HO\dot{O} + NO \rightarrow NO_2 + CH_3CHO$	1.0×10^{4}	-	2
33)	$CH_3\dot{C}HO\dot{O} + NO_2 \rightarrow NO_3 + CH_3CHO$	1.0×10^{3}	-	2
34)	$CH_3\dot{C}H\dot{O}\dot{O} + H_2O \rightarrow CH_3COOH + H_2O$	6.0×10^{-3}	-	2
C) Aromatic Reactions:				
35)	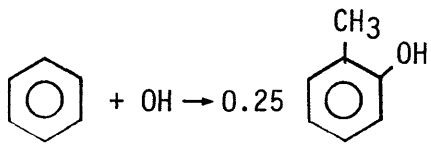 + 0.75 CH(O)CH=CHCHO + 0.75 $(CHO)_2$	1.8×10^{3}	-	10
36)	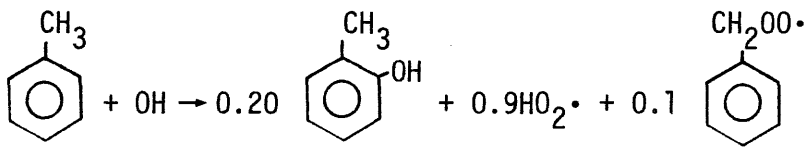 + 0.7NO_2 + 0.7$CH_3C(O)CHO$ + 0.7 CH(O)CH=CHCHO - 0.7NO	9.1×10^{3}	-	10
37)	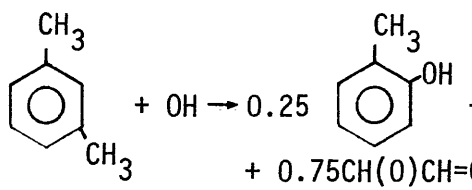 + 0.75CH(O)CH=CHCHO + 0.68$CH_3C(O)CHO$ + 0.07$(CHO)_2$	2.65×10^{4}	-	10

Table A.3 SUR1 Reaction Mechanism (continued)

	Reaction[1,2]	Rate Constant[3]	Activation Energy (K)	Note
38)	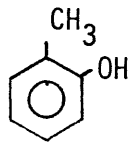 + OH → NO_2 - NO + HO_2· + CH(O)CH=CHCHO + $CH_3C(O)COOH$	8.0×10^4	-	11
39)	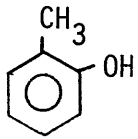 + NO_3 → 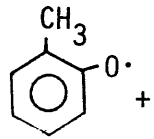 + HNO_3	1.5×10^4	-	2
40)	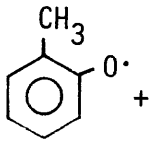 + NO_2 → Product	2.2×10^4	-	2
41)	CH(O)CH=CHCHO + OH → CH(O)CH=CHC(O)O_2· + H_2O	4.4×10^4	-	12
42)	CH(O)CH=CHC(O)O_2· + NO_2 → CH(O)CH=CHC(O)O_2NO_2	6.9×10^3	-	12
43)	CH(O)CH=CHC(O)O_2NO_2 → CH(O)CH=CHC(O)O_2· + NO_2	2.2×10^{-2}	1.354×10^4	12
44)	CH(O)CH=CHC(O)O_2· + NO → $3NO_2$ - 2NO + α(HO_2· + $(CHO)_2$+CO)+(1-α)(CH_3CO_3· + $CH_3C(O)CHO$)	1.1×10^4	-	12

Table A.3 SUR1 Reaction Mechanism (continued)

	Reaction[1,2]	Rate Constant[3]	Activation Energy (K)	Note
45)	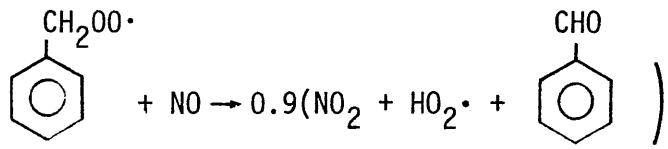	1.1×10^{4}	-	13
46)	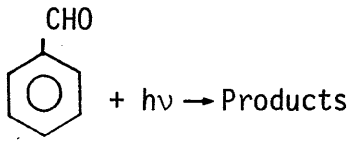	$5.3 \times 10^{-3} k_1$	-	14
47)	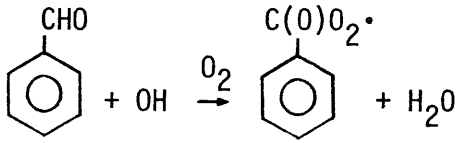	1.9×10^{4}	-	2
48)	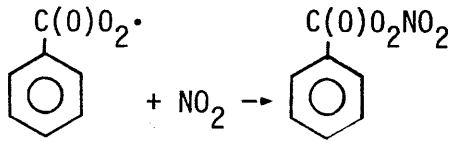	6.9×10^{3}	-	2
49)	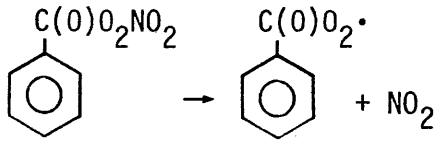	9.6×10^{-3}	1.304×10^{4}	2

Table A.3 SUR1 Reaction Mechanism (continued)

	Reaction[1,2]	Rate Constant[3]	Activation Energy (K)	Note
50)	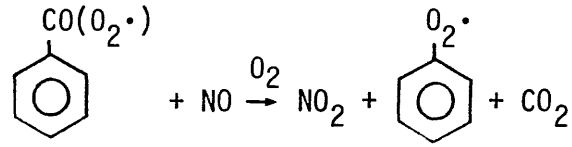	1.0×10^{4}	-	2
51)	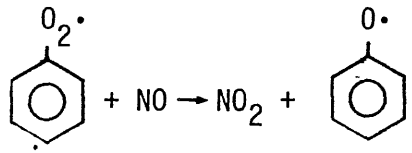	9.0×10^{3}	-	2
52)	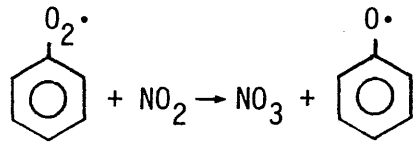	1.0×10^{4}	-	2
53)	$CH_3C(O)COOH + h\nu \rightarrow CH_3CHO + CO_2$	$3.6\times10^{-2}k_{NO_2}$	-	15
54)	$CH_3C(O)CHO + OH \xrightarrow{O_2} CH_3C(O)O_2\cdot + CO + H_2O$	2.5×10^{4}	-	2
55)	$CH_3C(O)CH) + h\nu \xrightarrow{2O_2} CH_3C(O)O_2\cdot + HO_2\cdot + CO$	$1.3\times10^{-2}k_{NO_2}$	-	2
56)	$CH_3C(O)CHO + h\nu \xrightarrow{2O_2} CH_3O_2\cdot + HO_2\cdot + 2CO$	$6.0\times10^{-3}k_{NO_2}$	-	2

Table A.3 SUR1 Reaction Mechanism (continued)

Reaction[1,2]	Rate Constant[3]	Activation Energy (K)	Note
57) $(CHO)_2 + OH \xrightarrow{O_2} HO_2\cdot + 2CO + H_2O$	1.7×10^{4}	-	2
58) $(CHO)_2 + h\nu \rightarrow 0.13HCHO + 0.87H_2 + 1.87CO$	$8.0\times10^{-3}k_{NO_2}$	-	2
D) Alkane Reactions:			
59) $CH_3CH_2CH_3 + OH \xrightarrow{O_2} CH_3CH(O_2\cdot)CH_3 + H_2O$	2.3×10^{3}	6.8×10^{2}	2
60) $CH_3CH(O_2\cdot)CH_3 + NO \rightarrow NO_2 + HO_2\cdot + 0.15CH_3CH_2CHO + 0.85CH_3C(O)CH_3$		1.0×10^{4}	16
61) $ALK + OH \xrightarrow{O_2} RO_2\cdot + H_2O$	5.8×10^{3}	4.0×10^{2}	17
62) $RO_2\cdot + NO \rightarrow 1.7NO_2 - 0.8NO + 0.9HO_2\cdot + 0.15HCHO + 0.3CH_3CHO + 0.10CH_3CH_2CHO + 0.30CH_3C(O)CH_3 + 0.45C_2H_5C(O)CH_3$	1.0×10^{4}	-	17
E) Carbonyl Reactions:			
63) $HCHO + h\nu \rightarrow H_2 + CO$	$3.3\times10^{-3}k_{NO_2}$	-	18
64) $HCHO + h\nu \xrightarrow{2O_2} 2HO_2\cdot + CO$	$2.35\times10^{-3}k_{NO_2}$	-	18
65) $HCHO + OH \xrightarrow{O_2} HO_2\cdot + CO + H_2O$	1.6×10^{4}	-	2
66) $CH_3CHO + h\nu \xrightarrow{2O_2} CH_3O_2\cdot + HO_2\cdot + CO$	$2.58\times10^{-4}k_{NO_2}$	-	18
67) $CH_3CHO + OH \xrightarrow{O_2} CH_3C(O)O_2\cdot + H_2O$	2.4×10^{4}	-2.6×10^{2}	2

Table A.3 SUR1 Reaction Mechanism (continued)

	Reaction[1,2]	Rate Constant[3]	Activation Energy (K)	Note
68)	$CH_3O_2\cdot + NO \rightarrow NO_2 + CH_3O\cdot$	1.1×10^{4}	-	2
69)	$CH_3O\cdot + O_2 \rightarrow HCHO + HO_2\cdot$	2.1×10^{0}	1.35×10^{3}	2
70)	$CH_3O\cdot + NO_2 \rightarrow CH_3ONO_2$	2.2×10^{4}	-	2
71)	$CH_3C(O)O_2\cdot + NO \xrightarrow{2O_2} NO_2 + CH_3O_2\cdot + CO_2$	1.1×10^{4}	-	2
72)	$CH_3C(O)O_2\cdot + NO_2 \rightarrow PAN$	6.9×10^{3}	-	2
73)	$PAN \rightarrow CH_3C(O)O_2\cdot + NO_2$	2.2×10^{-2}	1.354×10^{4}	2
74)	$C_2H_5CHO + OH \xrightarrow{O_2} H_2O + C_2H_5CO_3\cdot$	2.8×10^{4}	-2.5×10^{2}	2
75)	$C_2H_5CHO + h\nu \xrightarrow{O_2} C_2H_5O_2\cdot + HO_2\cdot + CO$	$2.6\times10^{-4}k_{NO_2}$	-	19
76)	$C_2H_5CO_3\cdot + NO_2 \rightarrow C_2H_5CO_3NO_2$	6.9×10^{3}	-	2
77)	$C_2H_5CO_3\cdot + NO \xrightarrow{O_2} C_2H_5O_2\cdot + NO_2 + CO$	1.1×10^{4}	-	2
78)	$C_2H_5CO_3NO_2 \rightarrow C_2H_5CO_3\cdot + NO_2$	2.2×10^{-2}	1.354×10^{4}	2
79)	$C_2H_5O_2\cdot + NO \rightarrow NO_2 + HO_2\cdot + CH_3CHO$	1.1×10^{4}	-	20
80)	$CH_3C(O)CH_3 + h\nu \xrightarrow{O_2} CH_3CO_3\cdot + CH_3O_2\cdot$	$1.7\times10^{-4}k_{NO_2}$	-	21
81)	$C_2H_5C(O)CH_3 + h\nu \xrightarrow{O_2} CH_3CO_3\cdot + C_2H_5O_2\cdot$	$1.7\times10^{-3}k_{NO_2}$	-	21
82)	$C_2H_5C(O)CH_3 + OH \rightarrow CH_3\overset{OO\cdot}{C}HC(O)CH_3 + H_2O$	1.3×10^{3}	-	22
83)	$CH_3\overset{OO\cdot}{C}HC(O)CH_3 + NO \rightarrow 0.9NO_2 + 0.9CH_3CHO + 0.9CH_3CO_3\cdot$	1.1×10^{4}	-	23

[1]One isomer is shown, even when several are possible

[2]CH_3CHCH_2 represents all terminal alkenes, $CH_3CH{=}CHCH_3$ represents all internal alkenes, toluene represents all mono-alkylbenzenes, xylene represents all di-

Table A.3 SUR1 Reaction Mechanism (continued)

and tri-alkylbenzenes, o-cresol represents phenol, o-cresol, and dimethylphenols, CH(O)CH=CHCHO represents all γ-dicarbonyls, C_4H_{10} represents all $\geq C_4$ alkanes, C_2H_5CHO represents all $\geq C_3$ aldehydes.

[3]Rate constants are for 298K, in ppm-min units.

Notes:

(1) For experiments EC-231 to EC-246, k_1 was measured at 0.30 min^{-1}.

(2) Reaction taken directly from the explicit mechanism.

(3) This reaction is formulated by combining reactions 16-18 of the explicit mechanism as suggested by Atkinson et al. (2).

(4) Rate constant obtained by averaging over zenith angles between 30° and 60° using the results of Demerjian et al. (24).

(5) Rate constant is specific for the evacuable chamber at SAPRC (19).

(6) Rate constant from Atkinson et al. (2).

(7) Represents reactions 125-129 of the explicit mechanism.

(8) Represents reactions 131-138 of the explicit mechanism. Five percent nitrate formation is assumed.

(9) Represents reactions 140-143 of the explicit mechanism. Ten percent nitrate formation is assumed.

(10) Ortho cresol is used to represent both phenol and the dimethylphenols and cis-2-butene-1,4-dial represents all γ-dicarbonyls. Ten percent of the initial toluene-OH reaction is assumed to proceed via OH abstraction. The abstraction pathway is neglected for both benzene and xylene. The rate constant and products shown for the xylene + OH reaction are for a lumped average xylene (2). If only m-xylene is present (as in experiments EC-231 to EC-246) the reaction should read

$$\text{m-xylene} + OH \rightarrow 0.25\ \text{o-cresol} + HO_2\cdot + 0.75NO_2 + 0.75\ CH(O)CH{=}CHCHO + 0.75CH_3C(O)CHO$$

with $k_{37} = 3.4\times10^4\ ppm^{-1}\ min^{-1}$

(11) Rate constant for reaction 38 is an average OH rate constant for o-cresol and dimenthylphenol.

(12) Reactions 41-44 are taken from Atkinson et al. (2) and represent reactions 82 through 90 of the explicit mechanism

$$\alpha = \frac{k_{35}[\text{benzene}]_o + k_{36}[\text{toluene}]_o + 0.5k_{37}[\text{xylene}]_o}{k_{35}[\text{benzene}]_o + k_{36}[\text{toluene}]_o + k_{37}[\text{xylene}]_o}$$

Table A.3 SUR1 Reaction Mechanism (continued)

Notes: (continued)

(12) See Atkinson et al. (2) for a discussion of these reactions.

(13) Represents reactions 49 through 51 of the explicit mechanism.

(14) Rate constant from Leone and Seinfeld (15).

(15) Based on measurements in sunlight by Grosjean (25).

(16) Represents reactions 152 through 155 of the explicit mechanism.

(17) ALK represents all $\geq C_4$ alkanes. See Atkinson et al. (2) for a discussion of these reactions. For explicit n-butane use (2):

$k_{61} = 4.1 \times 10^3\ ppm^{-1}\ min^{-1}$ $A_{61} = 560K$

$$RO_2\cdot + NO \xrightarrow{62} 1.3NO_2 - 0.4NO + 0.9HO_2\cdot + 0.6CH_3CHO + 0.1\ C_2H_5CHO + 0.5\ C_2H_5C(O)CH_3$$

(18) Photolysis rates calculated by averaging over zenith angles between 30° and 60° using the results of Demerjian et al. (24) followed by corrections based on the results of Horowitz and Calvert (26).

(19) Photolysis rate assumed to be similar to that of acetaldehyde.

(20) Represents reactions 170 and 173 of the explicit mechanism (reactions 171 and 172 are neglected).

(21) Photolysis rates from Atkinson et al. (2).

(22) Represents reactions 212 and 214 of the explicit mechanism.

(23) Represents reactions 215 through 217 of the explicit mechanism. Ten percent nitrate formation is assumed.

Table A.4. SUR2 Reaction Mechanism

Reaction[1,2]	Rate Constant[3,4]	Activation Energy (K)	Note
A) Inorganic Reactions:			
1) $NO_2 + h\nu \rightarrow NO + O_3$	*	-	1
2) $O_3 + NO \rightarrow NO_2 + O_2$	2.7×10^{1}	1.5×10^{3}	2
3) $O_3 + NO_2 \rightarrow NO_3 + O_2$	4.7×10^{-2}	2.45×10^{3}	2
4) $NO_3 + NO \rightarrow 2NO_2$	3.0×10^{4}	-	2
5) $HO_2 + NO_2 \rightarrow HO_2NO_2$	1.6×10^{3}	-	2
6) $NO_2 + OH \rightarrow HNO_3$	1.6×10^{4}	-	2
7) $O_3 + OH \rightarrow HO_2 + O_2$	9.9×10^{1}	9.7×10^{2}	2
8) $O_3 + HO_2 \rightarrow OH + 2O_2$	3.0×10^{0}	5.8×10^{2}	2
9) $HO_2NO_2 \rightarrow HO_2 + NO_2$	5.1×10^{0}	1.042×10^{4}	2
10) $HO_2 + NO \rightarrow NO_2 + OH$	1.2×10^{4}	-2.4×10^{2}	2
11) $HO_2 + HO_2 \rightarrow H_2O + O_2$	3.9×10^{3}	-1.2×10^{3}	2
12) $HO_2 + HO_2 + H_2O \rightarrow H_2O_2 + O_2 + H_2O$	2.2×10^{-1}	-5.8×10^{3}	2
13) $O_3 + H_2O + h\nu \rightarrow 2OH$	$2.8 \times 10^{-3}\ K_{NO_2}$		3
14) $NO + OH \rightarrow HONO$	9.7×10^{3}		2
15) $HONO + h\nu \rightarrow NO + OH$	$1.8 \times 10^{-1}\ k_{NO_2}$		4
16) $NO_3 + NO_2 \rightarrow N_2O_5$	1.6×10^{3}	-	2
17) $N_2O_5 \quad NO_2 + NO_3$	3.1×10^{0}	1.108×10^{4}	2
18) $N_2O_5 + H_2O \rightarrow 2HNO_3$	*	-	5
19) $H_2O_2 + OH \rightarrow HO_2 + H_2O$	2.5×10^{3}	-	2
20) $H_2O_2 + h\nu \rightarrow 2OH$	$8.4 \times 10^{-4}\ k_{NO_2}$	-	4
21) $CO + OH \xrightarrow{O_2} HO_2 + CO_2$	4.0×10^{2}	-	2
22) $NO_3 + h\nu \rightarrow 0.3NO + 0.7NO_2 + 0.70(^3P)$	$1.55 \times 10^{2}\ k_{NO_2}$	-	6

Table A.4. SUR2 Reaction Mechanism (continued)

	Reaction[1,2]	Rate Constant[3,4]	Activation Energy (K)	Note
	Alkene Reactions			
23)	$CH_2{=}CH_2 + OH \rightarrow NO_2 - NO + 2HCHO + HO_2\cdot$	1.2×10^{4}	-3.8×10^{2}	7
24)	$CH_2{=}CH_2 + O_3 \rightarrow HCHO + 0.42CO + 0.12HO_2\cdot$	2.5×10^{-3}	2.56×10^{3}	2
	$+ 0.4\dot{C}H_2O\dot{O} + 0.18CO_2$			
	$+ 0.12H_2 + 0.42H_2O$			
25)	$OLE + OH \rightarrow 0.95\gamma HCHO + (1.8-0.85\gamma)CH_3CHO$	*	-5.4×10^{2}	8
	$+ (0.9 + 0.05\gamma)(HO_2\cdot + NO_2) - NO$			
26)	$OLE + O_3 \rightarrow (1-0.5\gamma)CH_3CHO + (0.4-0.2\gamma)CH_3\dot{C}HO\dot{O}$	*	1.9×10^{3}	8,9
	$+ (0.24 + 0.09\gamma)CO + (0.29-0.09\gamma)HO_2\cdot$			
	$+ (0.19-0.09\gamma)OH + (0.43-0.21\gamma)CH_3O_2\cdot$			
	$+ (0.05-0.03\gamma)CH_3O\cdot + 0.2\gamma\dot{C}H_2O\dot{O}$			
27)	$\dot{C}H_2O\dot{O} + NO \rightarrow NO_2 + HCHO$	1.0×10^{4}	-	2
28)	$\dot{C}H_2O\dot{O} + NO_2 \rightarrow NO_3 + HCHO$	1.0×10^{3}	-	2
29)	$\dot{C}H_2O\dot{O} + H_2O \rightarrow HCOOH + H_2O$	6.0×10^{-3}	-	2
30)	$CH_3\dot{C}HO\dot{O} + NO \rightarrow NO_2 + CH_3CHO$	1.0×10^{4}	-	2
31)	$CH_3\dot{C}HO\dot{O} + NO_2 \rightarrow NO_3 + CH_3CHO$	1.0×10^{3}	-	2
32)	$CH_3\dot{C}HO\dot{O} + H_2O \rightarrow CH_3COOH + H_2O$	6.0×10^{-3}	-	2

Table A.4. SUR2 Reaction Mechanism (continued)

Reaction[1,2]	Rate Constant[3,4]	Activation Energy (K)	Note
Aromatic Reactions:			
33) + OH → 0.25 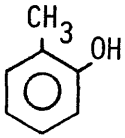 + HO_2• + 0.75CH(O)CH=CHCHO + 0.75$(CHO)_2$	1.8×10^3	-	10
34) ARO + OH → (0.25-0.05β) 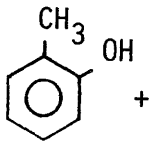 + (1-0.1β)HO_2•	*	-	10,11
(lumped xylene) + (0.75-0.05β)(NO_2 + CH(O)CH=CHCHO - NO) + (0.68 + 0.02β)$CH_3C(O)CHO$ + (0.08 - 0.08β)$(CHO)_2$ + 0.1β 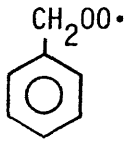			
(m-xylene) → (0.25-0.05β) 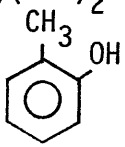 + (1-0.1β)HO_2•	*	-	
+ (0.75-0.05β)(NO_2 + CH(O)CH=CHCHO - NO) + (0.75-0.05β)$CH_3C(O)CHO$ + 0.1β 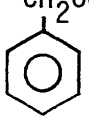			

Table A.4. SUR2 Reaction Mechanism (continued)

	Reaction[1,2]	Rate Constant[3,4]	Activation Energy (K)	Note
35)	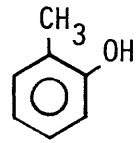 + OH → NO_2 - NO + HO_2· + CH(O)CH=CHCHO + $CH_3C(O)COOH$	8.0×10^4	-	12
36)	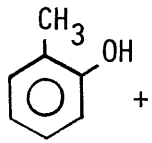 + NO_3 → 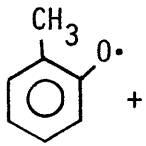 + HNO_3	1.5×10^4	-	2
37)	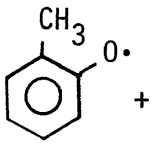 + NO_2 → Product	2.2×10^4	-	2
38)	CH(O)CH=CHCHO + OH → CH(O)CH=CHC(O)O_2· + H_2O	4.4×10^4	-	13
39)	CH(O)CH=CHC(O)O_2· + NO_2 → CH(O)CH=CHC(O)O_2NO_2	6.9×10^3	-	13
40)	CH(O)CH=CHC(O)O_2NO_2 → CH(O)CH=CHC(O)O_2· + NO_2	2.2×10^{-2}	1.354×10^4	13
41)	CH(O)CH=CHC(O)O_2· + NO → $3NO_2$-2NO + α(HO_2· + $(CHO)_2$ + CO) + (1-α)(CH_3CO_3· + $CH_3C(O)CHO$)	1.1×10^4	-	13

Table A.4. SUR2 Reaction Mechanism (continued)

	Reaction[1,2]	Rate Constant[3,4]	Activation Energy (K)	Note
42)	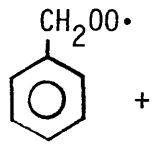 + NO → $0.9NO_2 + 0.9HO_2\cdot$	1.1×10^{4}	-	14
43)	$CH_3C(O)CHO + OH \xrightarrow{O_2} CH_3C(O)O_2\cdot + CO + H_2O$	2.5×10^{4}	-	2
44)	$CH_3C(O)CHO + h\nu \xrightarrow{2O_2} CH_3C(O)O_2\cdot + HO_2\cdot + CO$	$1.3\times10^{-2}k_{NO_2}$	-	2
45)	$CH_3C(O)CHO + h\nu \xrightarrow{2O_2} CH_3O_2\cdot + HO_2\cdot + 2CO$	$6.0\times10^{-3}k_{NO_2}$	-	2
	Alkane Reactions:			
46)	$ALK + OH \xrightarrow{O_2} RO_2\cdot$	5.8×10^{3}	4.0×10^{2}	15
47)	$RO_2\cdot + NO \rightarrow 1.7NO_2 - 0.8NO + 0.9HO_2\cdot + 0.15HCHO + 0.4CH_3CHO$	1.1×10^{4}	-	15

Table A.4. SUR2 Reaction Mechanism (continued)

	Reaction [1,2]	Rate Constant [3,4]	Activation Energy (K)	Note
	Carbonyl Reactions:			
48)	$HCHO + h\nu \rightarrow H_2 + CO$	$3.3\times10^{-3} k_{NO_2}$	-	16
49)	$HCHO + h\nu \xrightarrow{2O_2} 2HO_2\cdot + CO$	$2.35\times10^{-3} k_{NO_2}$	-	16
50)	$HCHO + OH \xrightarrow{O_2} HO_2\cdot + CO + H_2O$	1.6×10^{4}	-	2
51)	$CH_3CHO + h\nu \xrightarrow{2O_2} CH_3O_2\cdot + HO_2\cdot + CO$	$2.58\times10^{-4} k_{NO_2}$	-	16
52)	$CH_3CHO + OH \xrightarrow{O_2} CH_3C(O)O_2\cdot + H_2O$	2.4×10^{4}	-2.6×10^{2}	2
53)	$CH_3O_2\cdot + NO \rightarrow NO_2 + CH_3O\cdot$	1.1×10^{4}	-	2
54)	$CH_3O\cdot + O_2 \rightarrow HCHO + HO_2\cdot$	2.1×10^{0}	1.35×10^{3}	2
55)	$CH_3O\cdot + NO_2 \rightarrow CH_3ONO_2$	2.2×10^{4}	-	2
56)	$CH_3C(O)O_2\cdot + NO \xrightarrow{2O_2} NO_2 + CH_3O_2\cdot + CO_2$	1.1×10^{4}	-	2
57)	$CH_3C(O)O_2\cdot + NO_2 \rightarrow PAN$	6.9×10^{3}		
58)	$PAN \rightarrow CH_3C(O)O_2\cdot + NO_2$	2.2×10^{-2}	1.354×10^{4}	2

[1] One isomer is shown even when several are possible.

Table A.4. SUR2 Reaction Mechanism (Continued)

[2]o-cresol represents phenol, o-cresol, and dimethylphenols, CH(O)CH=CHCHO represents all γ-dicarbonyls, ALK represents all $\geq C_4$ alkanes, CH_3CHO represents all $\geq C_2$ aldehydes.

[3]298K, ppm-min units

[4]For rate constants marked *, see the appropriate note.

Notes:

(1) See Table A.2 for the k_1 values used in simulations of the SAPRC smog chamber experiments.

(2) Reaction taken directly from the explicit mechanism.

(3) This reaction is formulated by combining reactions 16-18 of the explicit mechanism as suggested by Atkinson et al. (2).

(4) Rate constant obtained by averaging over zenith angles between 30° and 60° using the results of Demerjian et al. (24).

(5) $k_{18} = 4.4\times10^{-6}$ ppm^{-1} - min^{-1} for SAPRC evacuable chamber
$k_{18} = 1.5\times10^{-5}$ ppm^{-1} - min^{-1} for UNC chamber.

(6) Rate constant from Atkinson et al. (2).

(7) Represents reactions 125-129 of the explicit mechanism.

(8) Represents reactions 131-138 and 140-143 of the explicit mechanism

$$\gamma = \frac{[\text{propene}]_o}{[\text{propene}]_o + [\text{butene}]_o}$$

where,
$[\text{propene}]_o \equiv$ initial concentration of terminal alkenes
$[\text{butene}]_o \equiv$ initial concentration of internal alkenes

$$k_{25} = 3.7\times10^{4}\gamma + 1.0\times10^{5}(1-\gamma)$$

(9) Represents reactions 139 and 144 of the explicit mechanism.

$$k_{26} = 1.6\times10^{-2}\gamma + 2.7\times10^{-1}\ (1-\gamma)$$

(10) Ortho-cresol is used to represent both phenol and the dimethylphenols, and cis-2-butene-1,4-dial represents all γ-dicarbonyls. The abstraction pathway for benzene is neglected.

Table A.4. SUR2 Reaction Mechanism (continued)

(11) Represents reactions 36 and 37 of the SUR1 mechanism.

$$\beta = \frac{[\text{toluene}]_o}{[\text{toluene}]_o+[\text{xylene}]_o}$$

where,

$[\text{toluene}]_o \equiv$ initial concentration of mono-alkylbenzenes
$[\text{xylene}]_o \equiv$ initial concentration of di- and tri-alkylbenzenes

$k_{34} = 9.1\text{x}10^3\beta + 2.65\text{x}10^4(1-\beta)$ for lumped xylene
$k_{34} = 9.1\text{x}10^3\beta + 3.4\text{x}10^4(1-\beta)$ for m-xylene

(12) k_{35} is an average OH rate constant for o-cresol and dimethylphenol.

(13) Reactions 38-41 are taken from Atkinson et al. (2) and represent reactions 82 through 90 of the explicit mechanism.

for lumped xylene,

$$\alpha = \frac{1.8\text{x}10^3[\text{benzene}]_o+9.1\text{x}10^3[\text{toluene}]_o+1.35\text{x}10^4[\text{xylene}]_o}{1.8\text{x}10^3[\text{benzene}]_o+9.1\text{x}10^3[\text{toluene}]_o+2.65\text{x}10^4[\text{xylene}]_o}$$

where,

$[\text{toluene}]_o \equiv$ initial concentration of mono-alkylbenzenes
$[\text{xylene}]_o \equiv$ initial concentration of di- and tri-alkylbenzenes

(14) Benzaldehyde formation is neglected.

(15) ALK represents all $\geq C_4$ alkanes. See Atkinson et al. (2) for a discussion of these reactions. For explicit n-butane use (2):

$$k_{46} = 4.1\text{x}10^3 \text{ ppm}^{-1}\text{-min}^{-1} \qquad A_{61} = 560\text{K}$$

$$C_4H_{11}O_3\cdot + NO \rightarrow 1.3NO_2 - 0.4NO + 0.9HO_2\cdot + 0.7CH_3CHO$$

(16) Photolysis rates calculated by averaging over zenith angles between 30° and 60° using the results of Demerjian et al. (24) followed by corrections based on the results of Horowitz and Calvert (26). CH_3CHO represents all $\geq C_2$ aldehydes.

Table A.5 Non-Steady-State Species Appearing in the SUR2 Mechanism[1]

NO	HONO	ARO	$CH_3C(O)CHO$
NO_2	N_2O_5	CH(O)CH=CHCHO	ALK
O_3	CO	benzene	HCHO
HO_2NO_2	ethene	o-cresol	CH_3CHO
H_2O_2	OLE	$CH(O)CH=CHC(O)O_2NO_2$	PAN

[1]In most cases the additional non-steady-state species appearing in the SUR2 mechanism (H_2O,HCOOH, etc.) would either be held constant or ignored. There are cases where one would include additional non-steady state species. For instance, HNO_3 would definitely be included in studies on acid rain.

Table A.6 Chamber Dependent Reactions for the SAPRC and UNC Chambers[1]

Reaction	Rate Constant[2,3] SAPRC	UNC
$O_3 \rightarrow$ wall	1.65×10^{-3}	1.5×10^{-4}
$N_2O_5 + H_2O \xrightarrow{\text{wall}} 2HNO_3$	4.4×10^{-6}	1.5×10^{-5}
Wall $\rightarrow HO_2\cdot$	-	$1.5 \times 10^{-4} k_1$
wall $\rightarrow$ OH	$0.39 k_1$	-
$NO_2 \xrightarrow{\text{wall}}$ OH	$1.37 k_1$	-
Wall $\rightarrow$ NO	1.0×10^{-4}	-

[1]The reactions shown here are the chamber dependent reactions recommended by the chamber operators (18,19,27).

[2]ppm-min units

[3]k_1 is the NO_2 photolysis rate.

Table A.7 Initial Conditions and Physical Parameters for University of North Carolina Smog Chamber Experiments.[1-4]

Experiment	Concentration (ppbC)[5]					
	7/8/82-Red	7/8/82-Blue	8/26/81-Blue	9/2/81-Red	10/14/81-Red	8/26/81-Red
NO	212	210	182	191	174	184
NO_2	78	73	51	55	106	47
n-butane	863	801	582	-	-	840
propene	327	278	171	143	71	259
toluene	370	220	293	194	-	-
m-xylene	365	170	214	176	685	-
ethene	-	-	235	230	216	346
HCHO	4	4	-	-	-	-
CO	355	300	355[6]	355[6]	300[6]	355[6]
H_2O(ppm)	15,000	15,500	17,500	21,000	5,500	20,000
n-propylbenzene	-	183	-	-	-	-
1,2,4-trimethylbenzene	160	287	-	-	-	-
sec-butylbenzene	-	172	-	-	-	-
n-pentane	-	442	-	419	519	665
2,4-dimethylpentane	-	-	-	275	353	-
2,2,4-trimethylpentane	-	-	-	184	270	-
1-butene	-	-	-	61	67	-
cis-2-butene	-	-	-	56	53	-
isopentane	-	-	-	250	317	-

Table A.7 Initial Conditions and Physical Parameters for University of North Carolina Smog Chamber Experiments.[1-4] (continued)

	Concentration (ppbC)[5]					
Experiment	7/8/82-Red	7/8/82-Blue	8/26/81-Blue	9/2/81-Red	10/14/81-Red	8/26/81-Red
2-methyl-1-butene	-	-	-	73	88	-
2-methyl-2-butene	-	-	-	110	92	-
2-methylpentane	-	-	-	226	339	-
Start time (EDT)	06:00	06:00	06:00	06:55	07:30	06:30
Dilution Rate (min^{-1})[7]	$3.7x10^{-4}$	$4.8x10^{-4}$	$3.6x10^{-4}$	$3.6x10^{-4}$	$9.6x10^{-5}$	$3.6x10^{-4}$

[1]The UNC chamber has two sides, one is labeled red, the other blue.

[2]Since the chamber temperature varied throughout the experiment, no temperature data are presented presented here. Consult Jeffries et al. (27).

[3]k_1 is not given because it varied throughout the experiment. The k_1 values used in our simulations were calculated as k_1 = 0.4 x total solar radiation, increased by 15 percent between 9 AM and 3 PM (27).

[4]5 ppb of initial HONO is assumed in each simulation.

[5]Note that the units of concentration are ppbC for the organics, ppb for NO and NO_2.

[6]CO was not measured in these experiments, so the initial CO concentration had to be estimated.

[7]The average dilution rate recommended by Jeffries et al. (27), $3.6x10^{-4}$ min^{-1}, was used if detailed dilution data was not available.

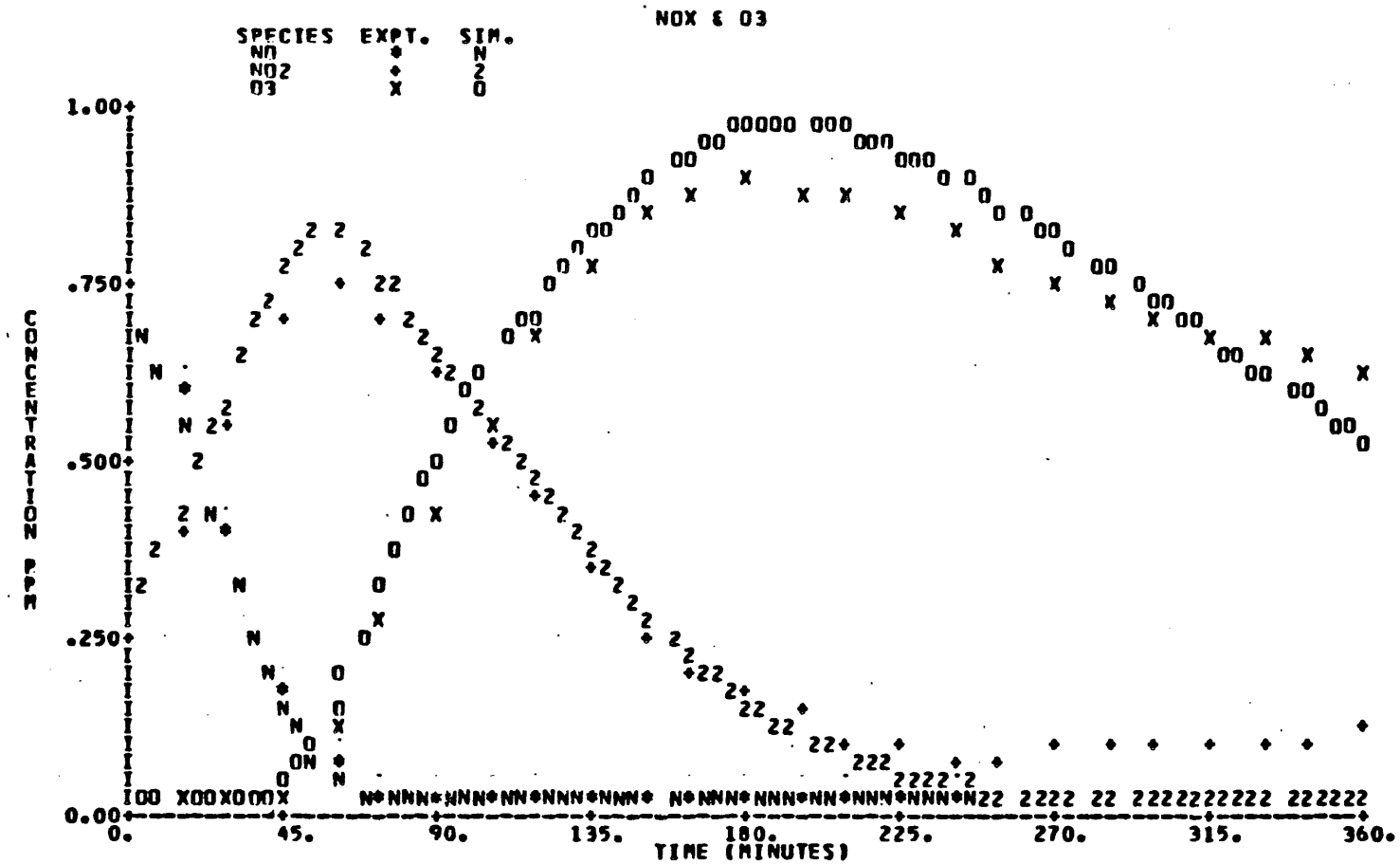

Figure A.10.a. Comparison of Concentration-Time Profiles Predicted by the SUR2 Mechanism with Experimental Data from SAPRC Experiment EC-245.

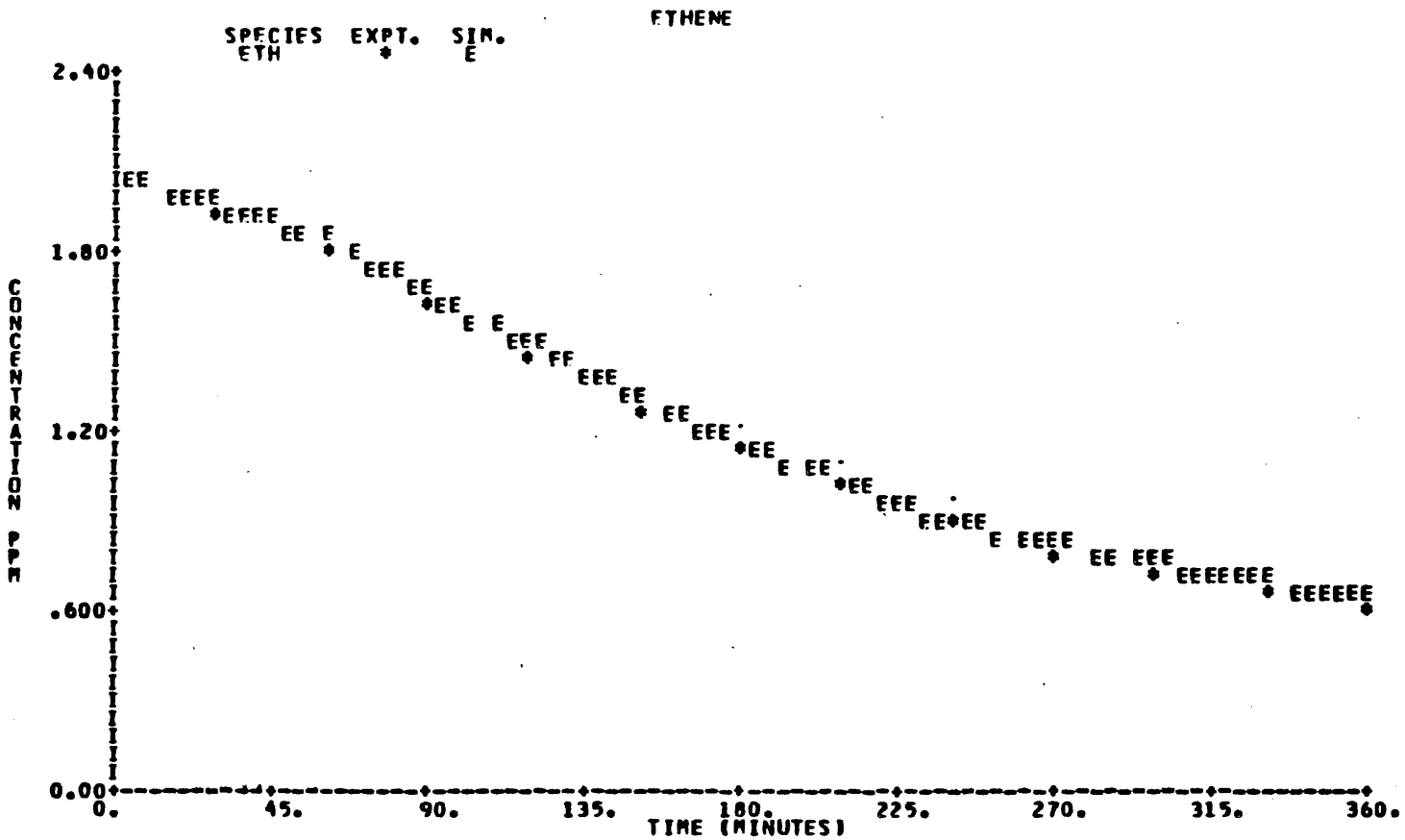

Figure A.10.b. Comparison of Concentration-Time Profiles Predicted by the SUR2 Mechanism with Experimental Data from SAPRC Experiment EC-245.

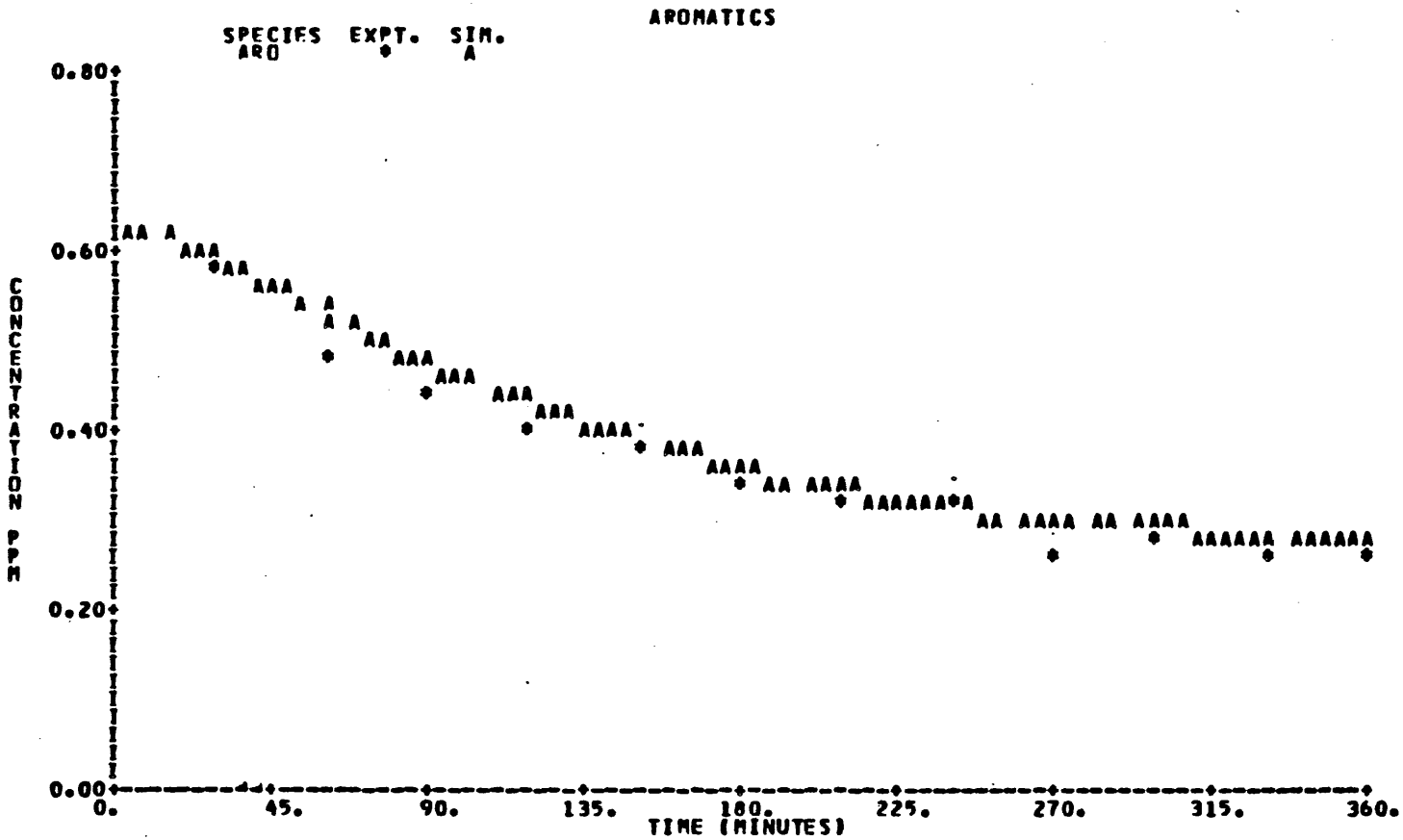

Figure A.10.c. Comparison of Concentration-Time Profiles Predicted by the SUR2 Mechanism with Experimental Data from SAPRC Experiment EC-245.

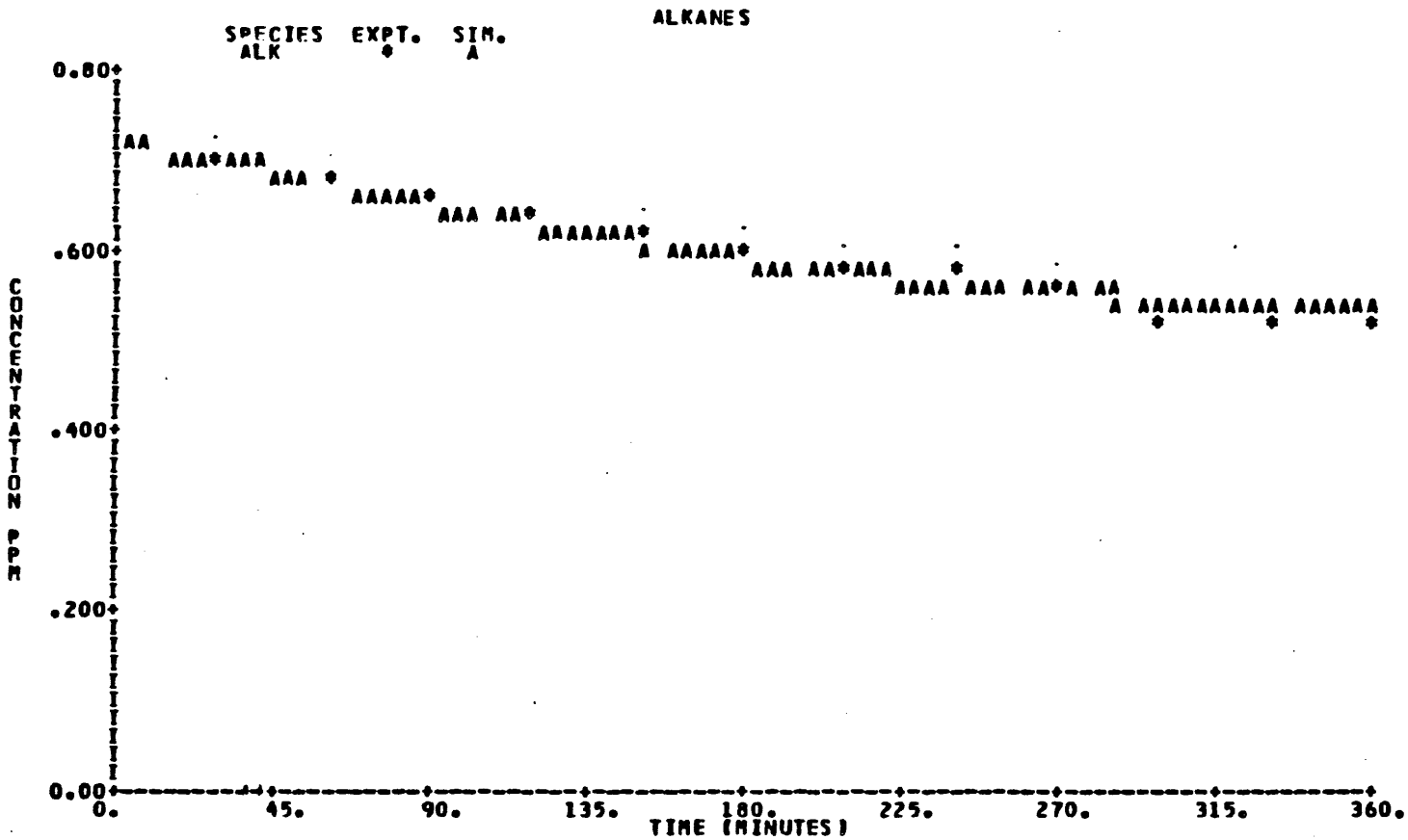

Figure A.10.d. Comparison of Concentration-Time Profiles Predicted by the SUR2 Mechanism with Experimental Data from SAPRC Experiment EC-245.

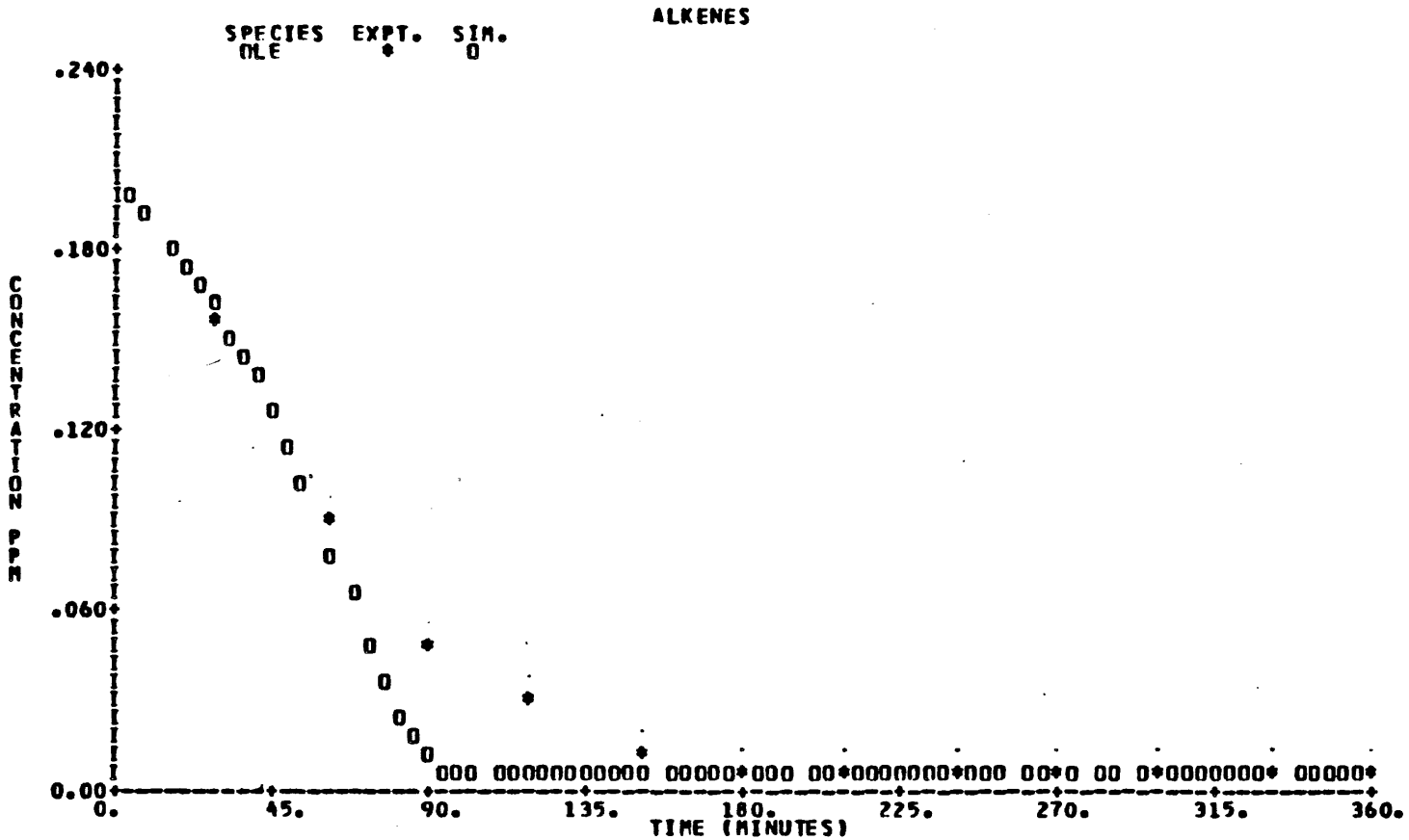

Figure A.10.e. Comparison of Concentration-Time Profiles Predicted by the SUR2 Mechanism with Experimental Data from SAPRC Experiment EC-245.

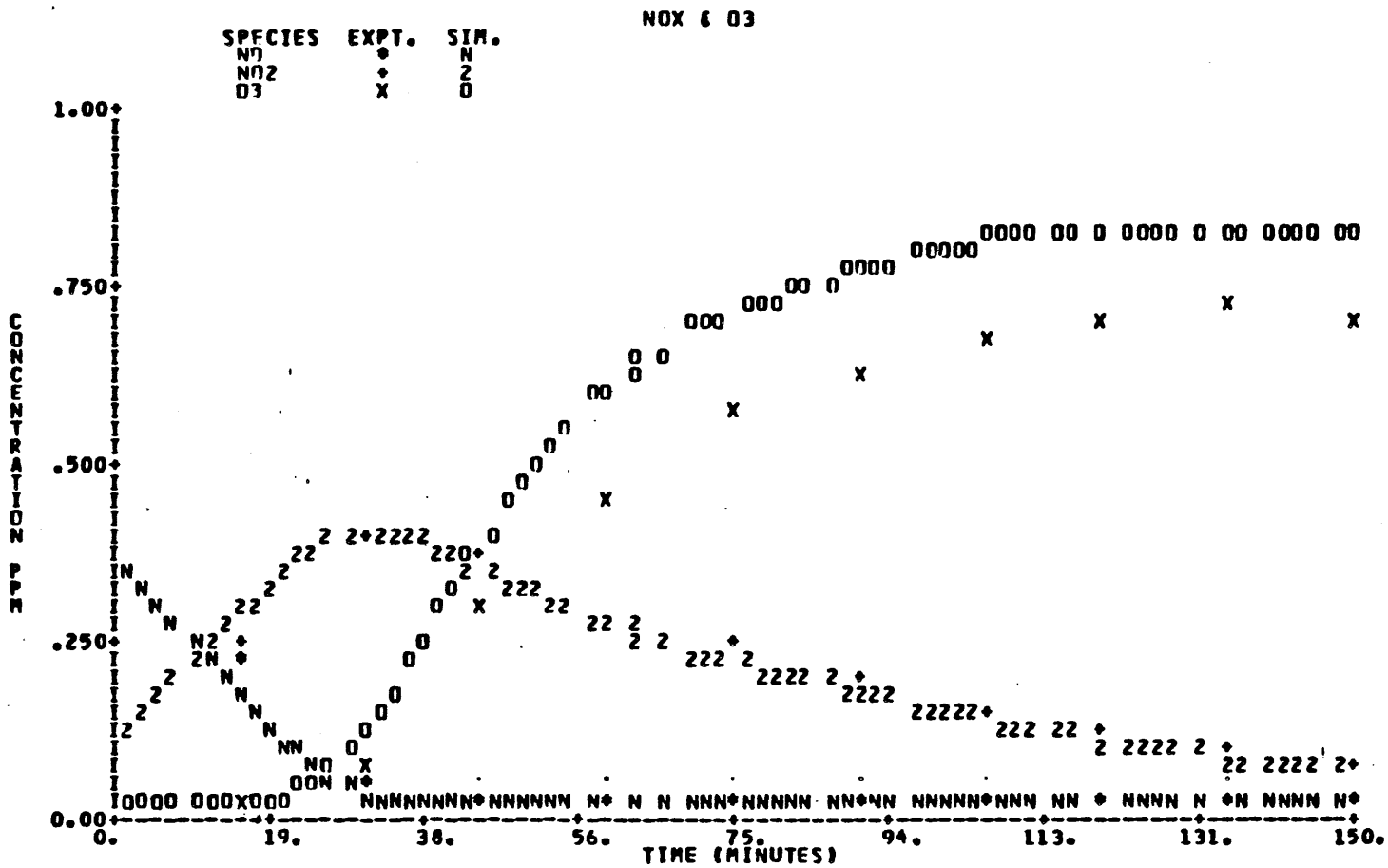

Figure A.11.a. Comparison of Concentration-Time Profiles Predicted by the SUR2 Mechanism with Experimental Data from SAPRC Experiment EC-243.

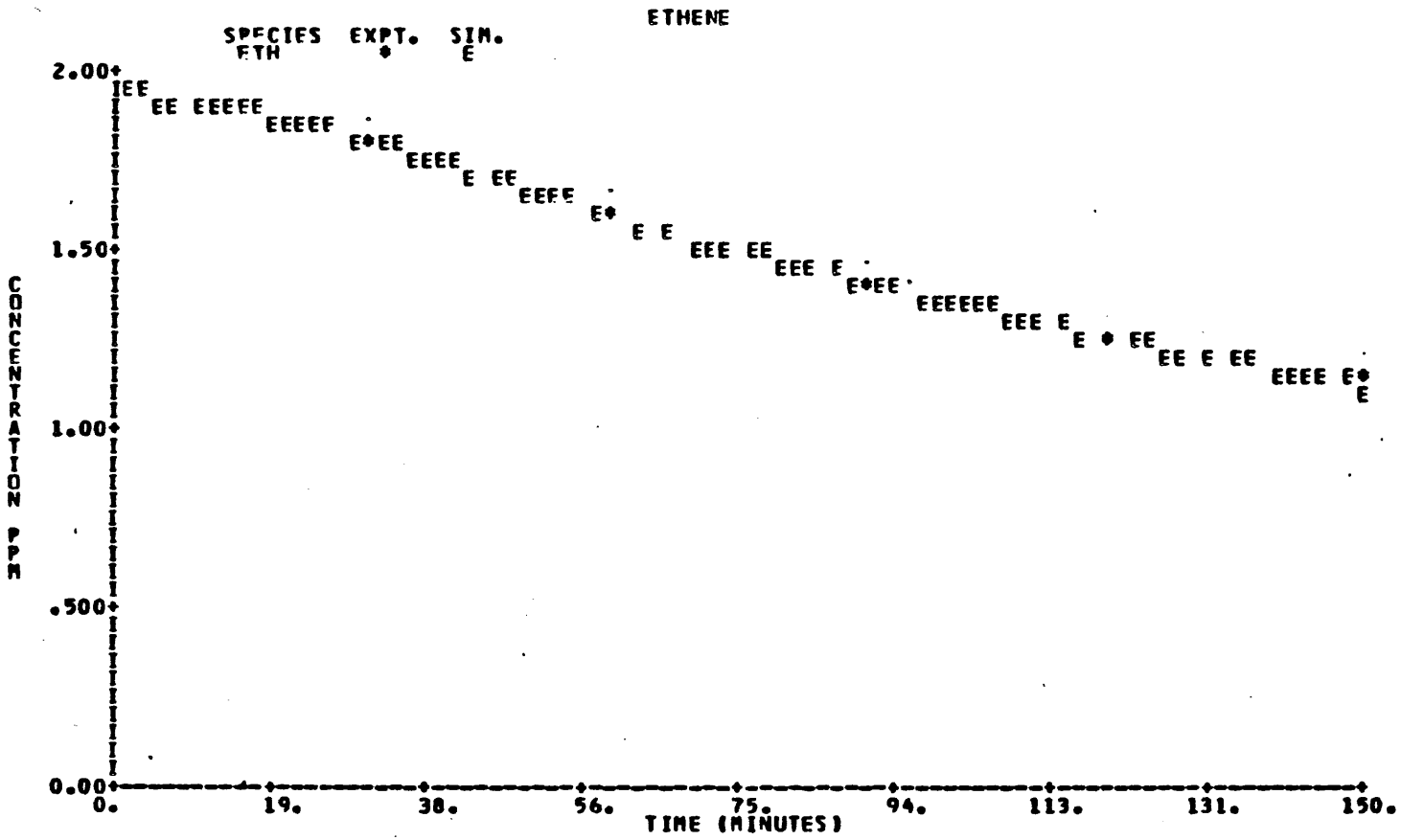

Figure A.11.b Comparison of Concentration-Time Profiles Predicted by the SUR2 Mechanism with Experimental Data from SAPRC Experiment EC-243.

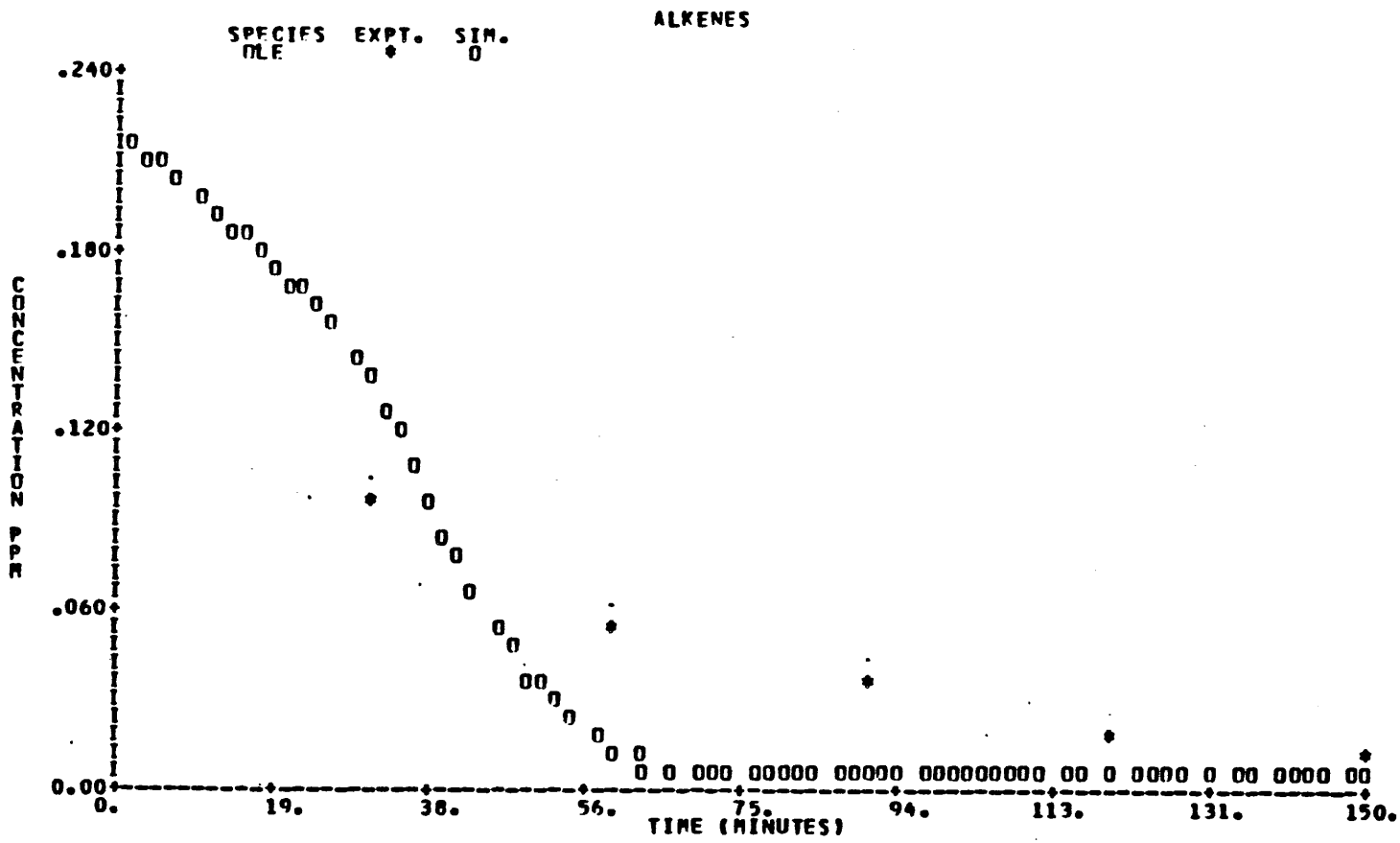

Figure A.11.c. Comparison of Concentration-Time Profiles Predicted by the SUR2 Mechanism with Experimental Data from SAPRC Experiment EC-243.

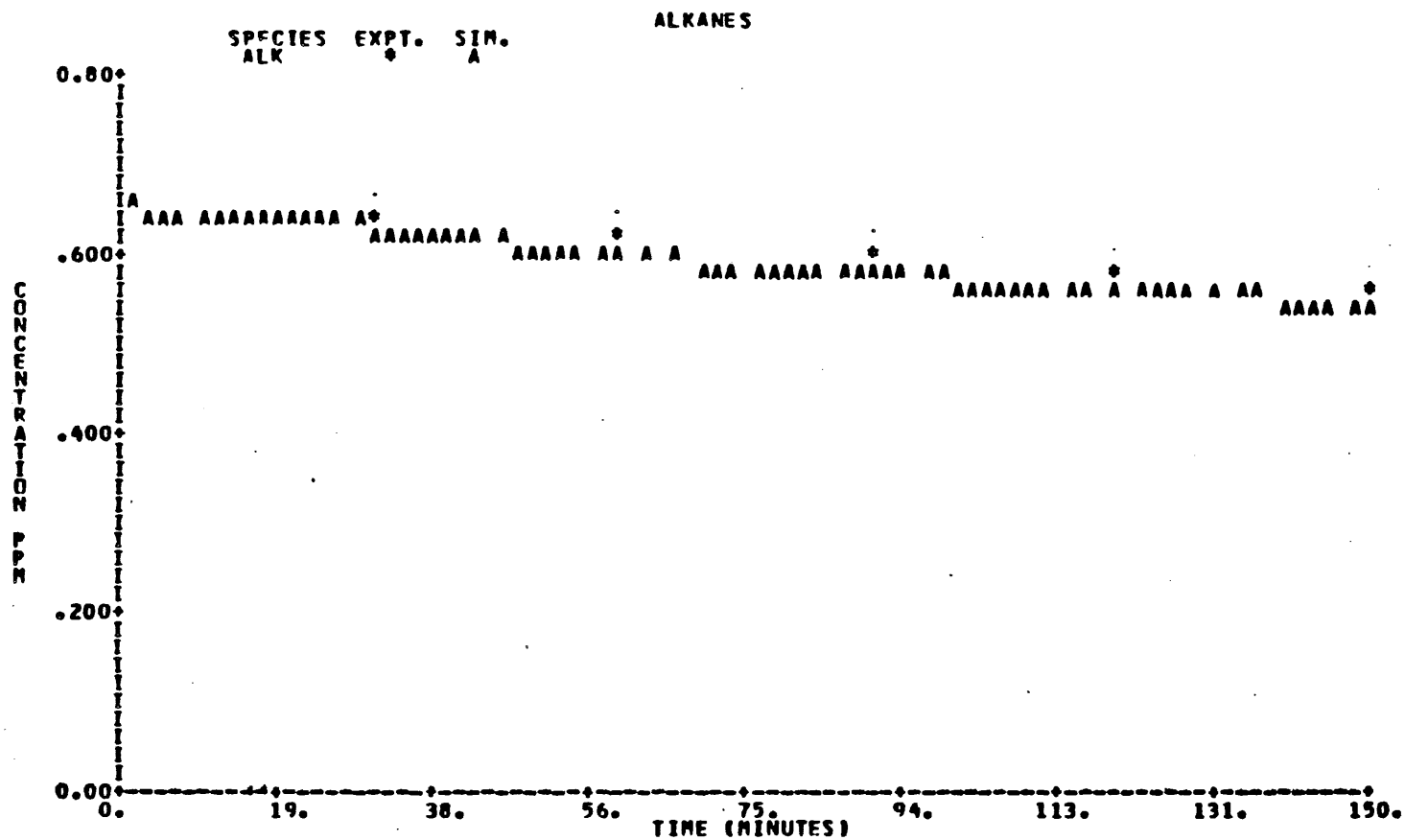

Figure A.11.d. Comparison of Concentration-Time Profiles Predicted by the SUR2 Mechanism with Experimental Data from SAPRC Experiment EC-243.

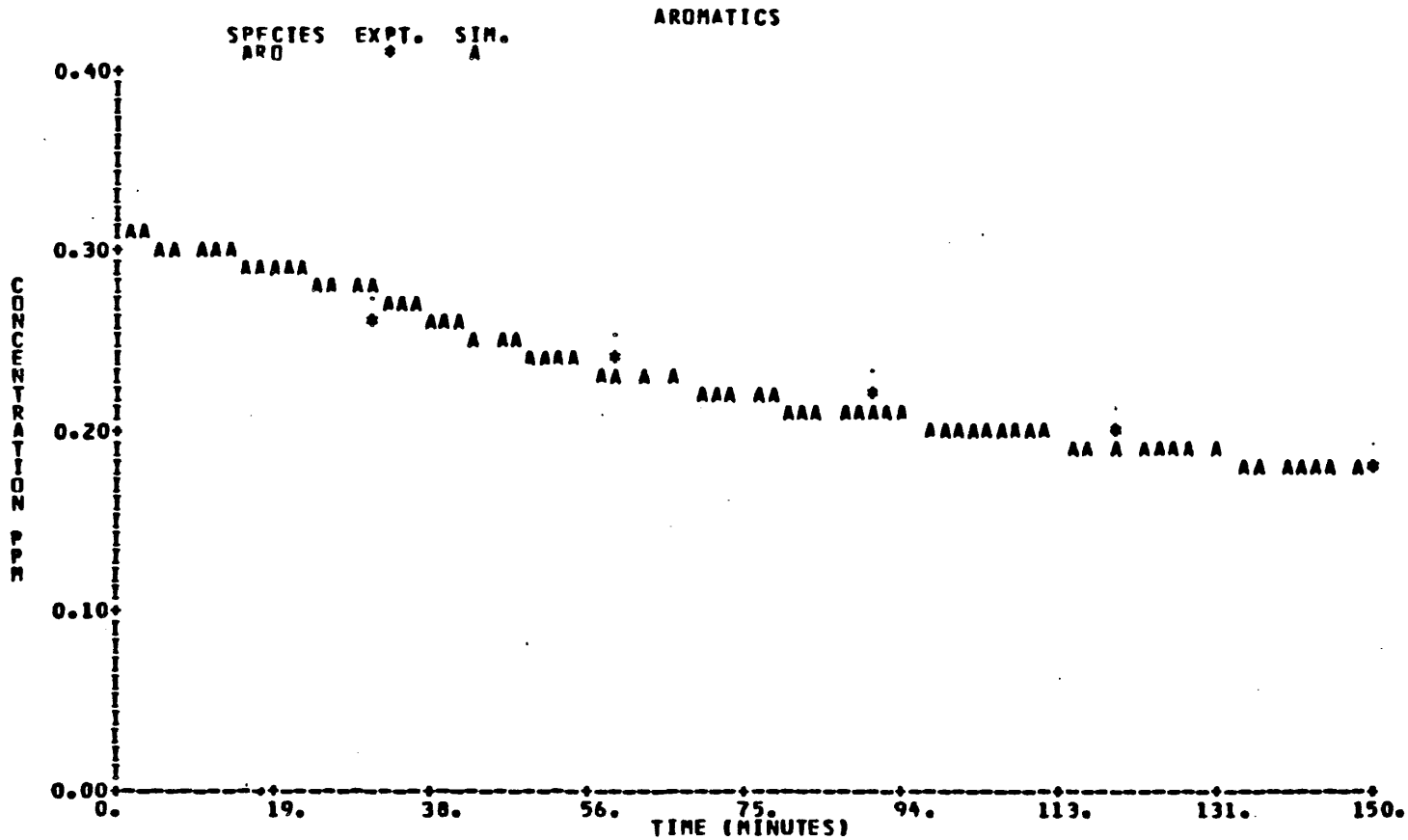

Figure A.11.e. Comparison of Concentration-Time Profiles Predicted by the SUR2 Mechanism with Experimental Data from SAPRC Experiment EC-243.

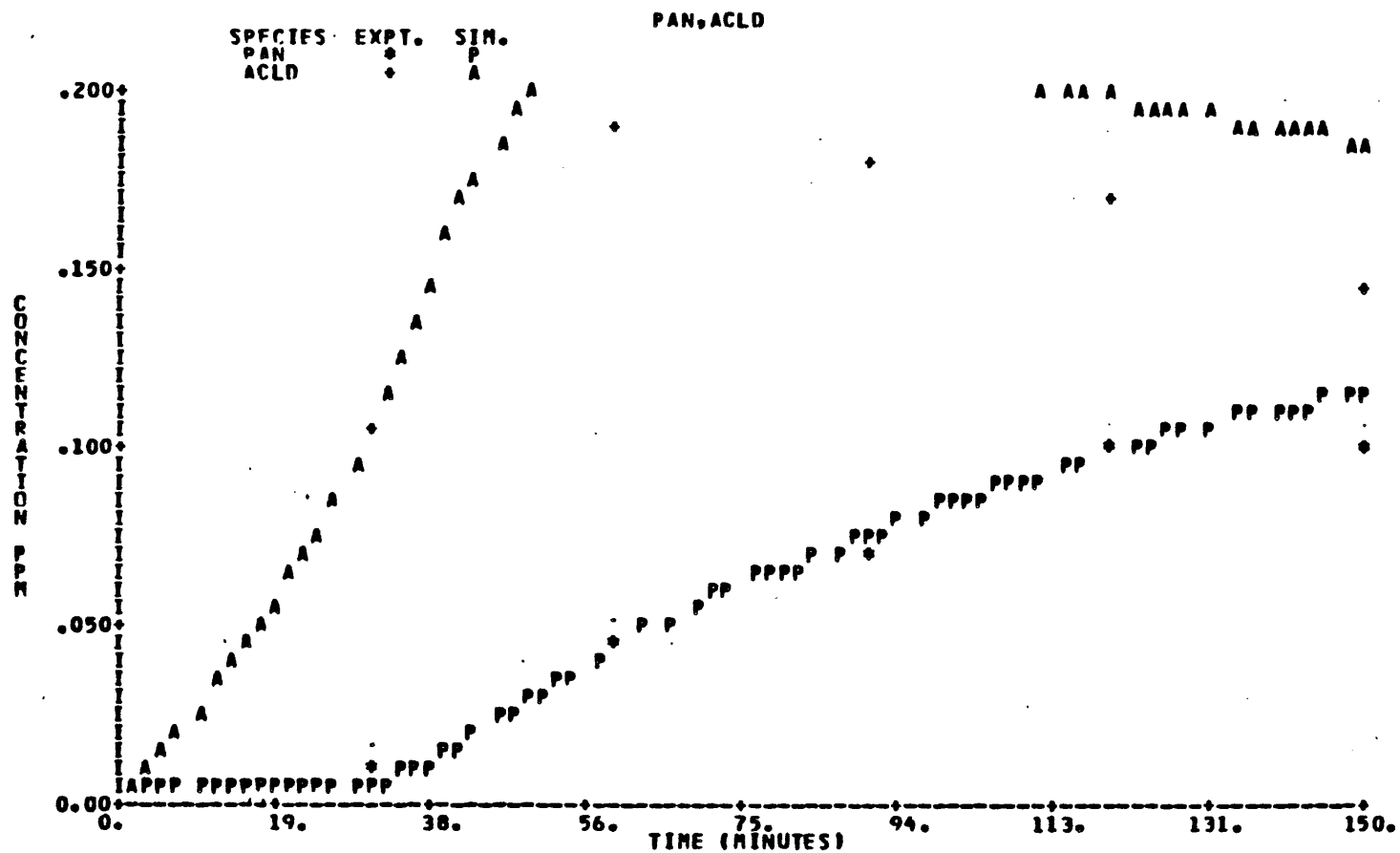

Figure A.11.f. Comparison of Concentration-Time Profiles Predicted by the SUR2 Mechanism with Experimental Data from SAPRC Experiment EC-243.

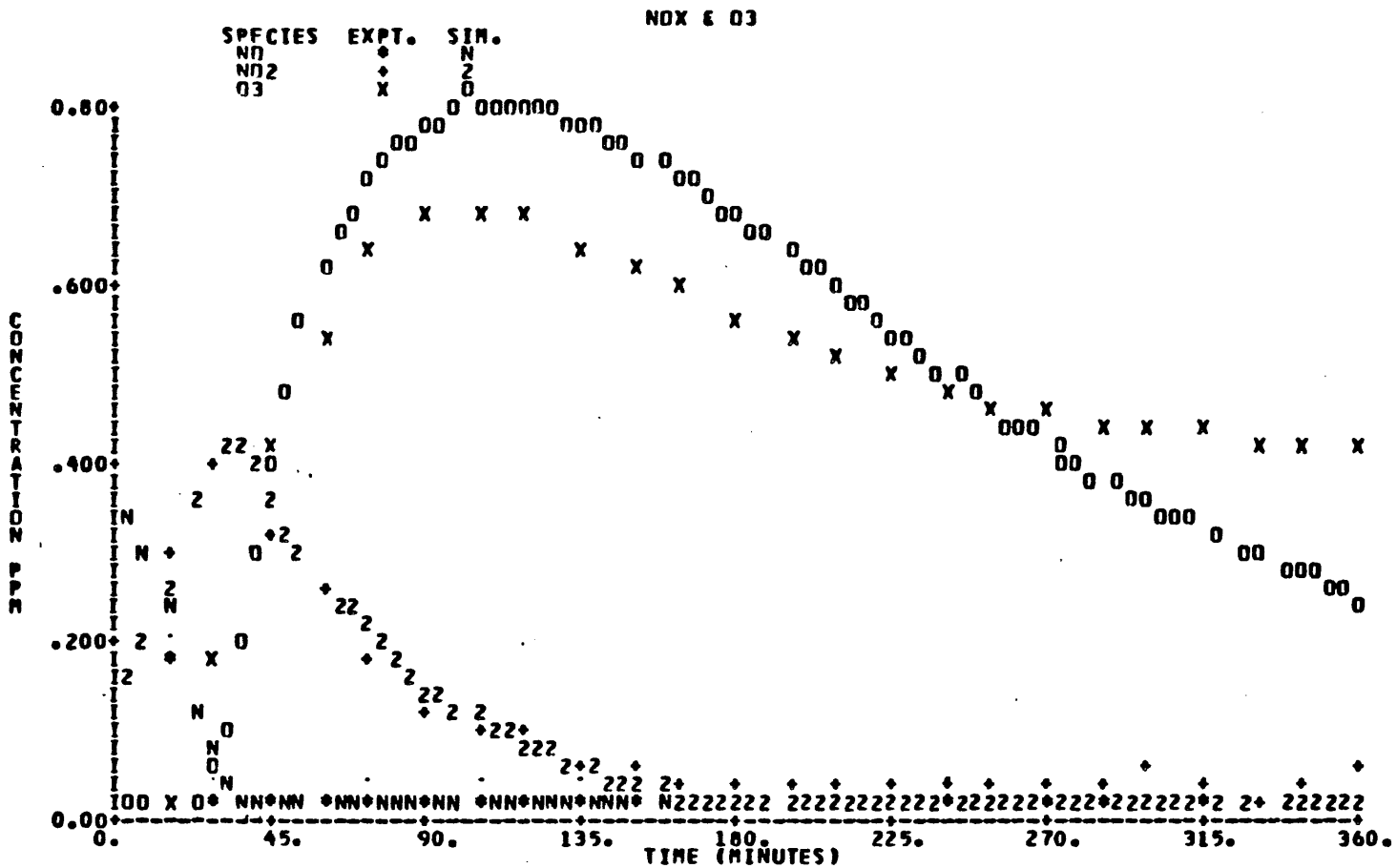

Figure A.12.a. Comparison of Concentration-Time Profiles Predicted by the SUR2 Mechanism with Experimental Data from SAPRC Experiment EC-242.

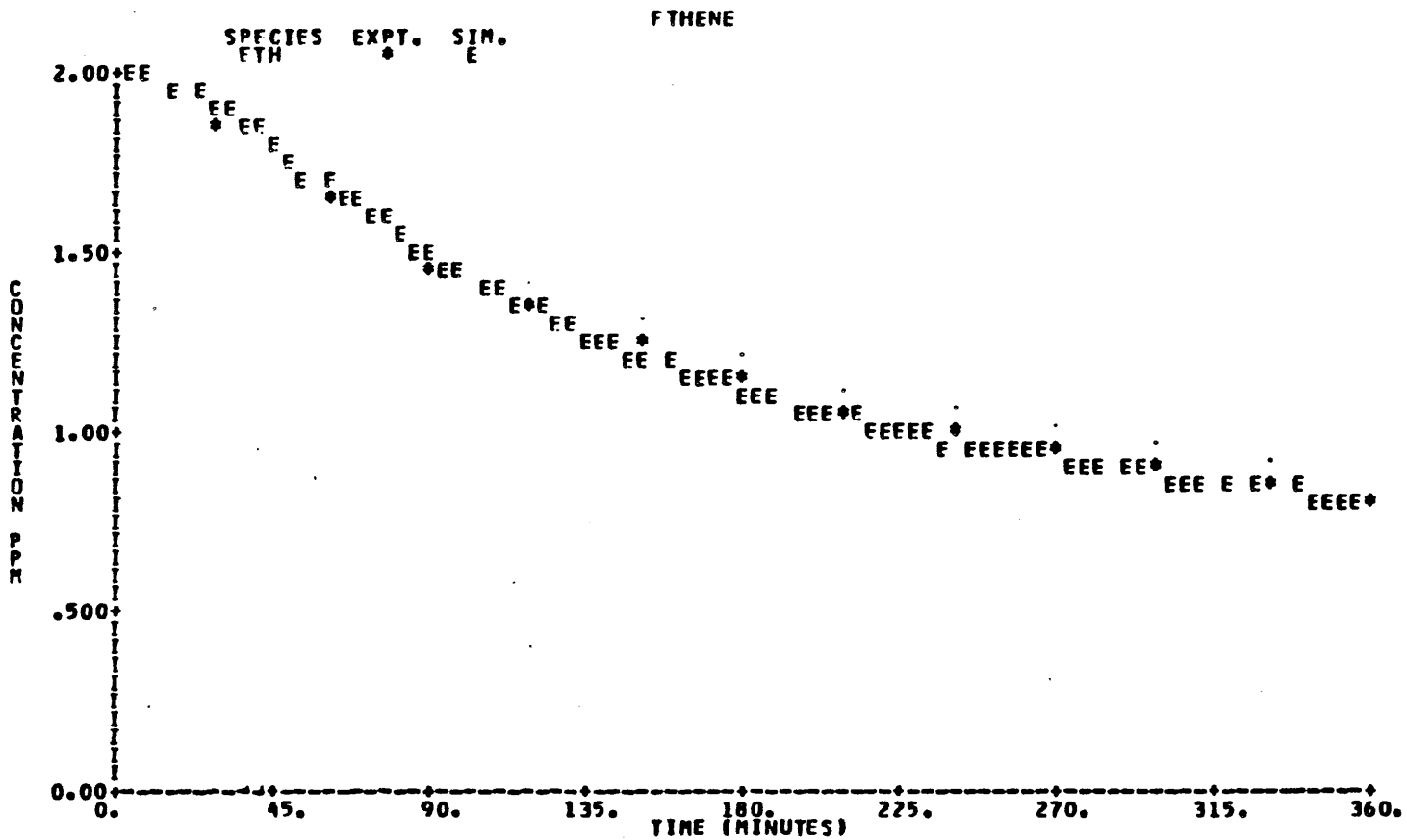

Figure A.12.b. Comparison of Concentration-Time Profiles Predicted by the SUR2 Mechanism with Experimental Data from SAPRC Experiment EC-242.

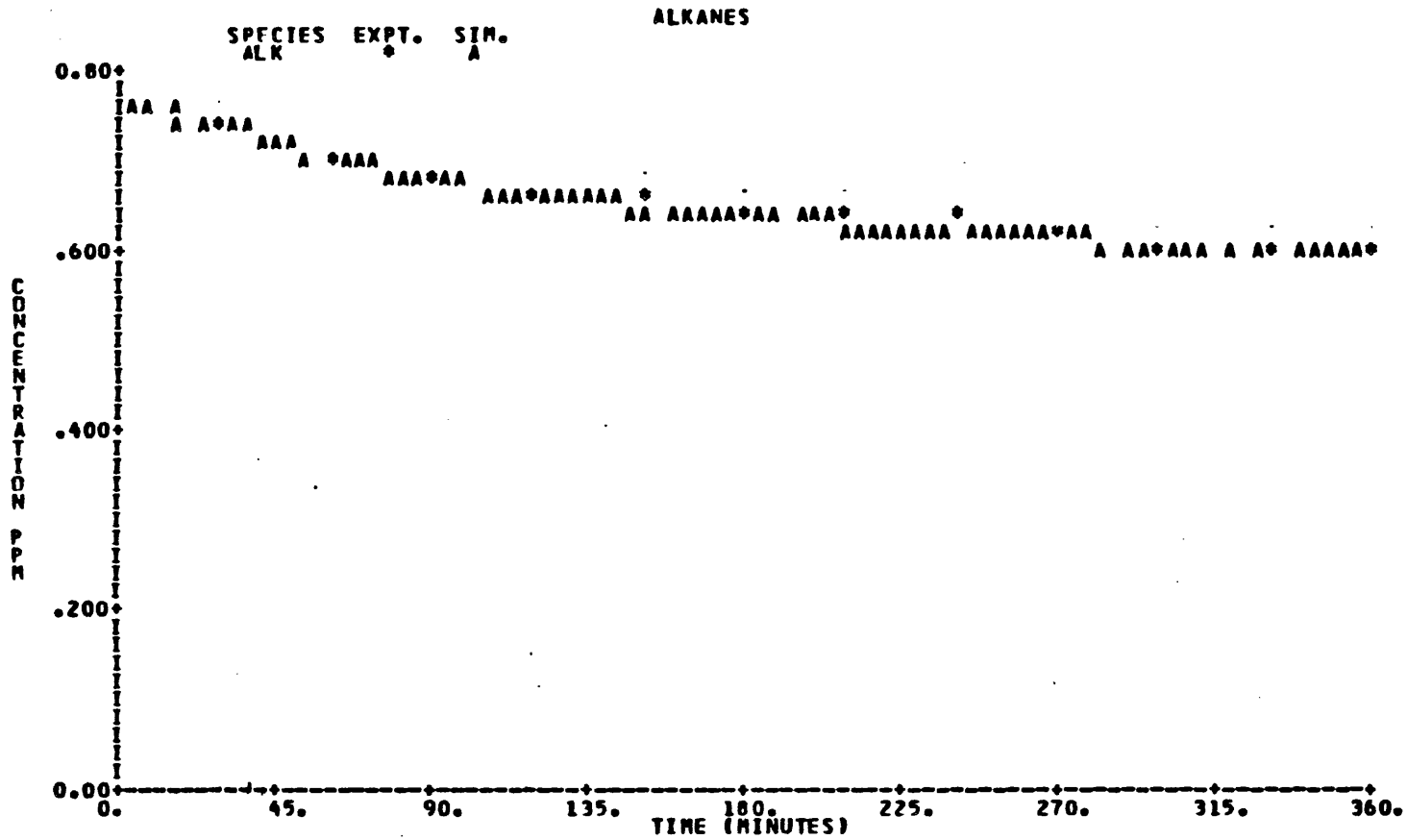

Figure A.12.c. Comparison of Concentration-Time Profiles Predicted by the SUR2 Mechanism with Experimental Data from SAPRC Experiment EC-242.

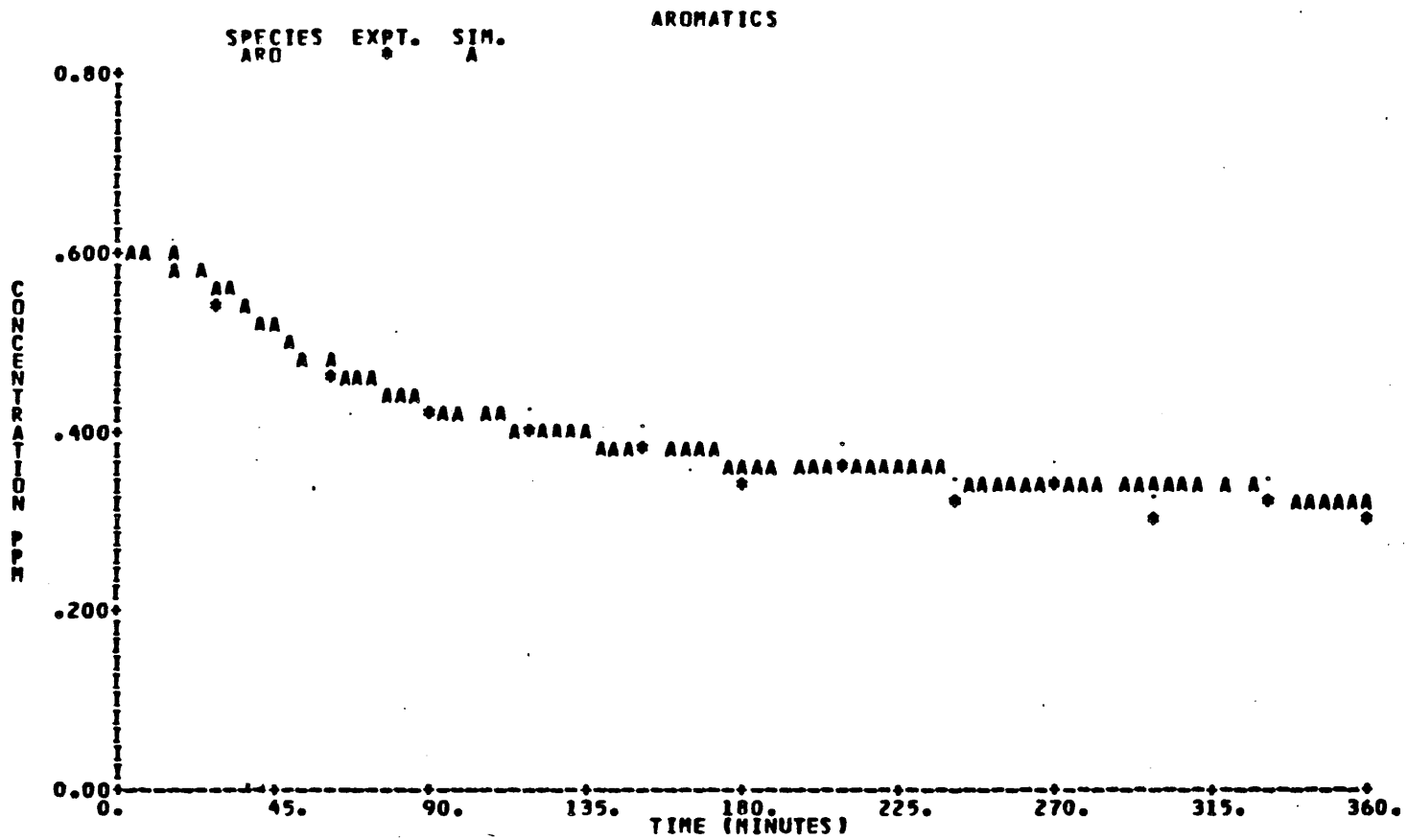

Figure A.12.d. Comparison of Concentration-Time Profiles Predicted by the SUR2 Mechanism with Experimental Data from SAPRC Experiment EC-242.

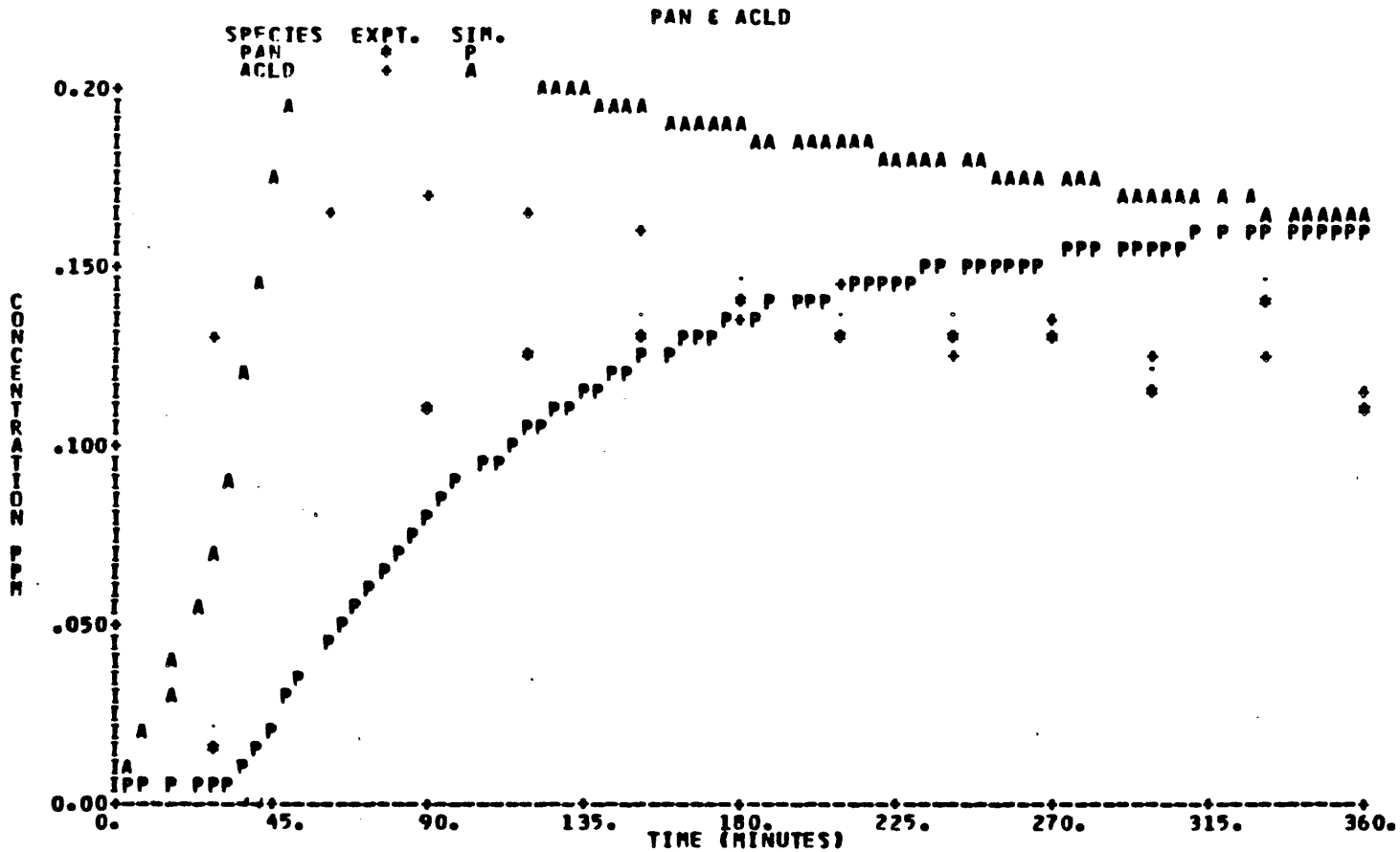

Figure A.12.e. Comparison of Concentration-Time Profiles Predicted by the SUR2 Mechanism with Experimental Data from SAPRC Experiment EC-242.

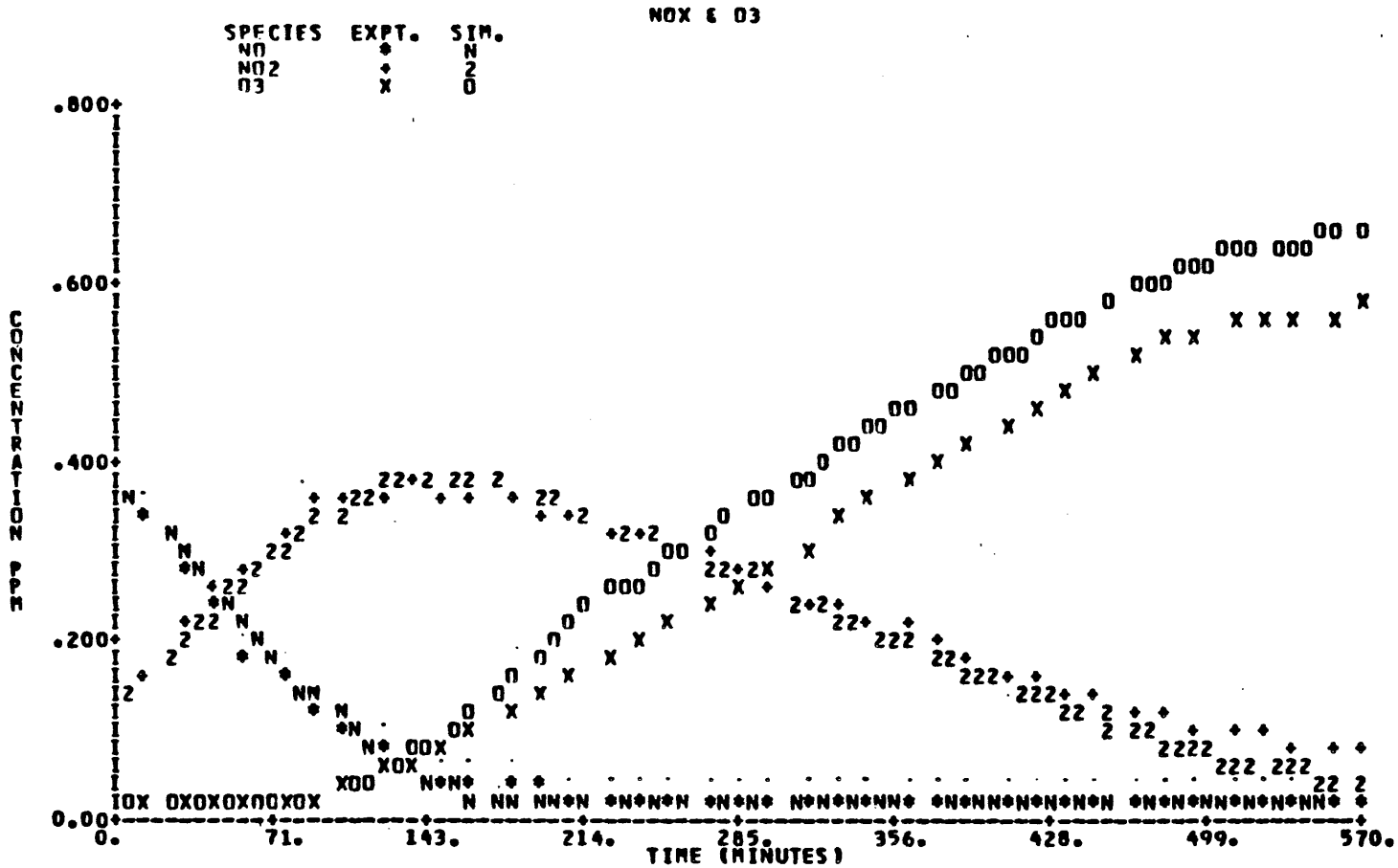

Figure A.13.a. Comparison of Concentration-Time Profiles Predicted by the SUR2 Mechanism with Experimental Data from SAPRC Experiment EC-246.

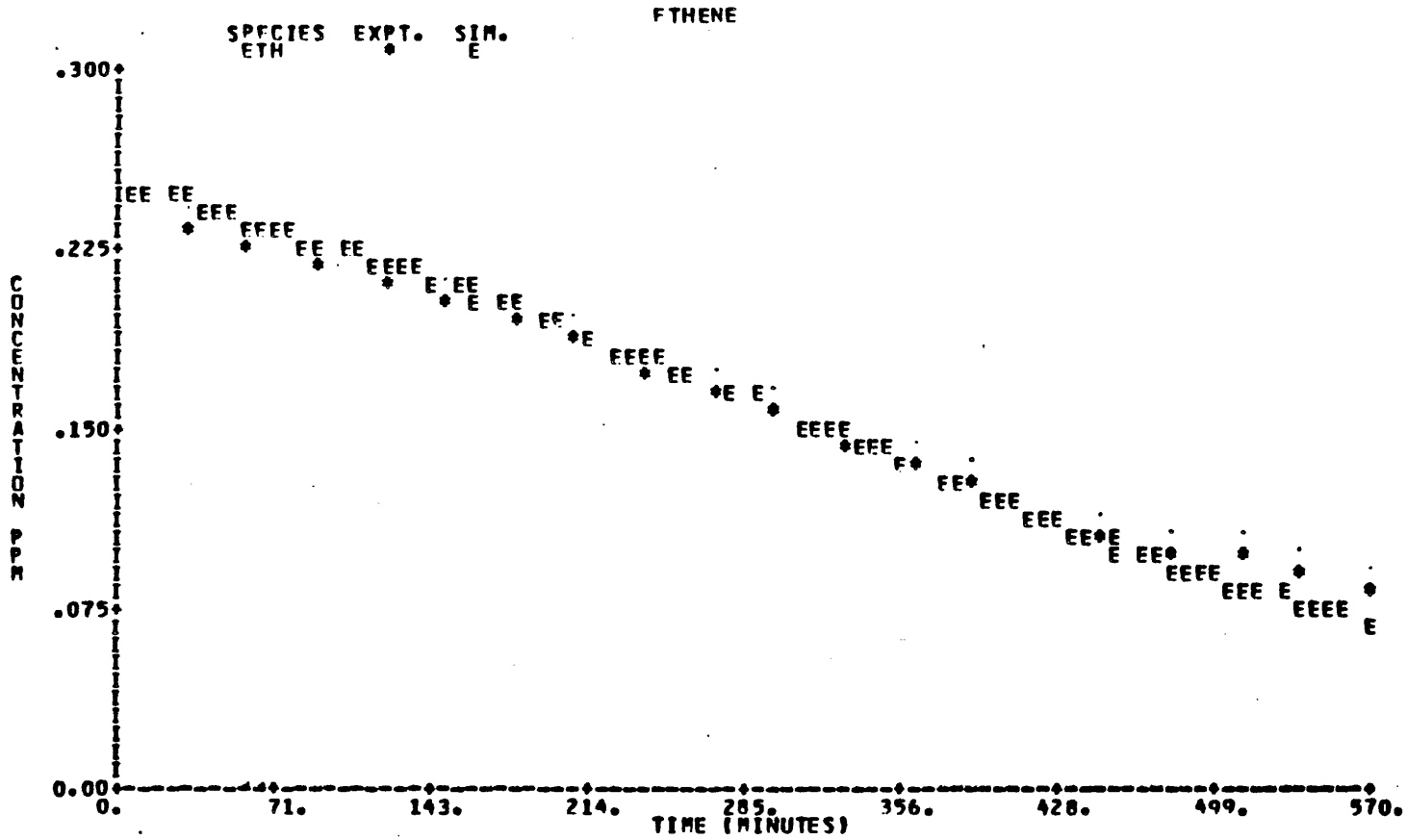

Figure A.13.b. Comparison of Concentration-Time Profiles Predicted by the SUR2 Mechanism with Experimental Data from SAPRC Experiment EC-246.

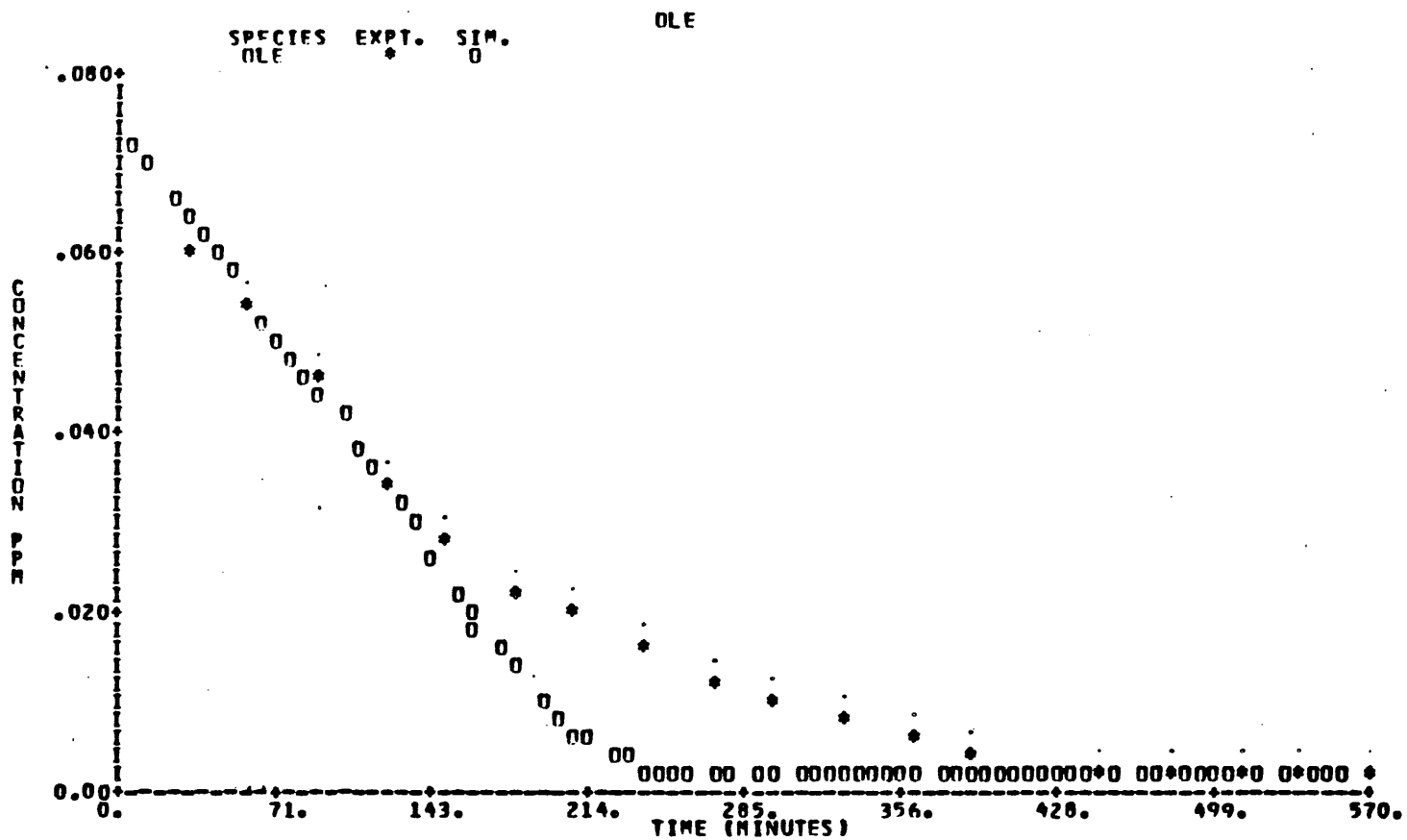

Figure A.13.c. Comparison of Concentration-Time Profiles Predicted by the SUR2 Mechanism with Experimental Data from SAPRC Experiment EC-246.

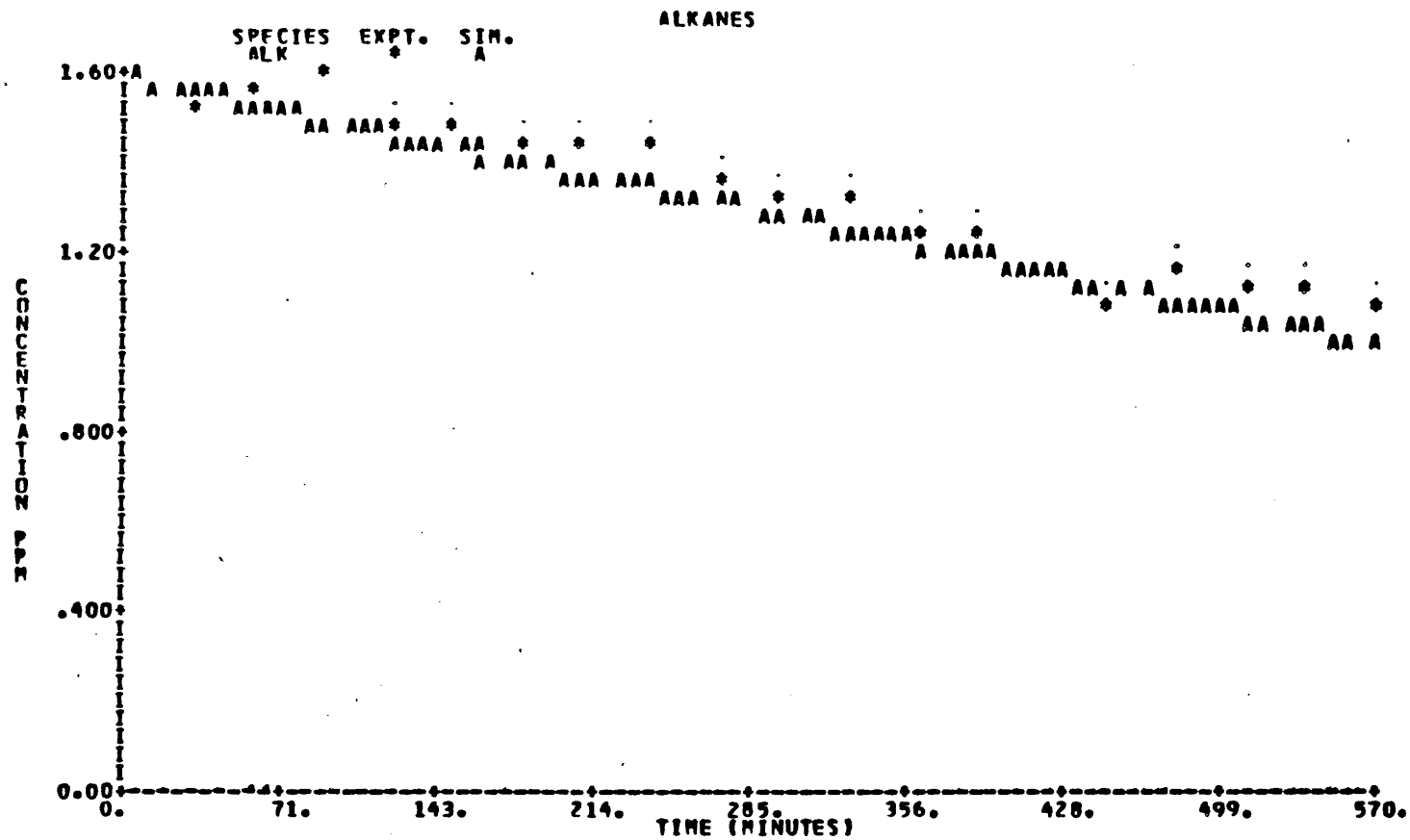

Figure A.13.d. Comparison of Concentration-Time Profiles Predicted by the SUR2 Mechanism with Experimental Data from SAPRC Experiment EC-246.

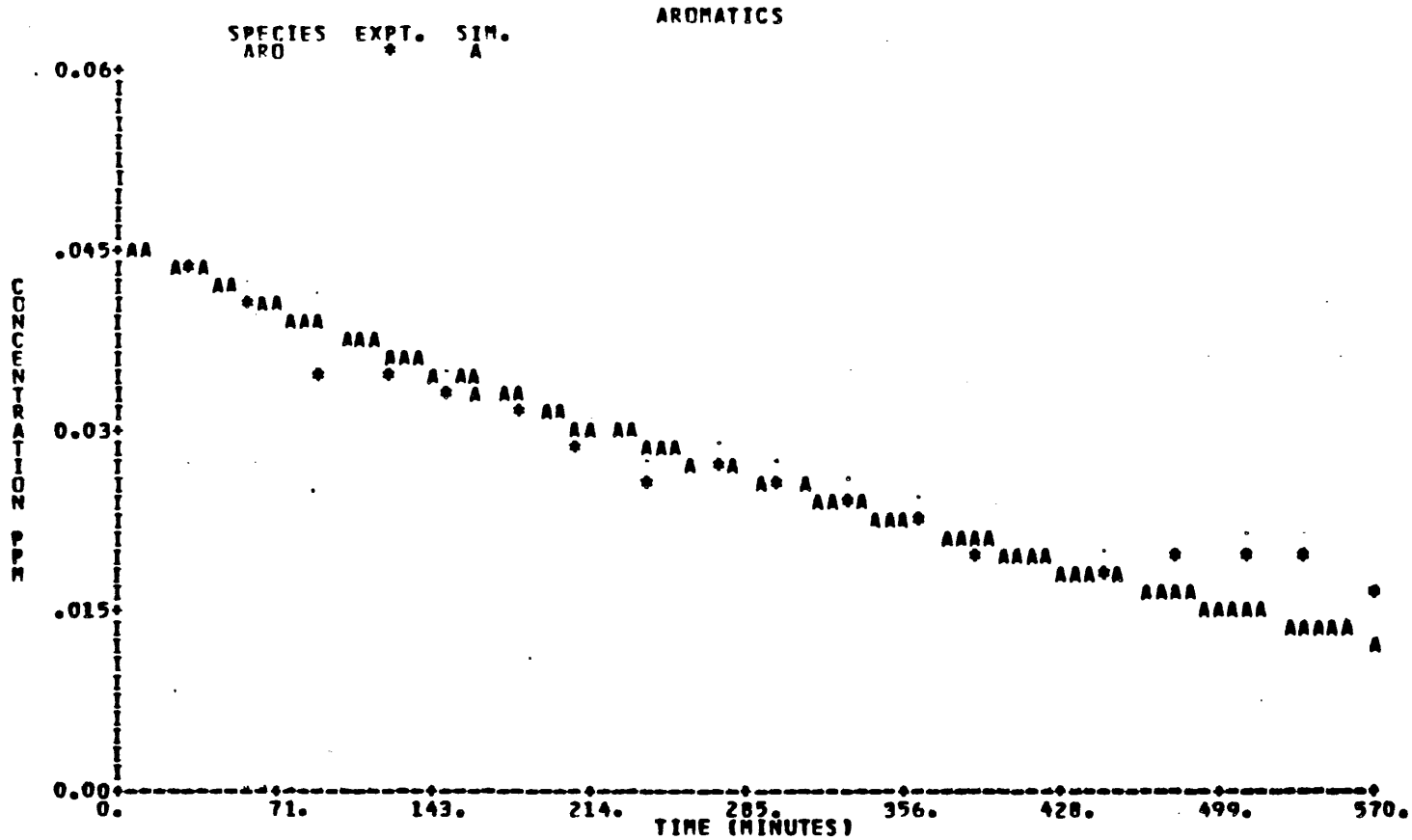

Figure A.13.e. Comparison of Concentration-Time Profiles Predicted by the SUR2 Mechanism with Experimental Data from SAPRC Experiment EC-246.

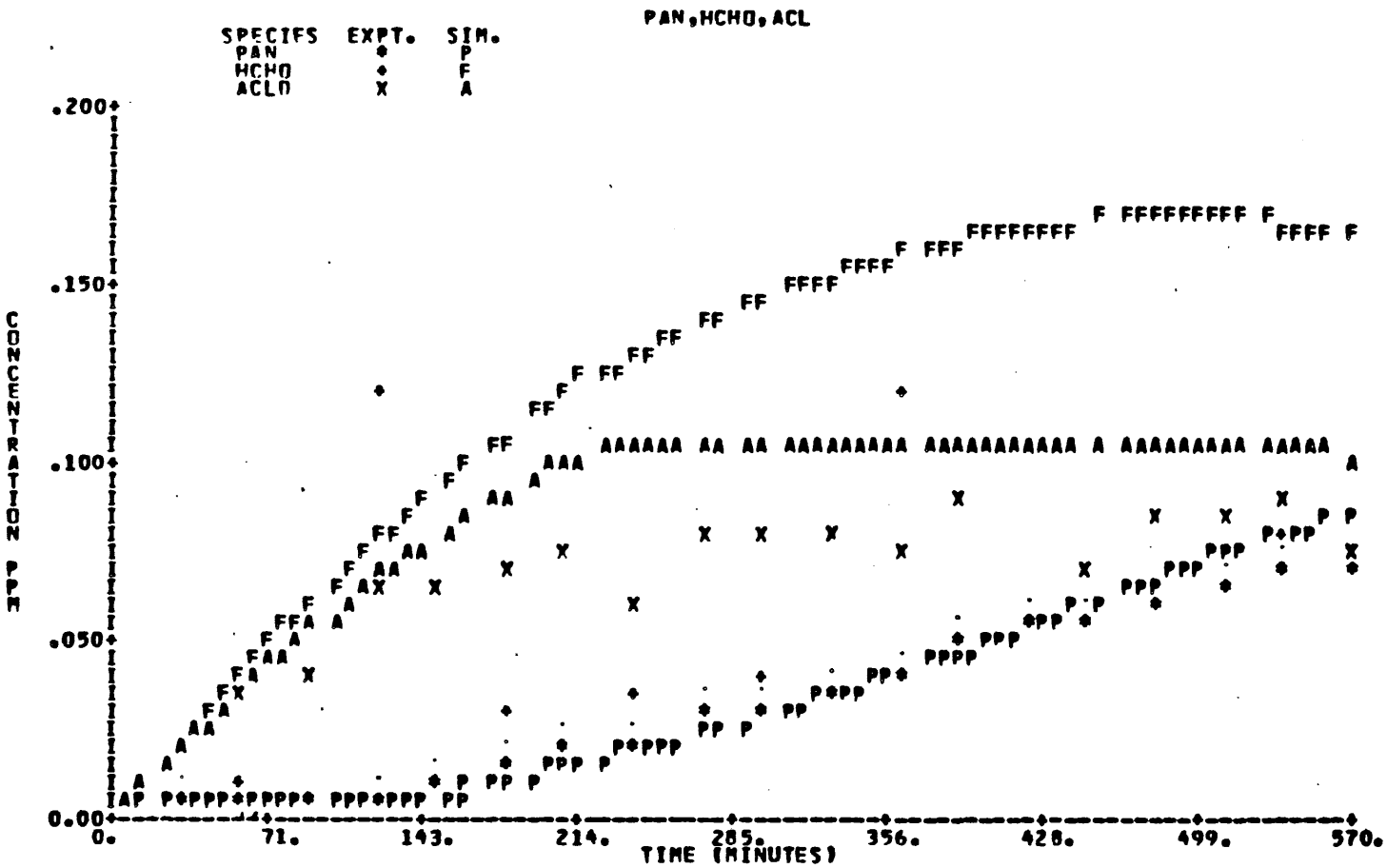

Figure A.13.f. Comparison of Concentration-Time Profiles Predicted by the SUR2 Mechanism with Experimental Data from SAPRC Experiment EC-246.

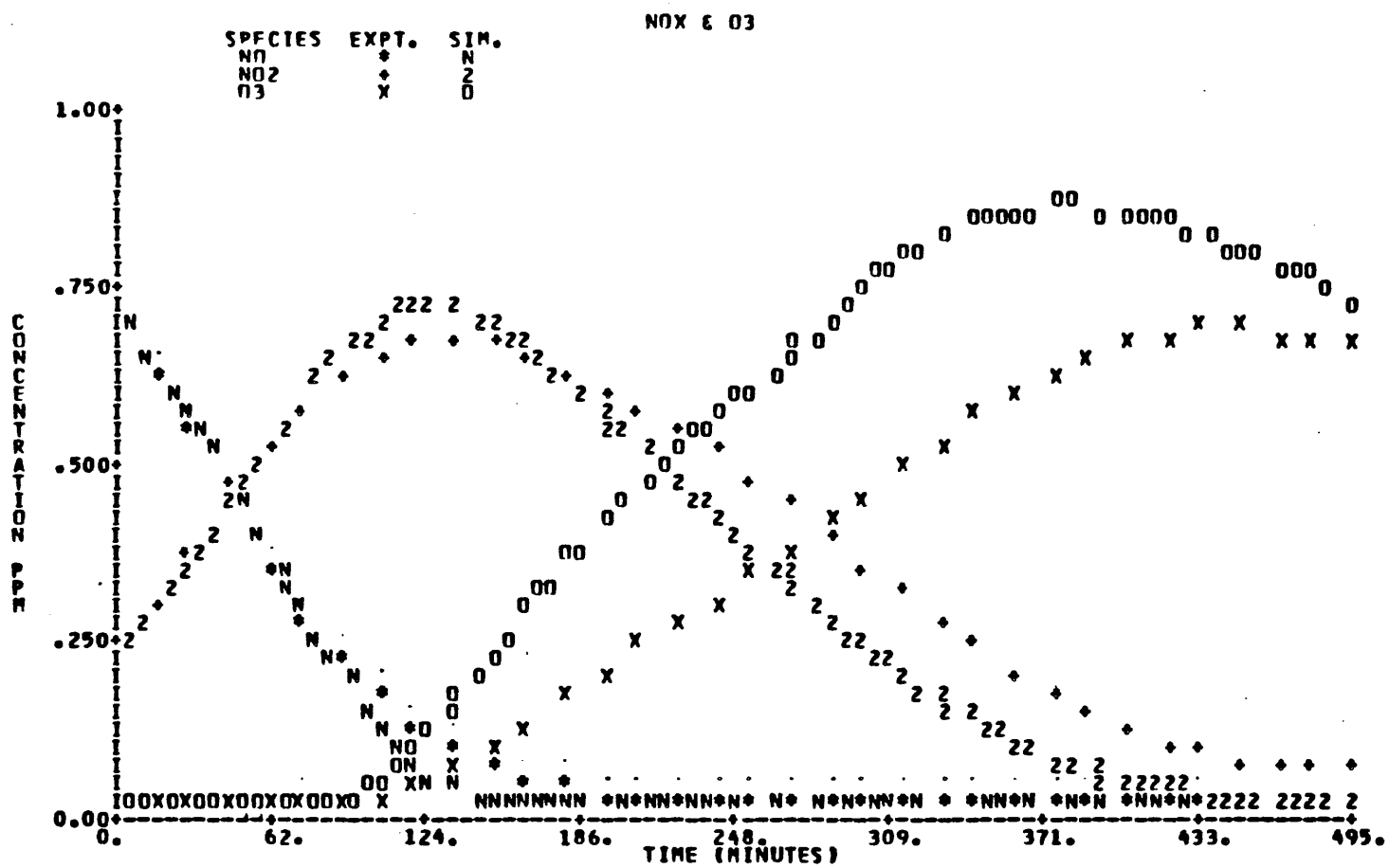

Figure A.14.a. Comparison of Concentration-Time Profiles Predicted by the SUR2 Mechanism with Experimental Data from SAPRC Experiment EC-238.

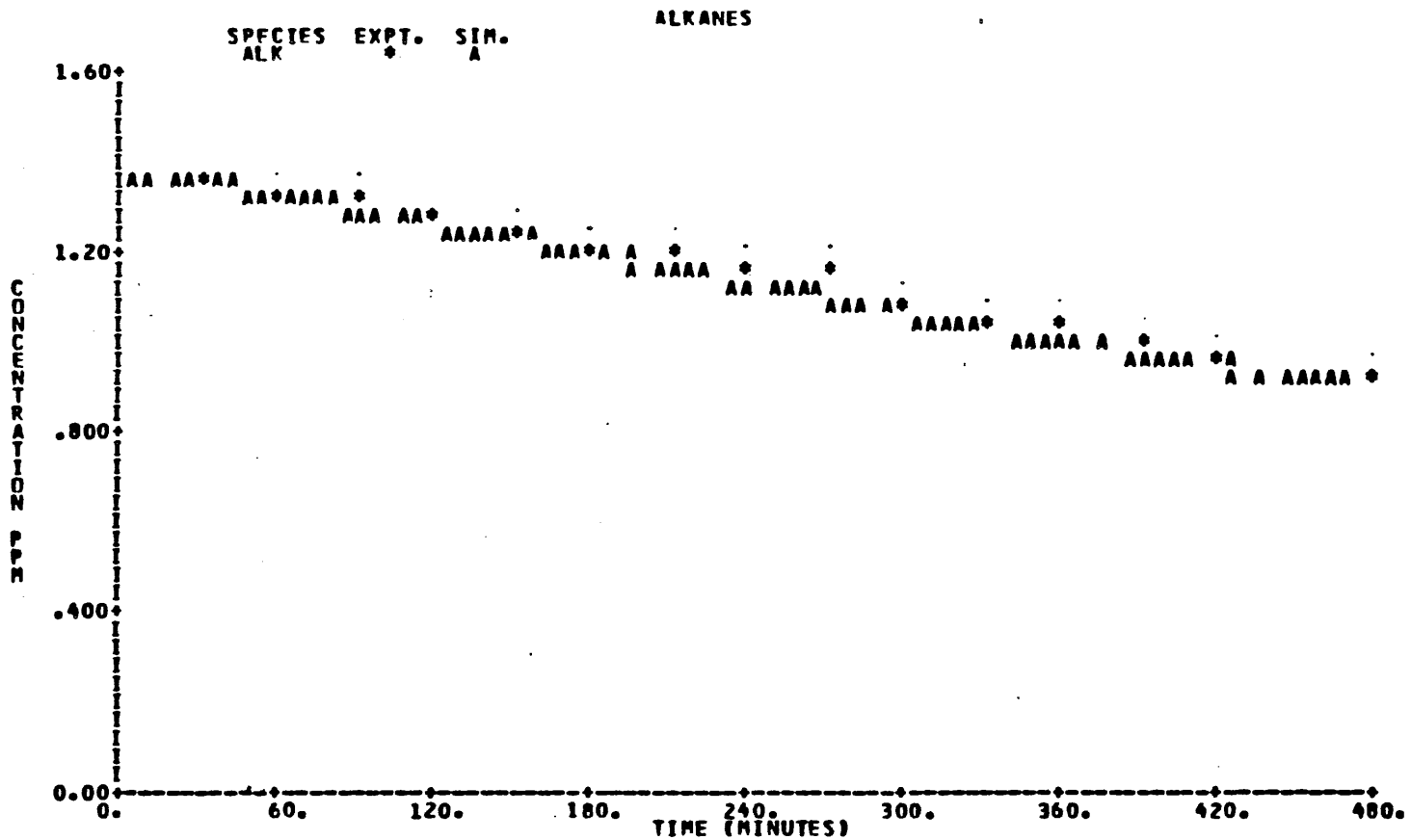

Figure A.14.b. Comparison of Concentration-Time Profiles Predicted by the SUR2 Mechanism with Experimental Data from SAPRC Experiment EC-238.

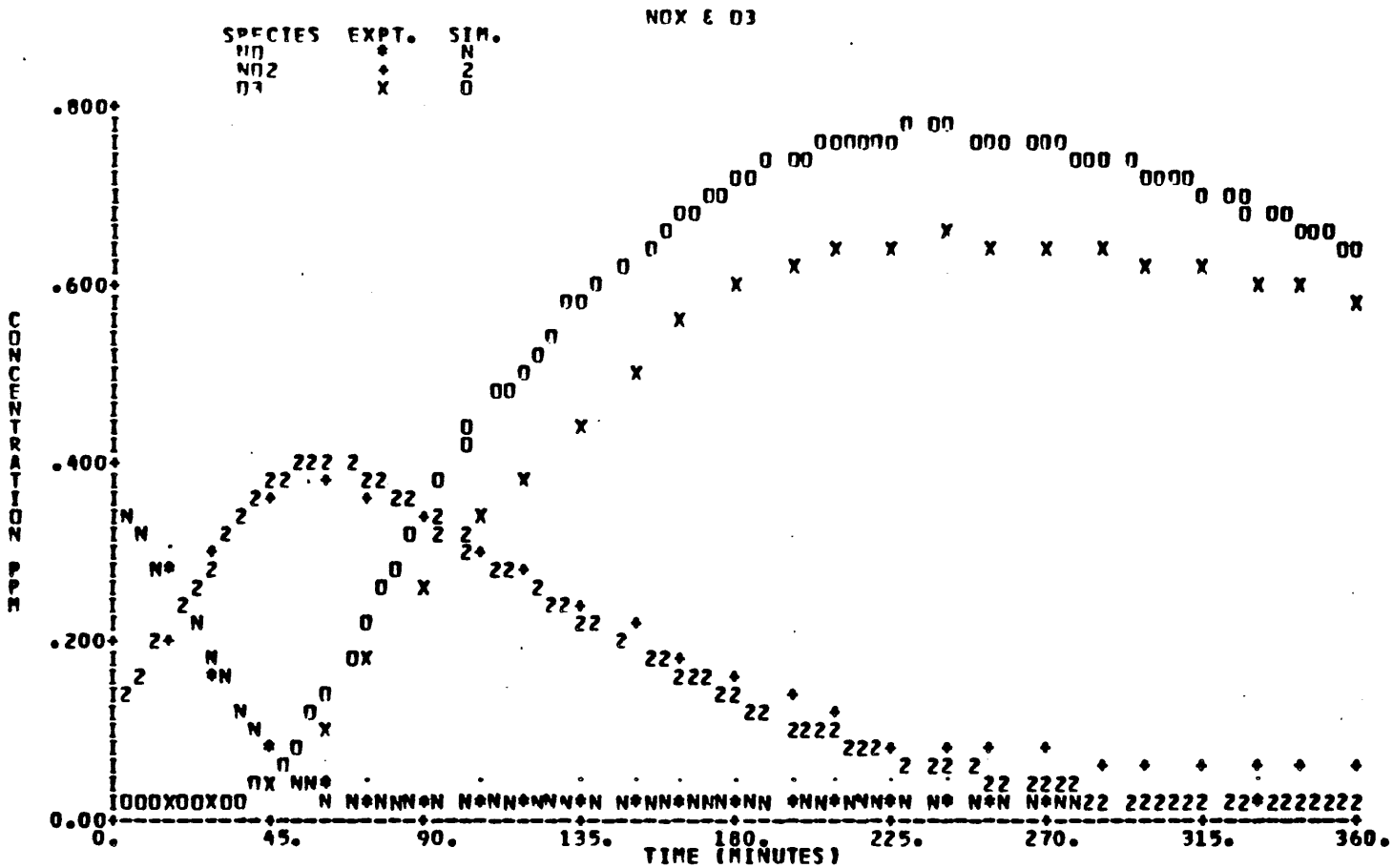

Figure A.15.a. Comparison of Concentration-Time Profiles Predicted by the SUR2 Mechanism with Experimental Data from SAPRC Experiment EC-237.

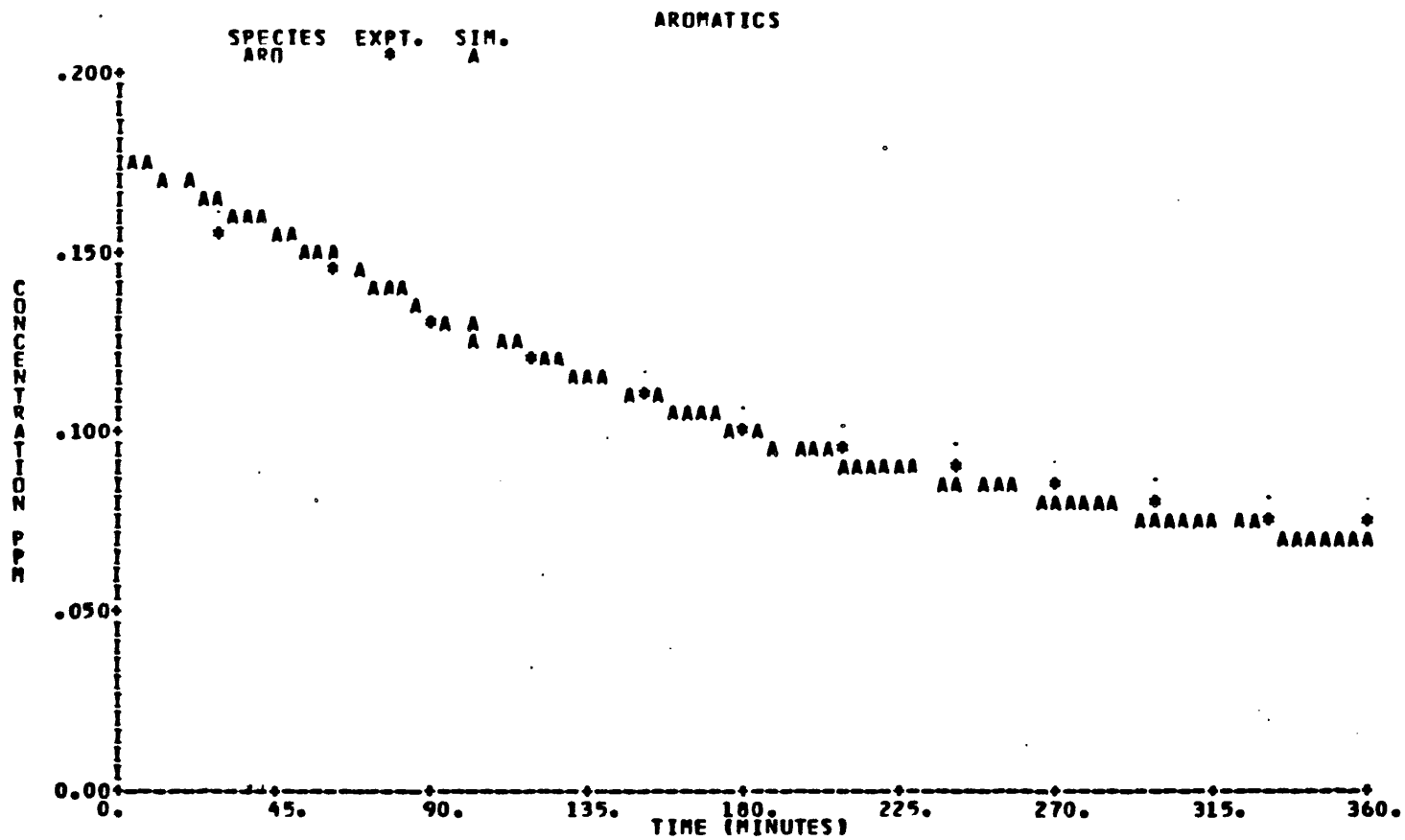

Figure A.15.b. Comparison of Concentration-Time Profiles Predicted by the SUR2 Mechanism with Experimental Data from SAPRC Experiment EC-237.

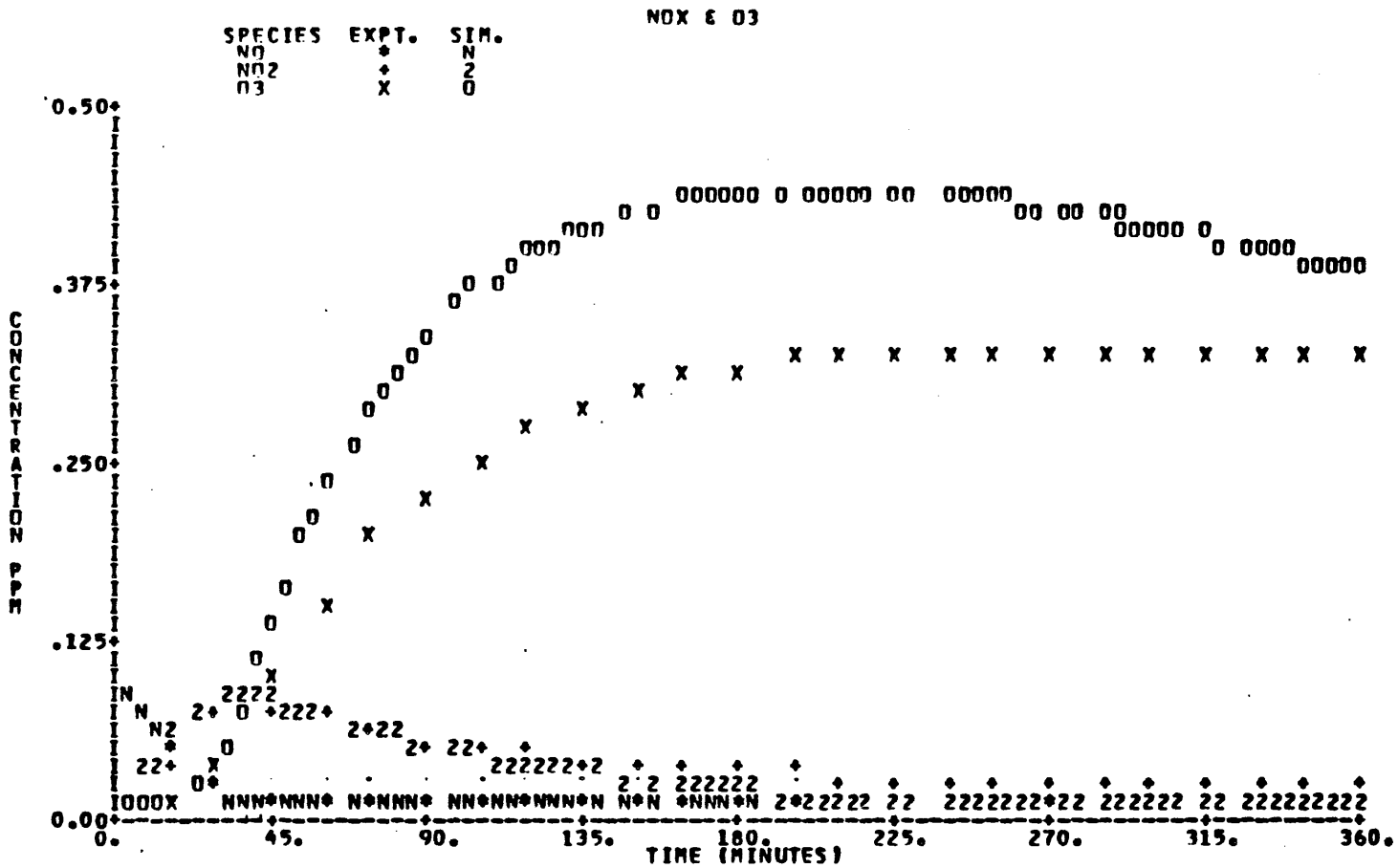

Figure A.16.a. Comparison of Concentration-Time Profiles Predicted by the SUR2 Mechanism with Experimental Data from SAPRC Experiment EC-233.

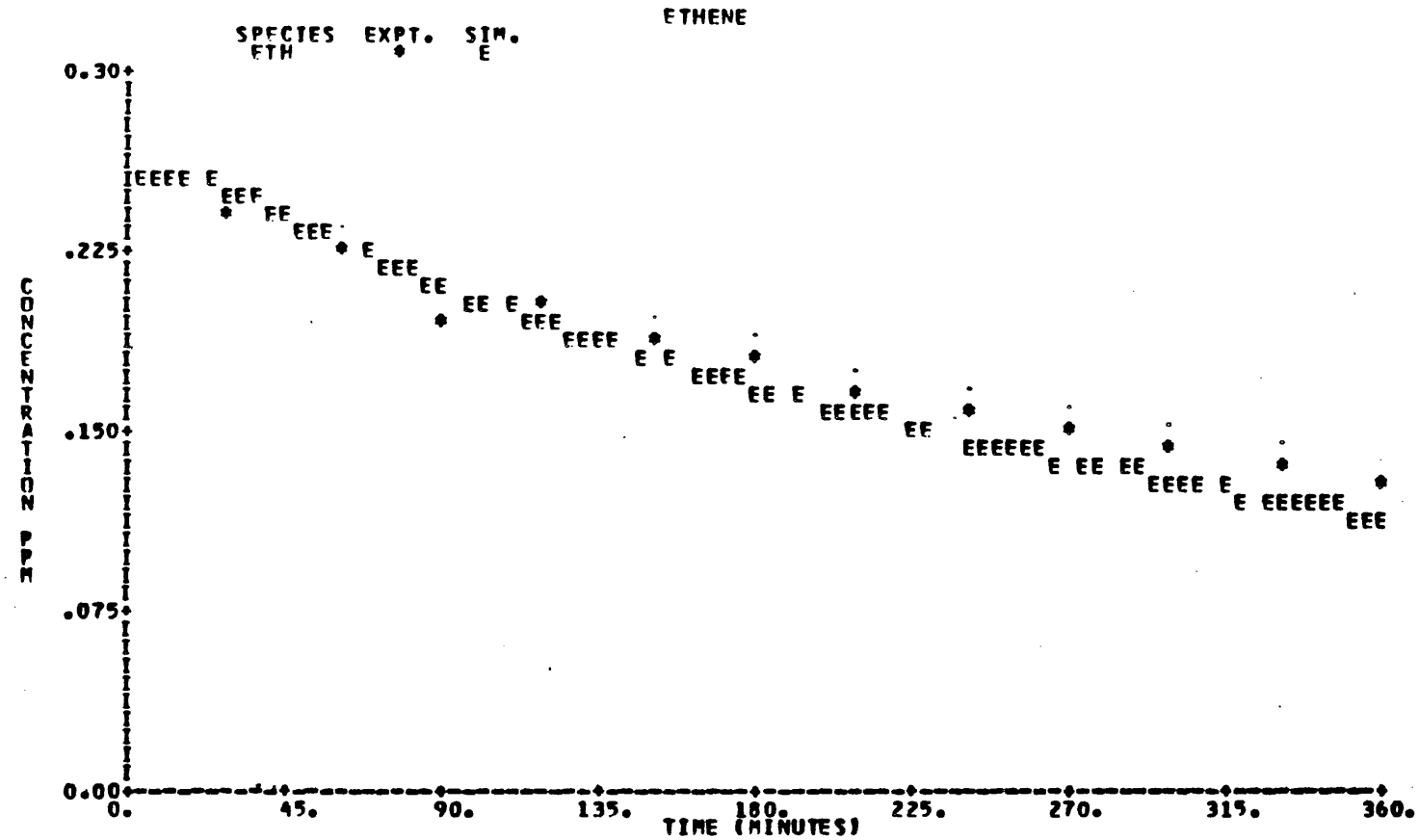

Figure A.16.b. Comparison of Concentration-Time Profiles Predicted by the SUR2 Mechanism with Experimental Data from SAPRC Experiment EC-233.

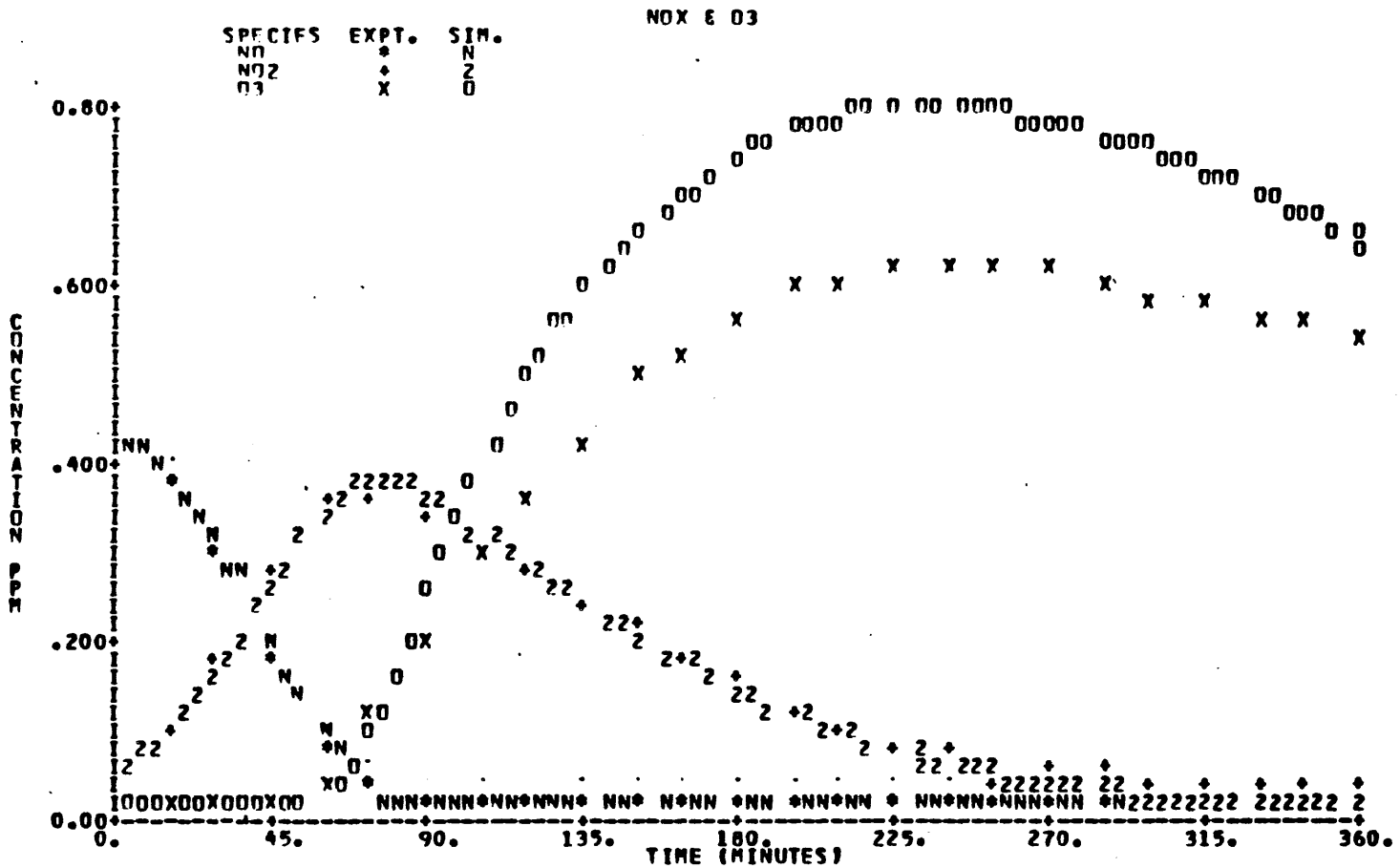

Figure A.17.a. Comparison of Concentration-Time Profiles Predicted by the SUR2 Mechanism with Experimental Data from SAPRC Experiment EC-231.

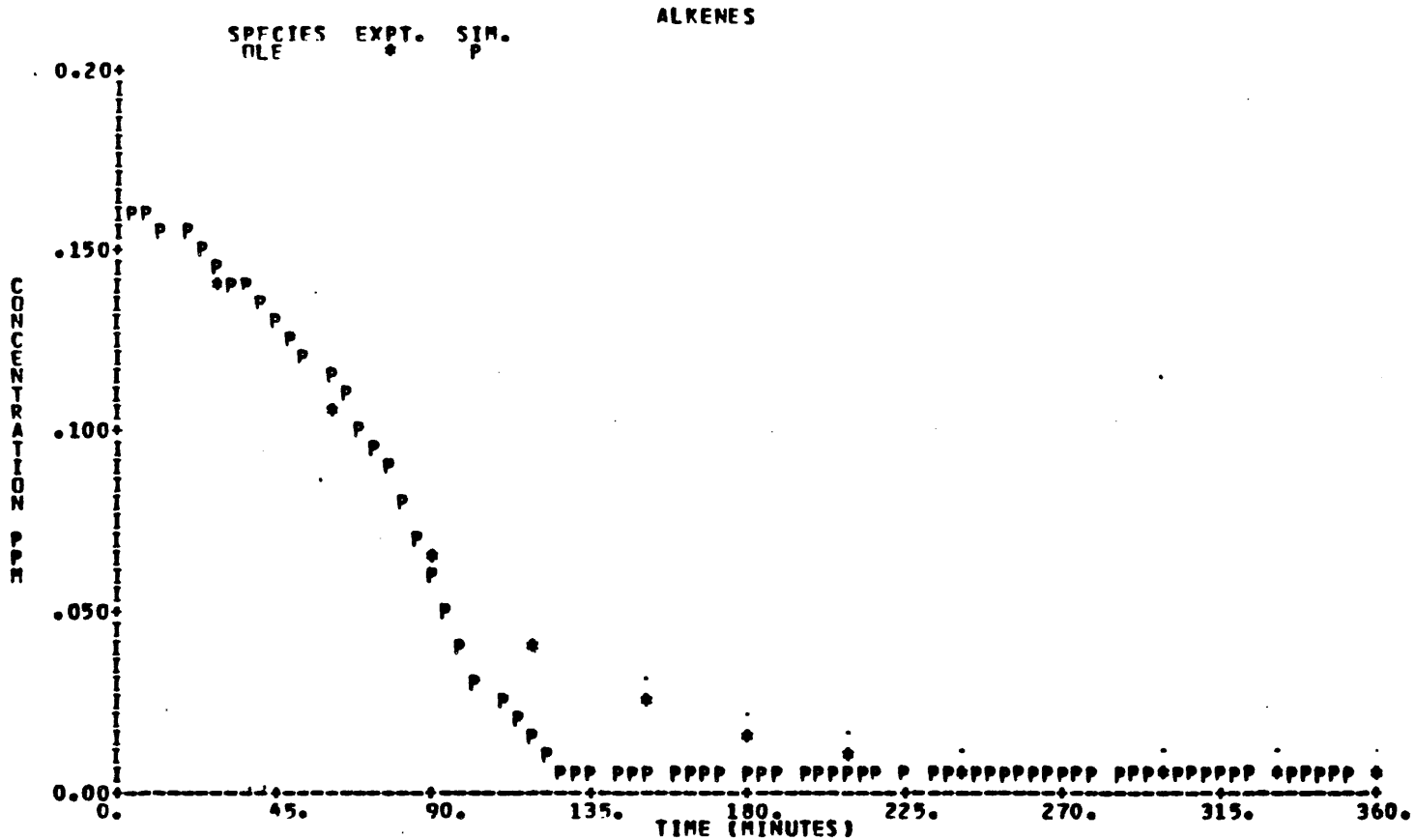

Figure A.17.b. Comparison of Concentration-Time Profiles Predicted by the SUR2 Mechanism with Experimental Data from SAPRC Experiment EC-231.

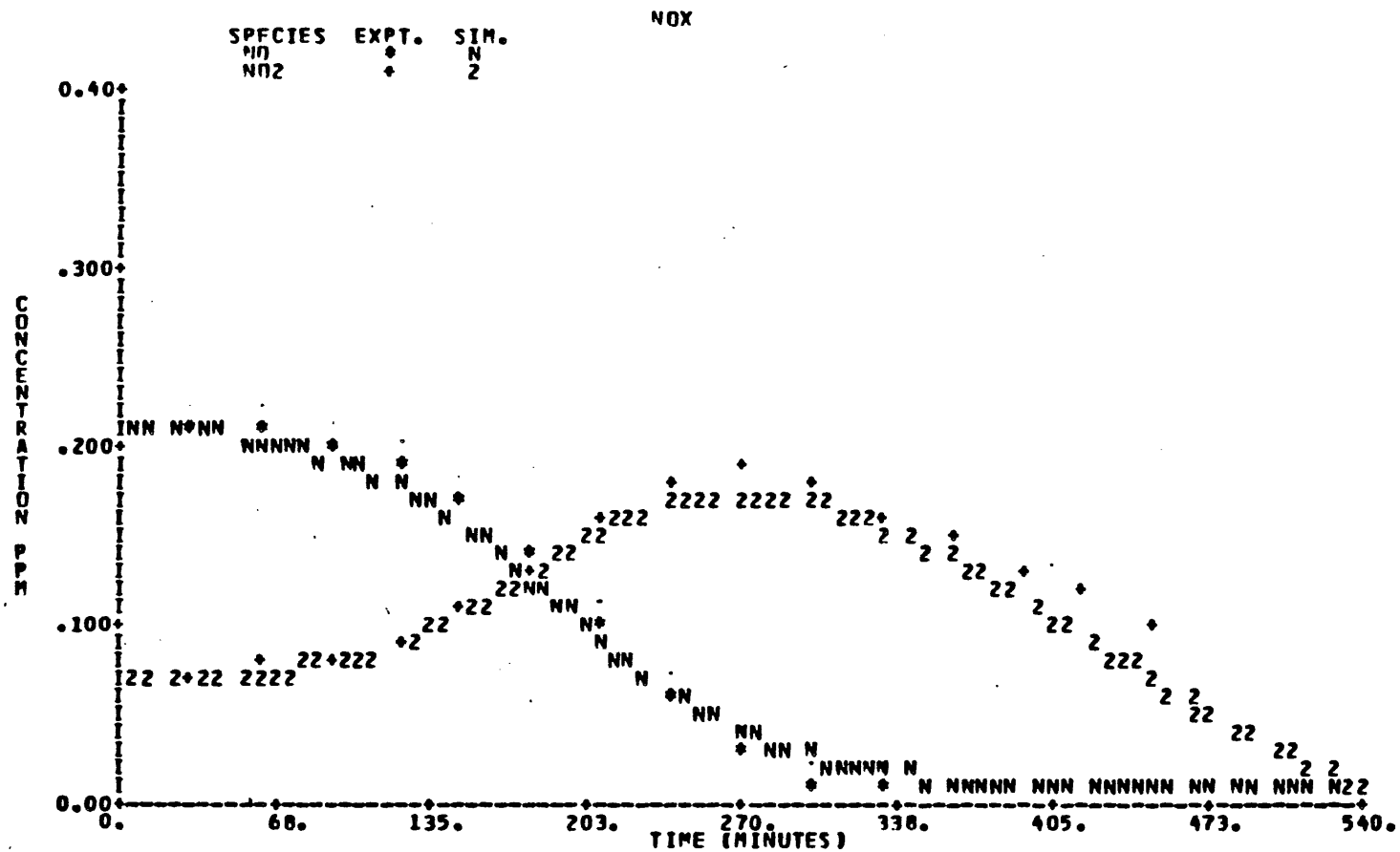

Figure A.18.a. Comparison of Concentration-Time Profiles Predicted by the SUR2 Mechanism with Experimental Data from the Blue Side of the UNC Experiment of July 8, 1982.

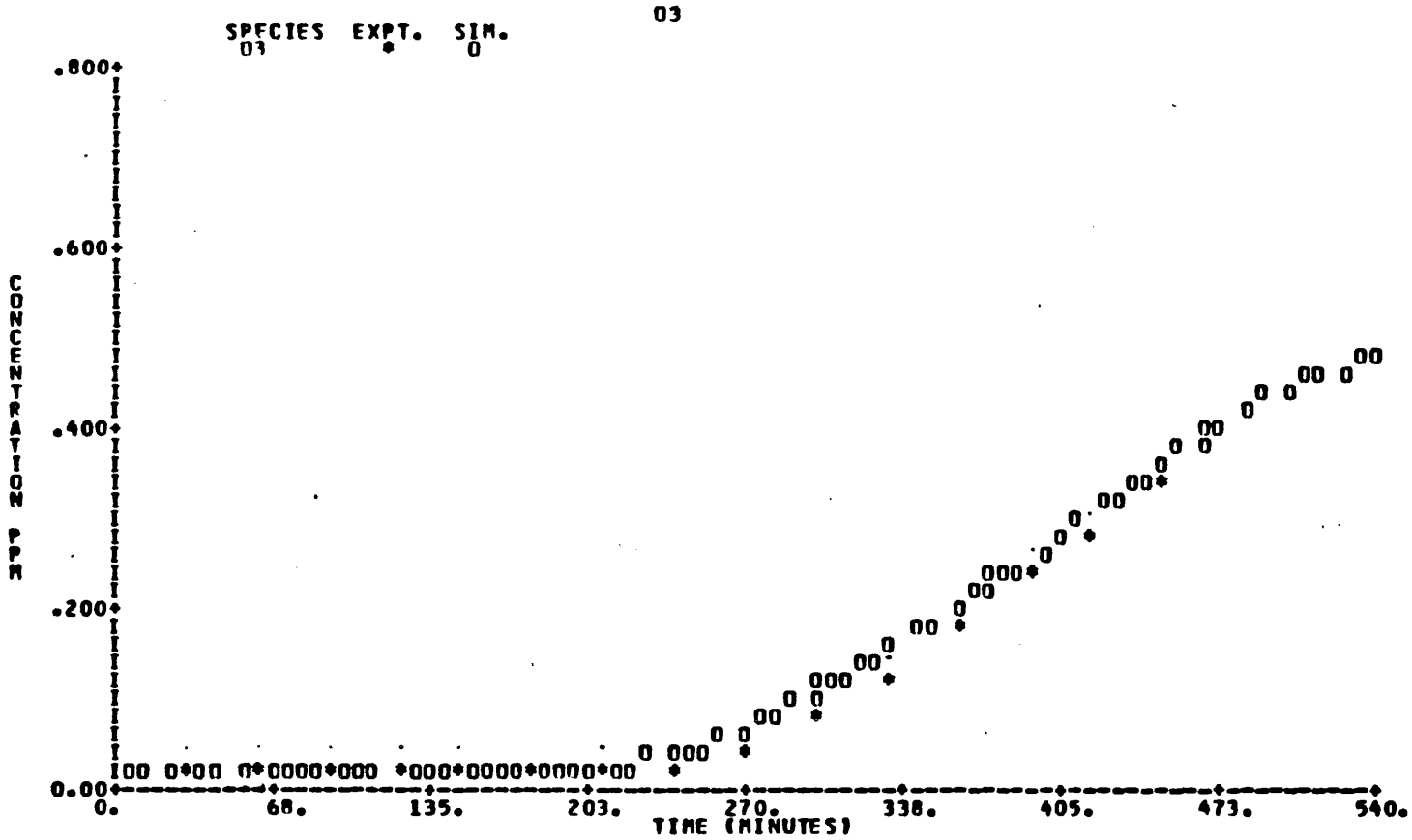

Figure A.18.b. Comparison of Concentration-Time Profiles Predicted by the SUR2 Mechanism with Experimental Data from the Blue Side of the UNC Experiment of July 8, 1982.

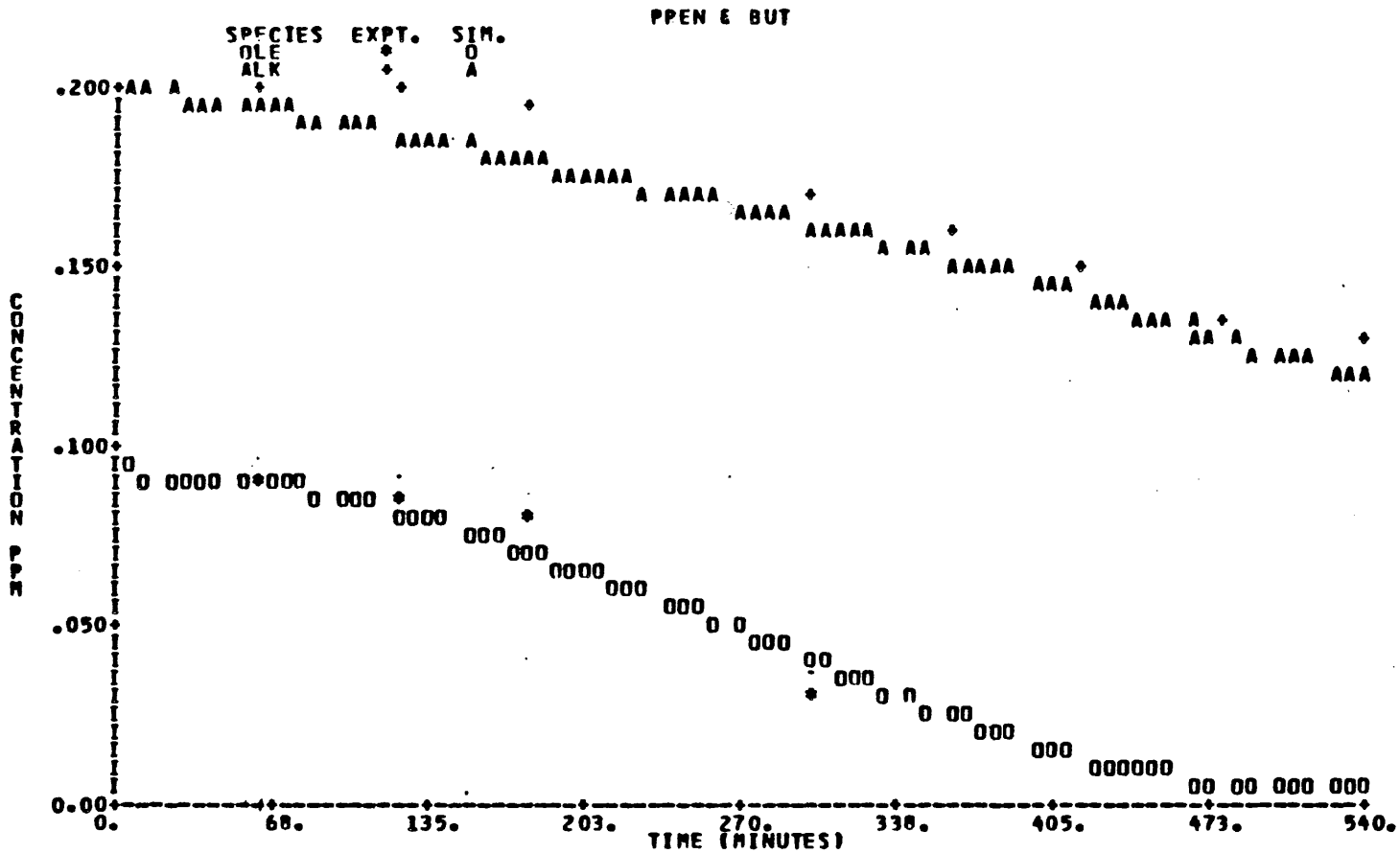

Figure A.18.c. Comparison of Concentration-Time Profiles Predicted by the SUR2 Mechanism with Experimental Data from the Blue Side of the UNC Experiment of July 8, 1982.

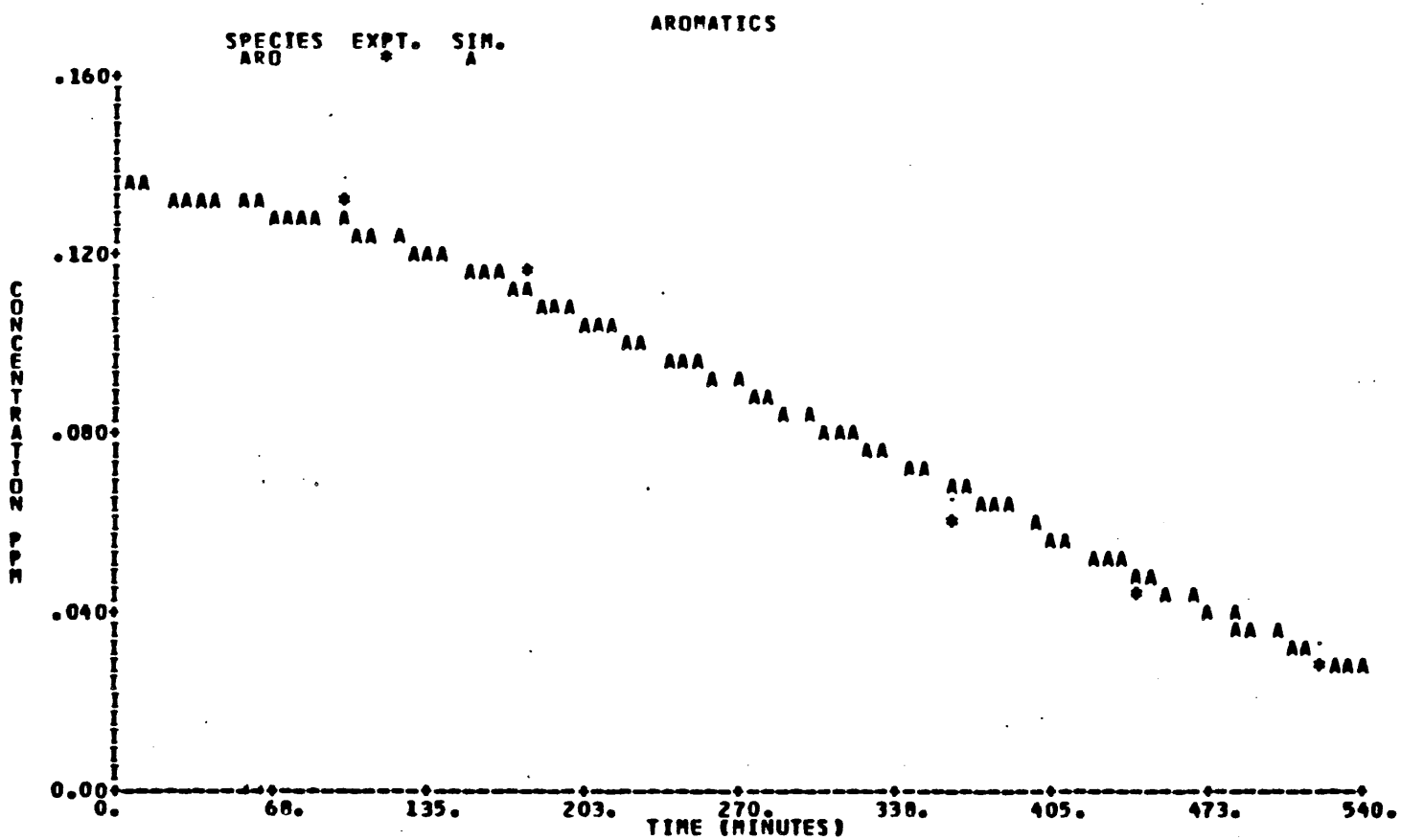

Figure A.18.d. Comparison of Concentration-Time Profiles Predicted by the SUR2 Mechanism with Experimental Data from the Blue Side of the UNC Experiment of July 8, 1982.

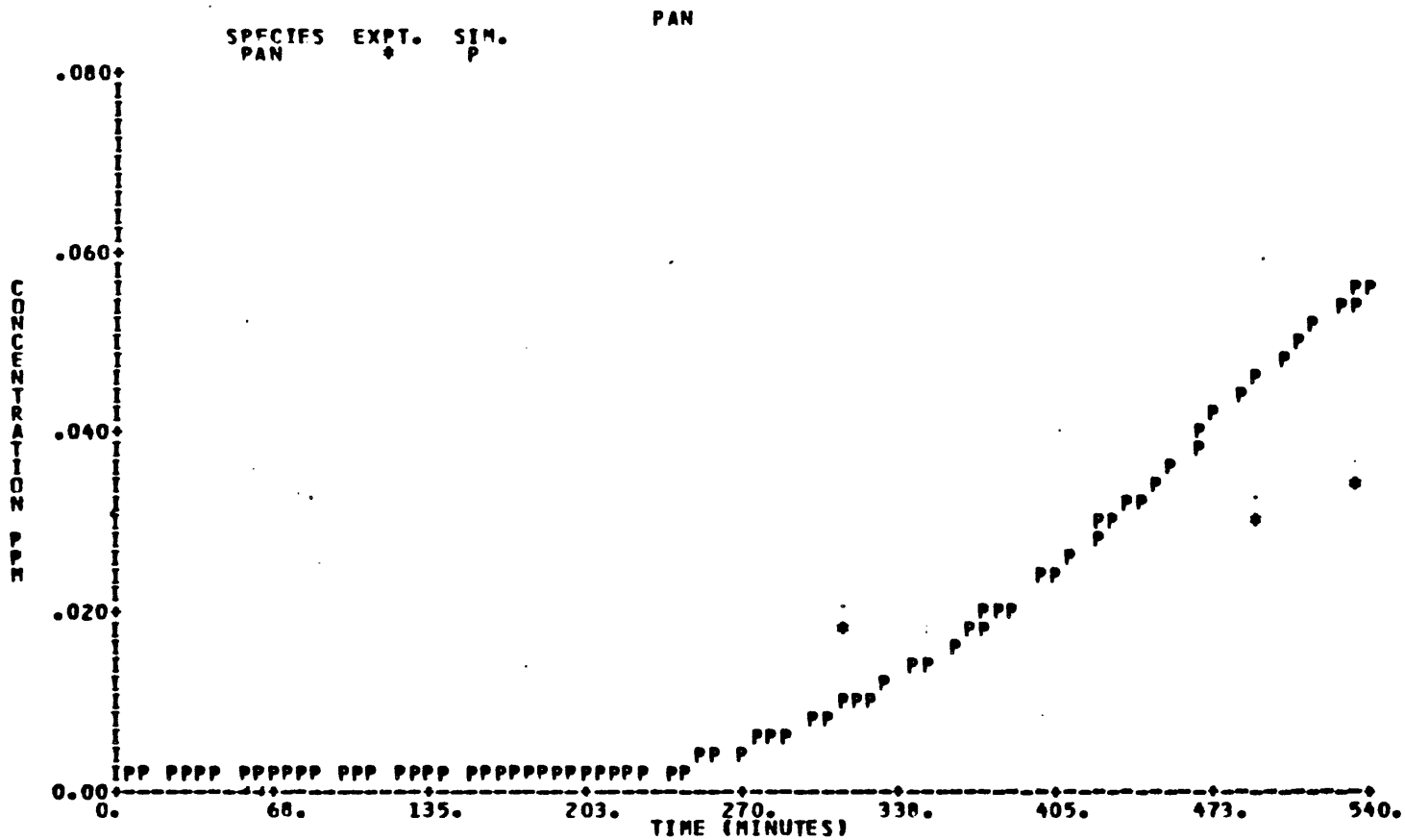

Figure A.18.e. Comparison of Concentration-Time Profiles Predicted by the SUR2 Mechanism with Experimental Data from the Blue Side of the UNC Experiment of July 8, 1982.

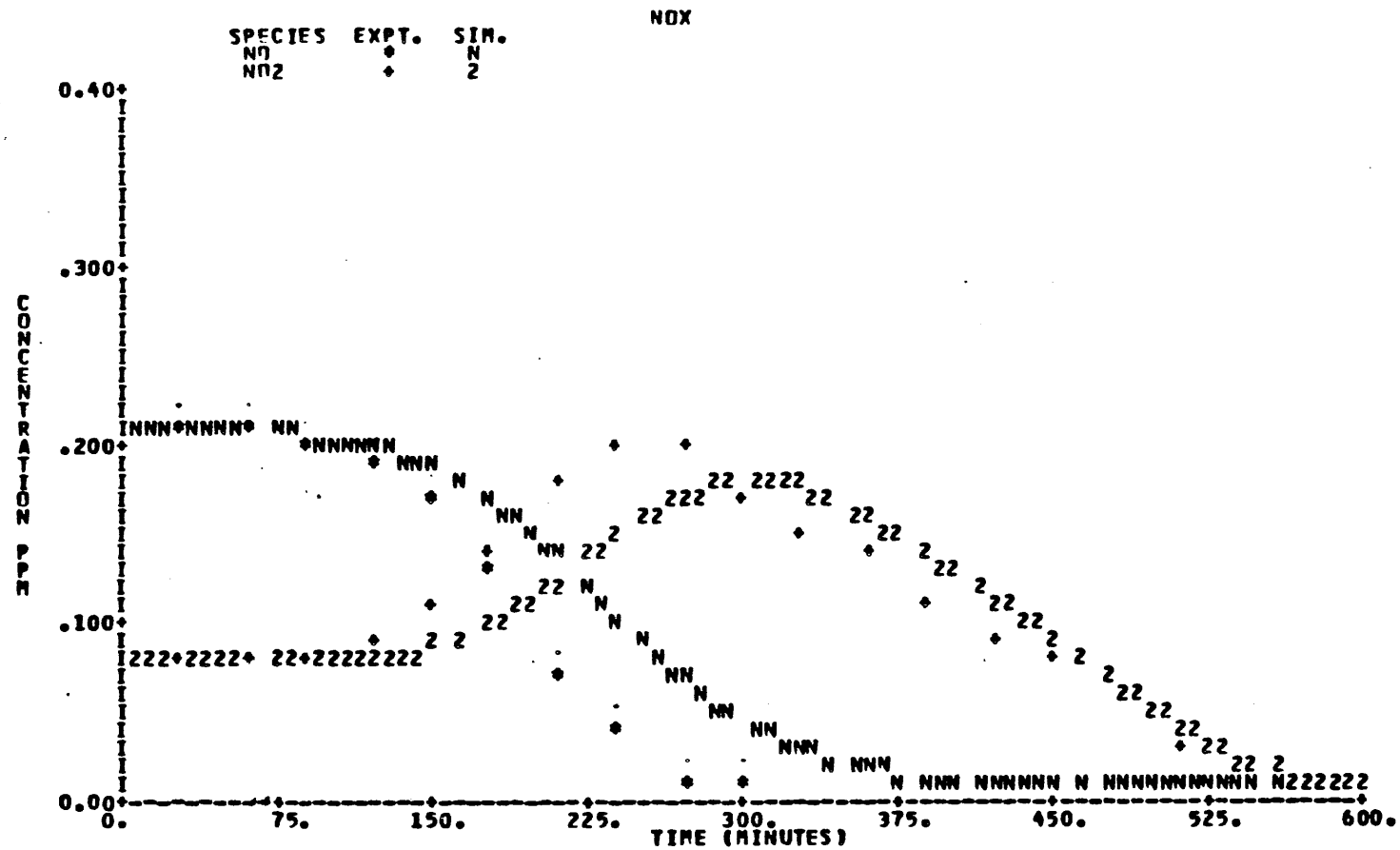

Figure A.19.a. Comparison of Concentration-Time Profiles Predicted by the SUR2 Mechanism with Experimental Data from the Red Side of the UNC Experiment of July 8, 1982.

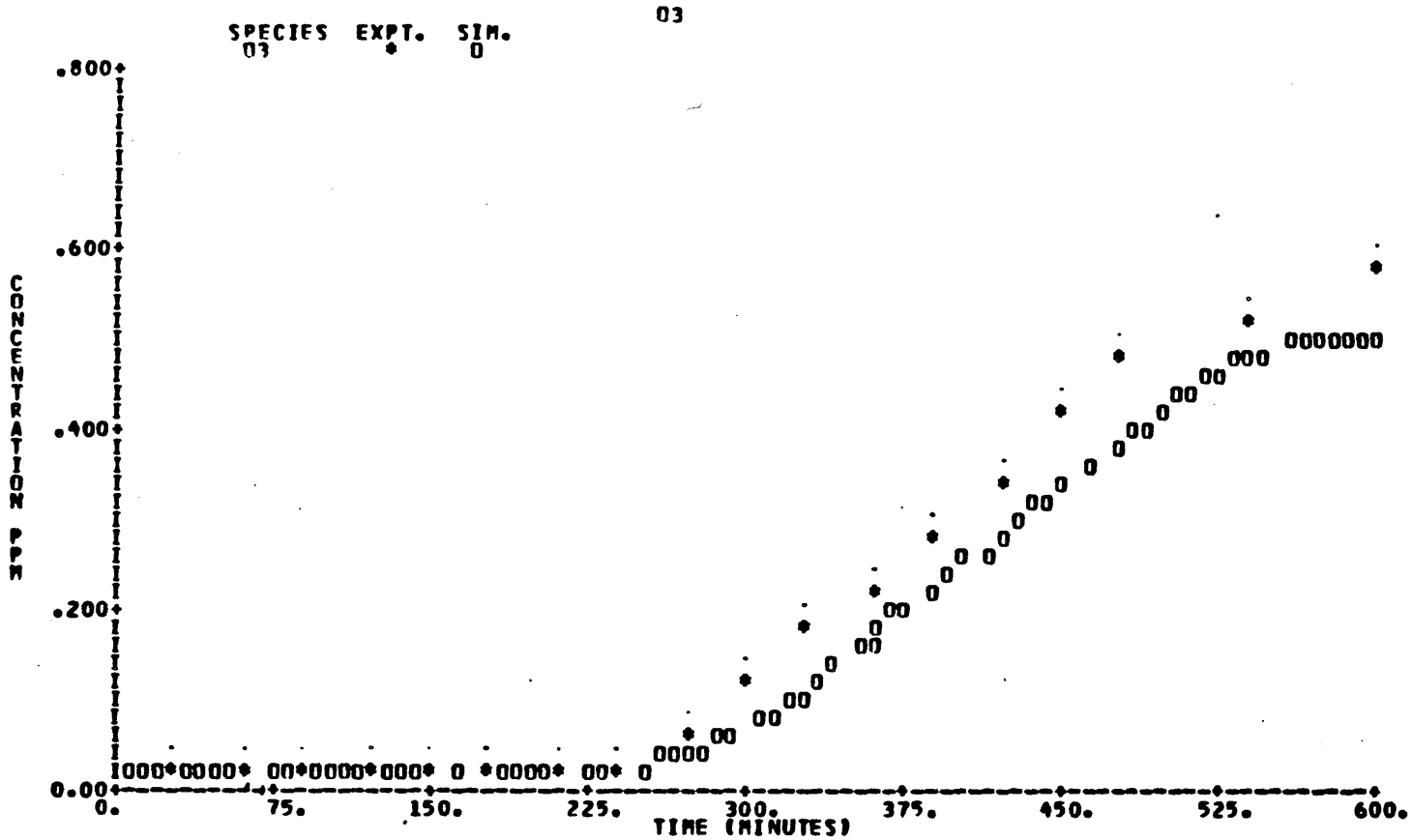

Figure A.19.b. Comparison of Concentration-Time Profiles Predicted by the SUR2 Mechanism with Experimental Data from the Red Side of the UNC Experiment of July 8, 1982.

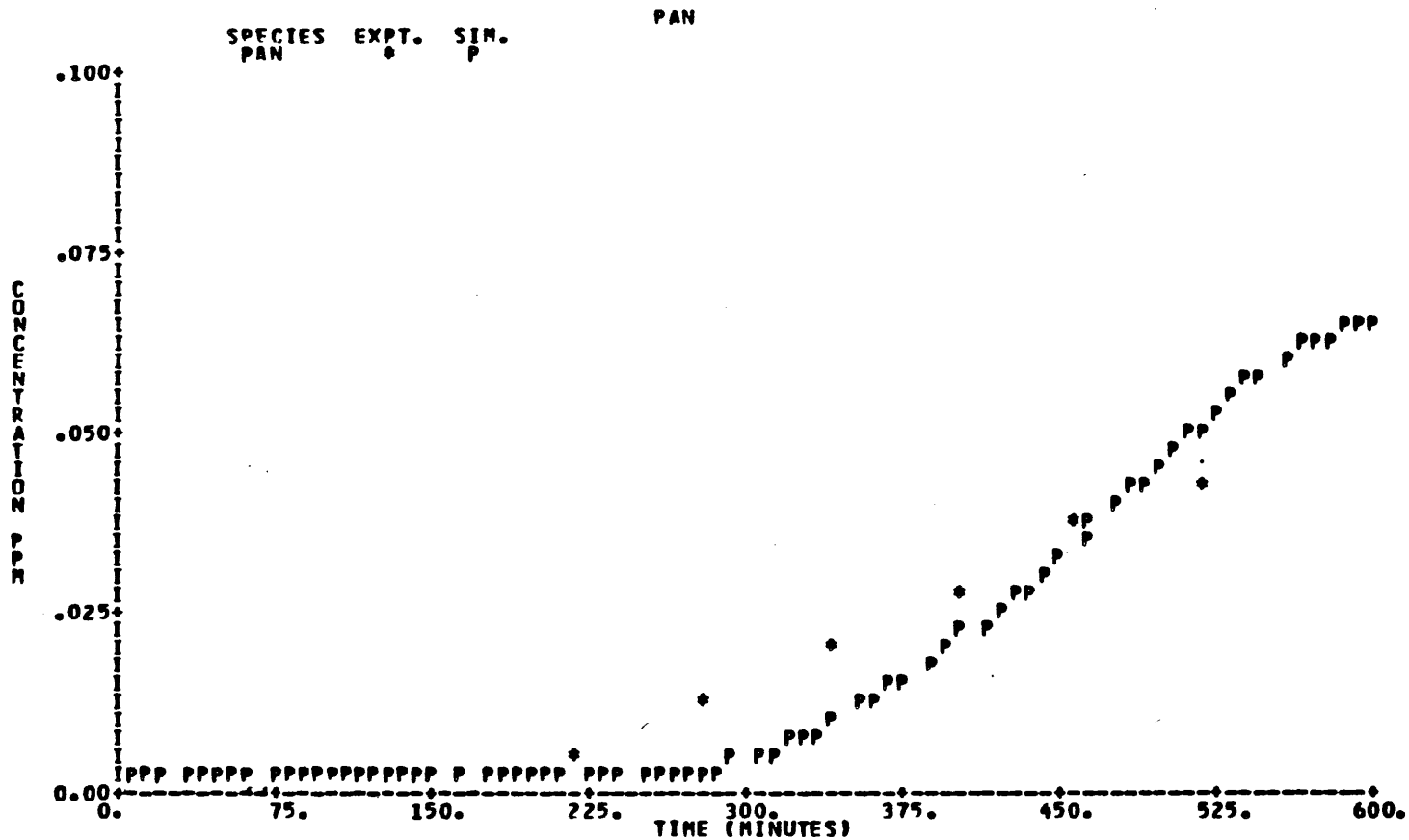

Figure A.19.c. Comparison of Concentration-Time Profiles Predicted by the SUR2 Mechanism with Experimental Data from the Red Side of the UNC Experiment of July 8, 1982.

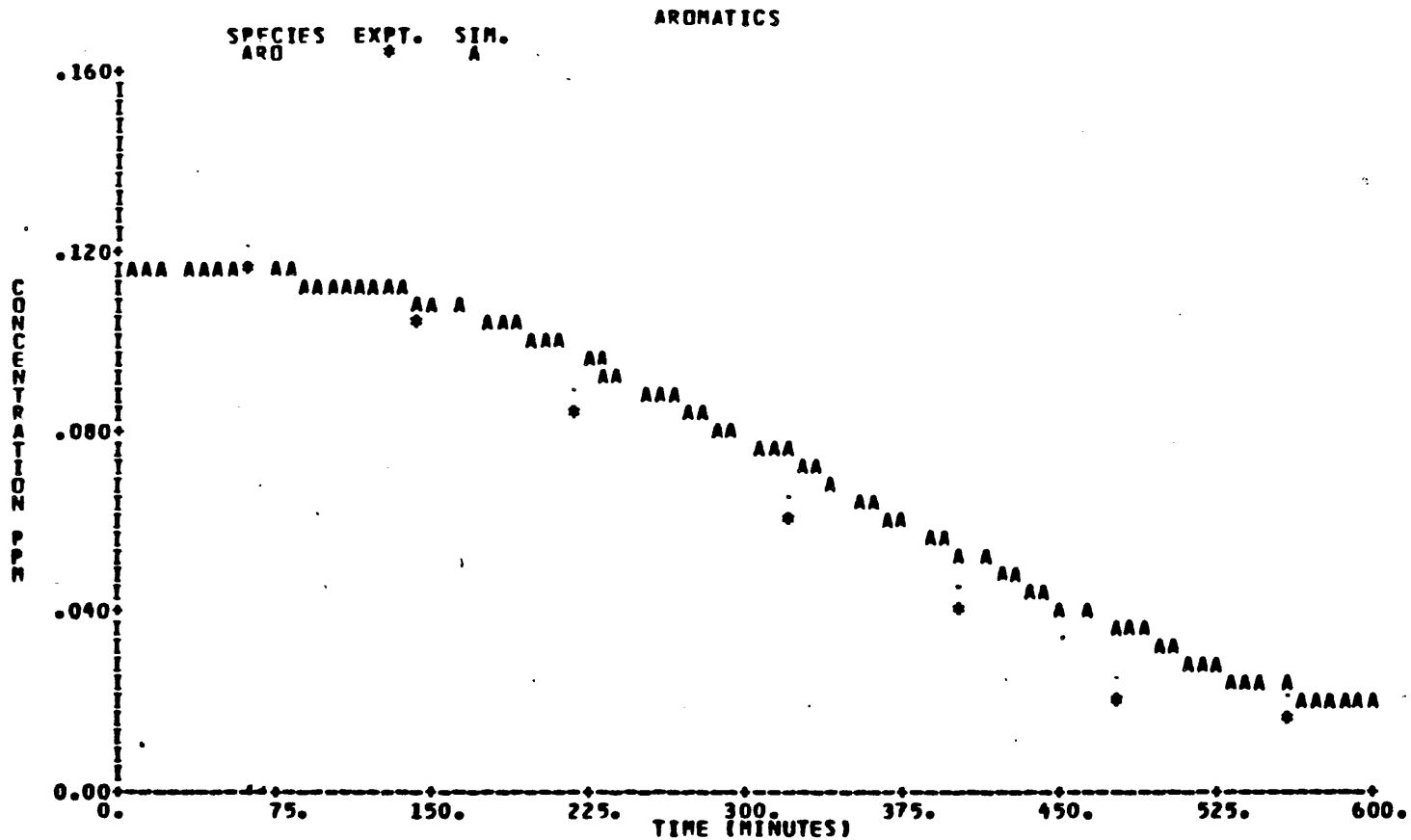

Figure A.19.d. Comparison of Concentration-Time Profiles Predicted by the SUR2 Mechanism with Experimental Data from the Red Side of the UNC Experiment of July 8, 1982.

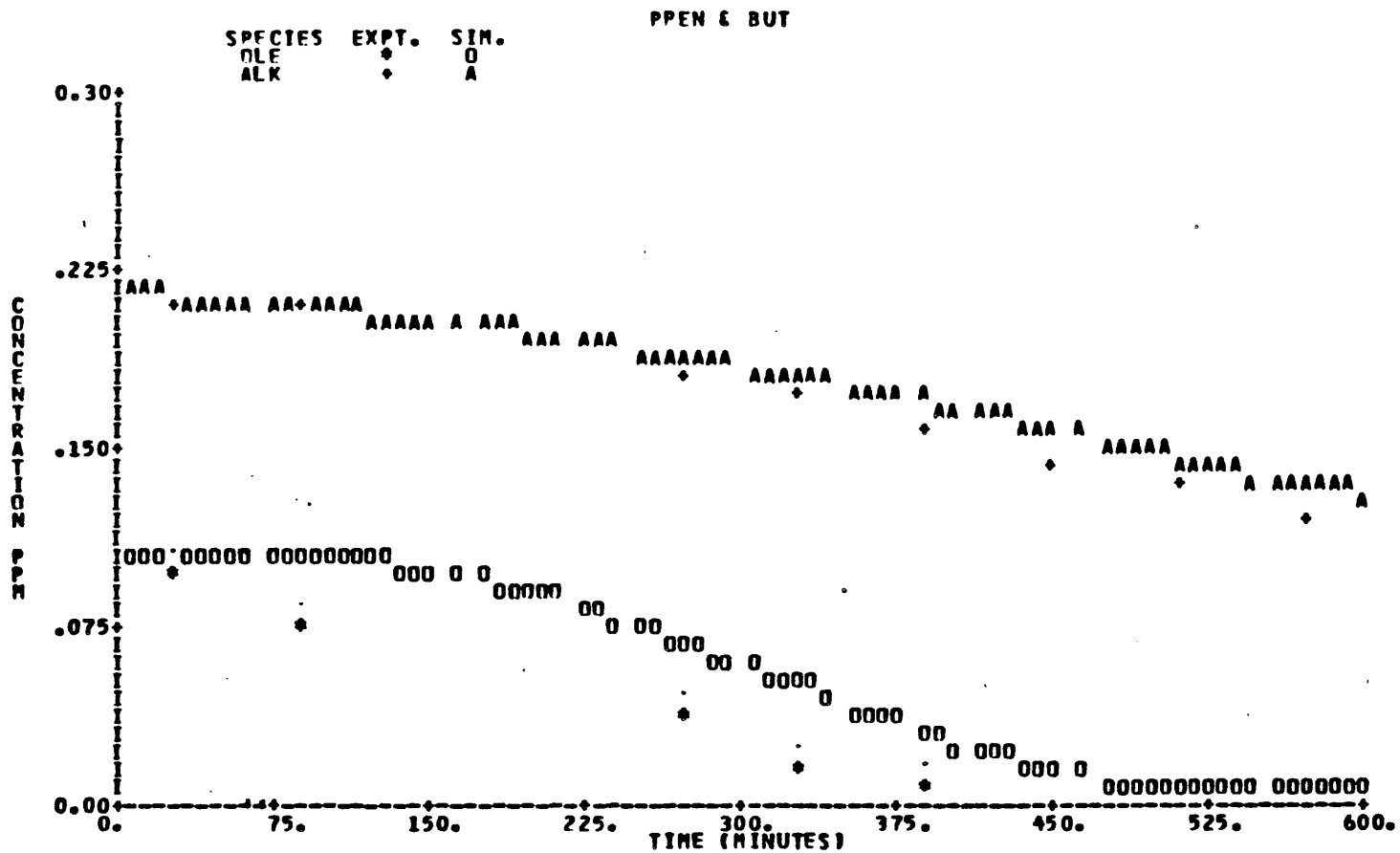

Figure A.19.e. Comparison of Concentration-Time Profiles Predicted by the SUR2 Mechanism with Experimental Data from the Red Side of the UNC Experiment of July 8, 1982.

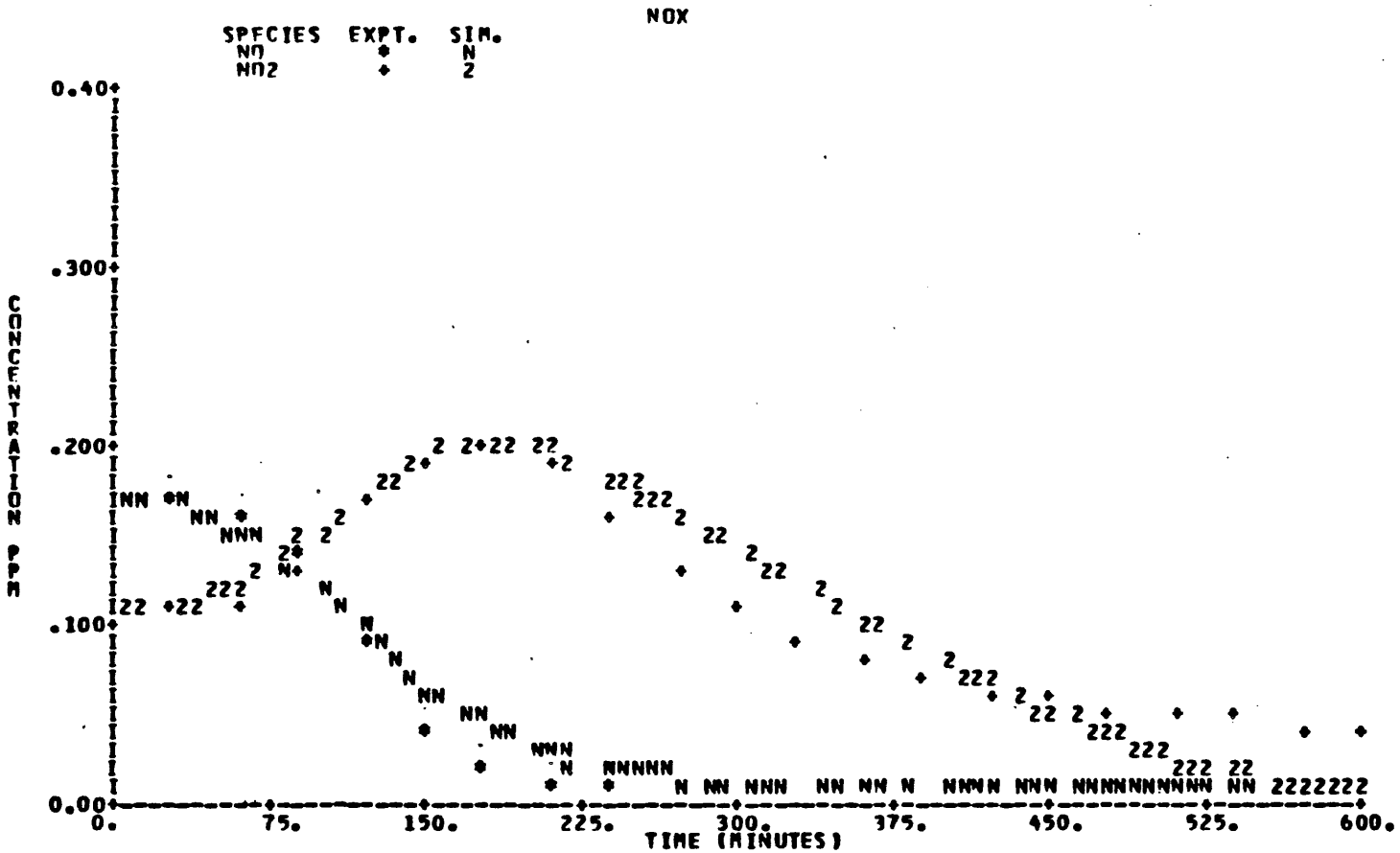

Figure A.20.a. Comparison of Concentration-Time Profiles Predicted by the SUR2 Mechanism with Experimental Data from the Red Side of the UNC Experiment of October 14, 1981.

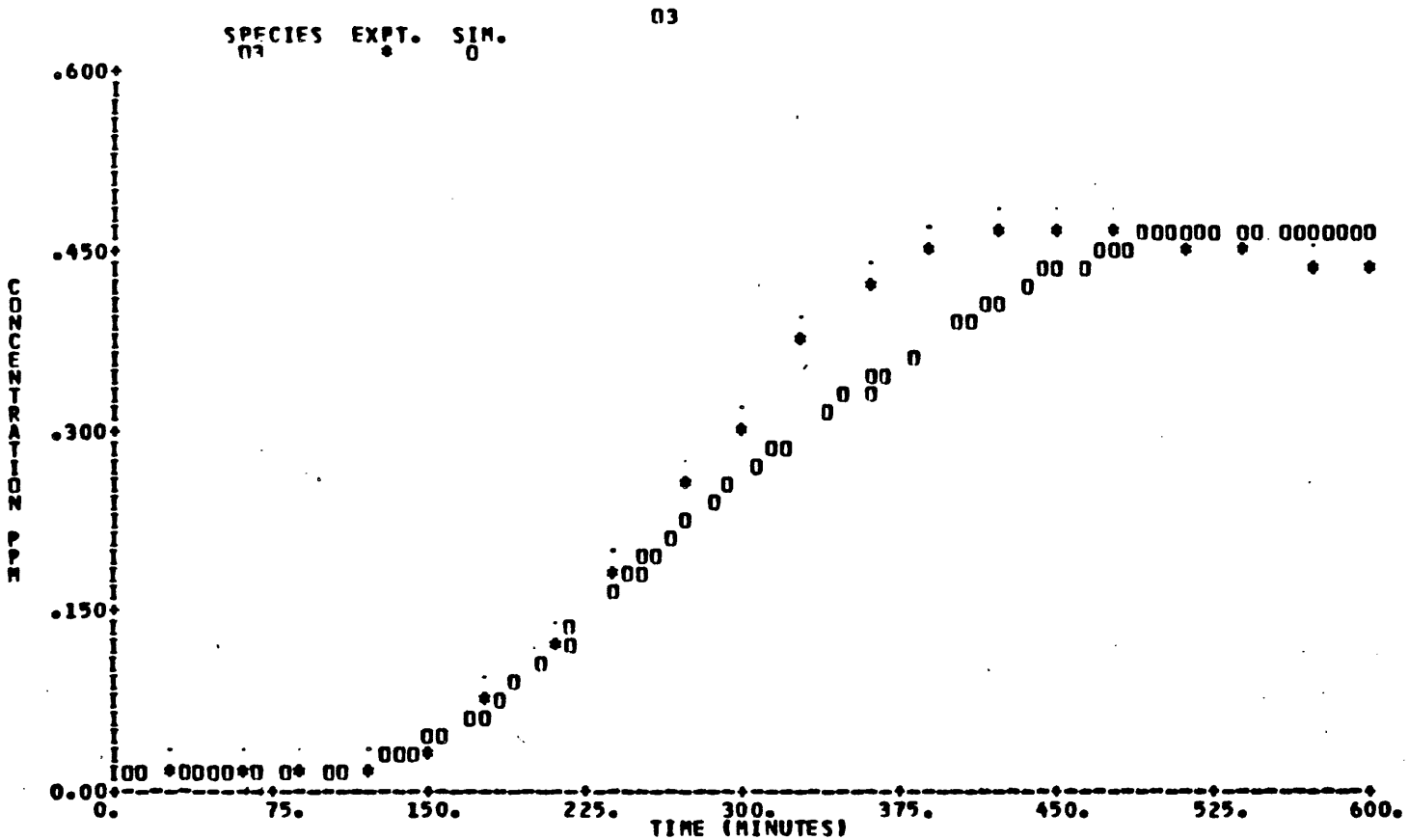

Figure A.20.b. Comparison of Concentration-Time Profiles Predicted by the SUR2 Mechanism with Experimental Data from the Red Side of the UNC Experiment of October 14, 1981.

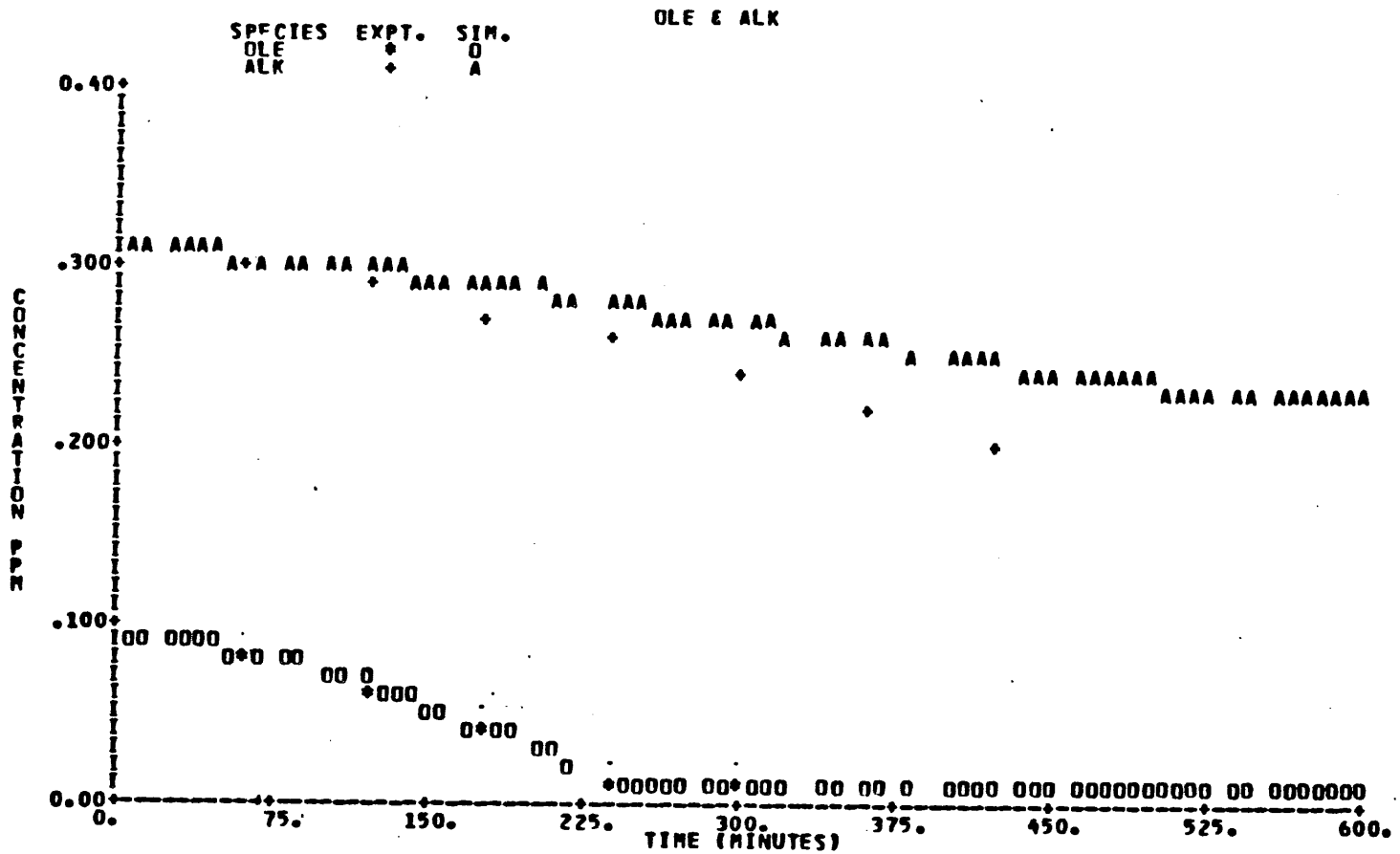

Figure A.20.c. Comparison of Concentration-Time Profiles Predicted by the SUR2 Mechanism with Experimental Data from the Red Side of the UNC Experiment of October 14, 1981.

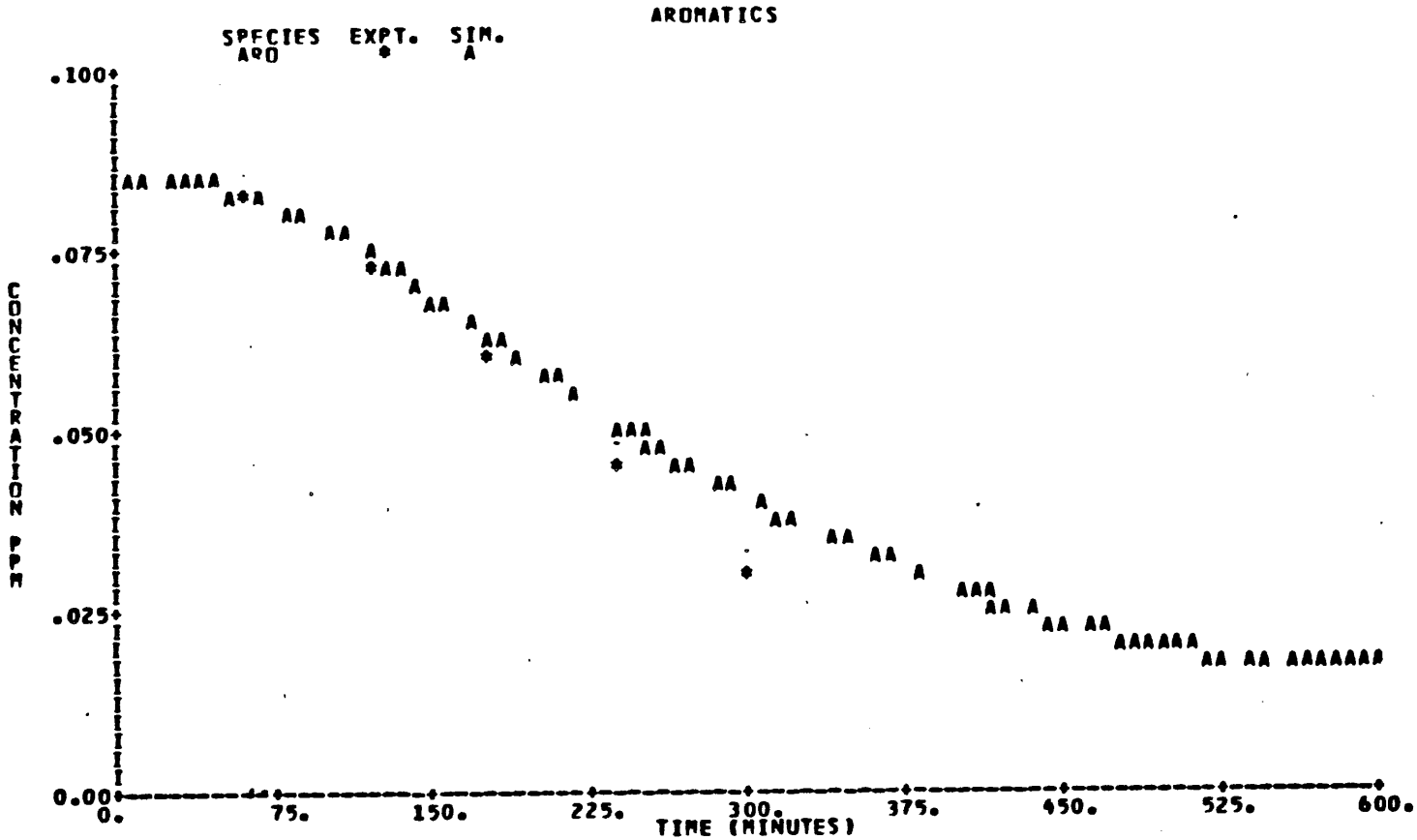

Figure A.20.d. Comparison of Concentration-Time Profiles Predicted by the SUR2 Mechanism with Experimental Data from the Red Side of the UNC Experiment of October 14, 1981.

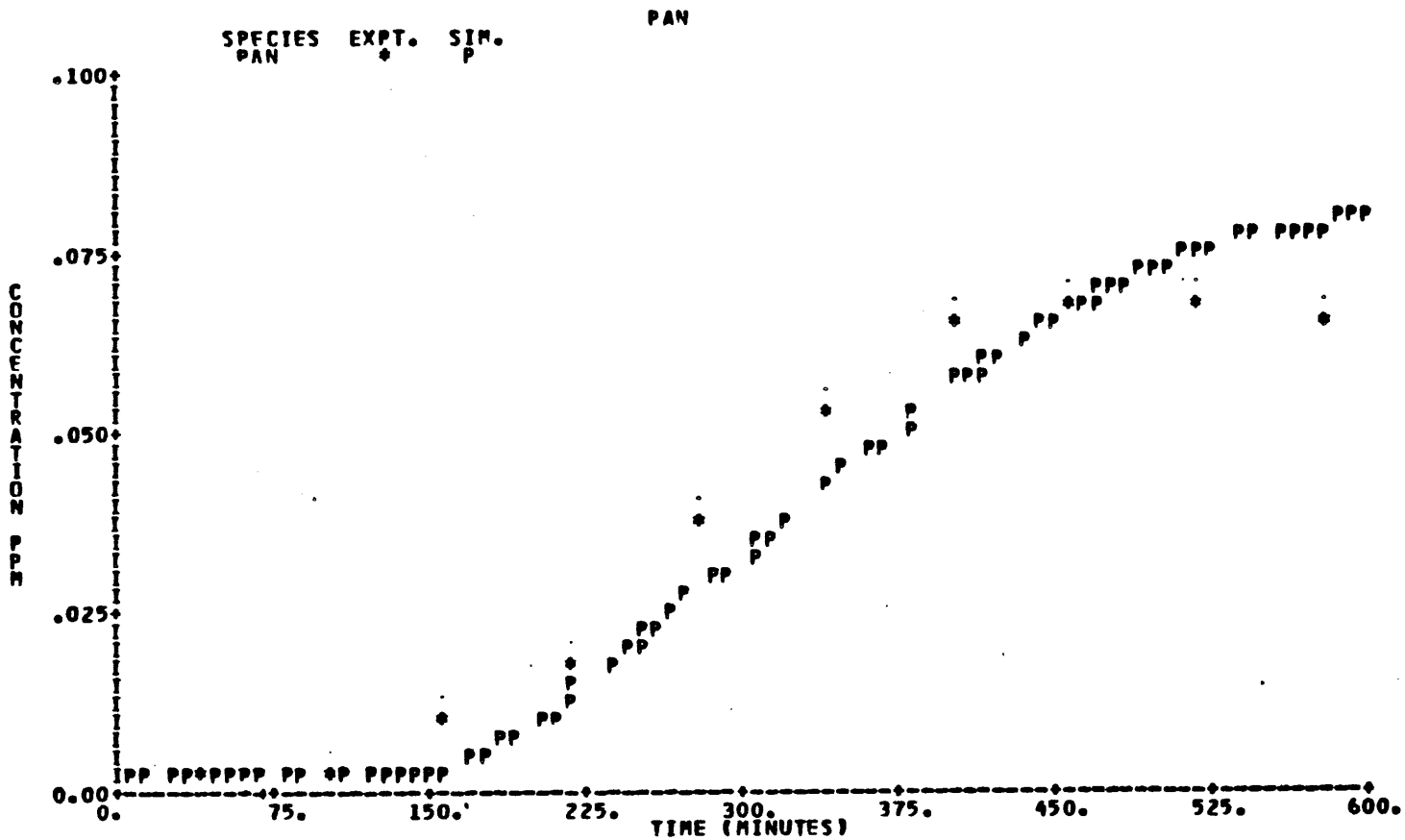

Figure A.20.e. Comparison of Concentration-Time Profiles Predicted by the SUR2 Mechanism with Experimental Data from the Red Side of the UNC Experiment of October 14, 1981.

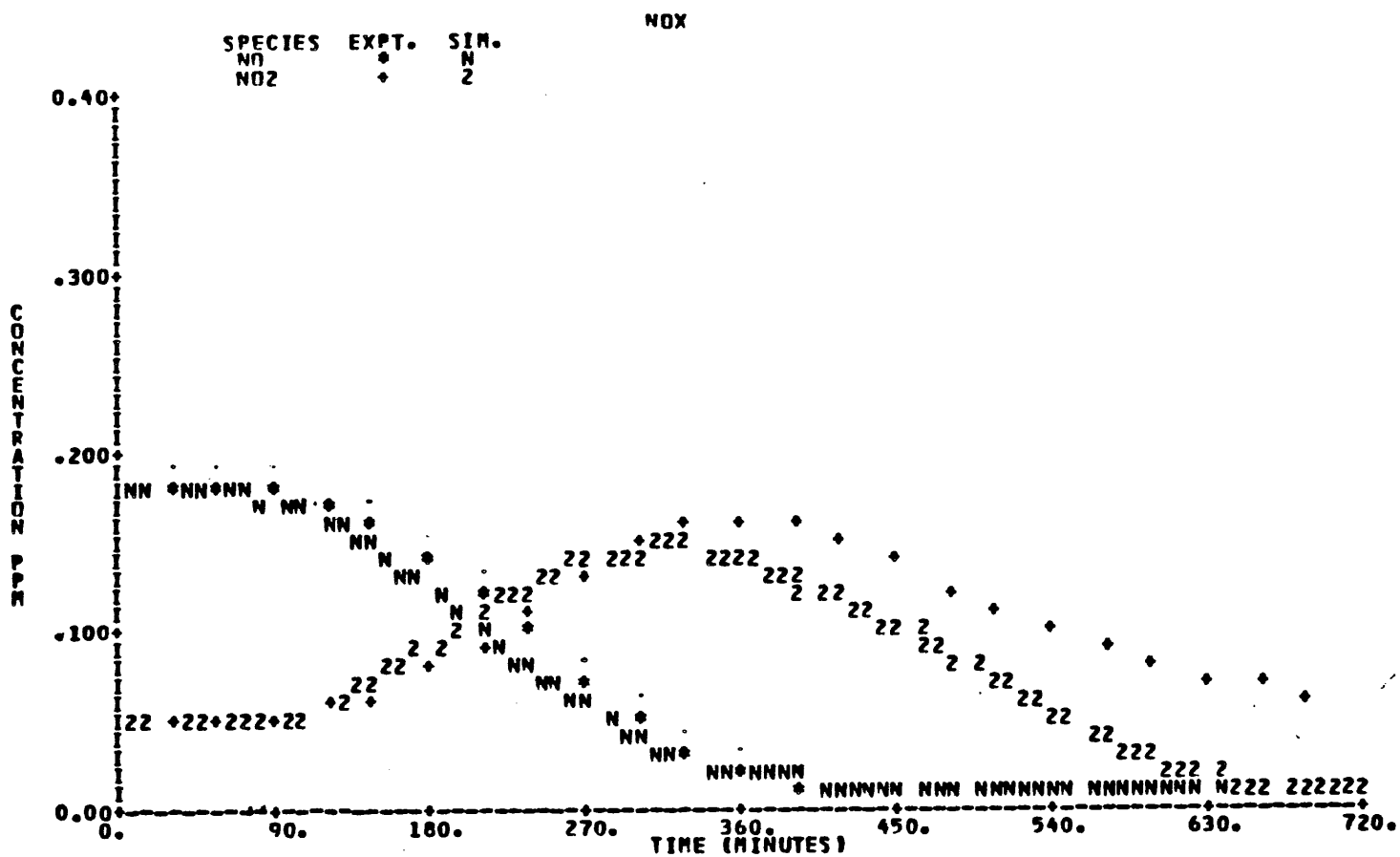

Figure A.21.a. Comparison of Concentration-Time Profiles Predicted by the SUR2 Mechanism with Experimental Data from the Red Side of the UNC Experiment of August 26, 1981.

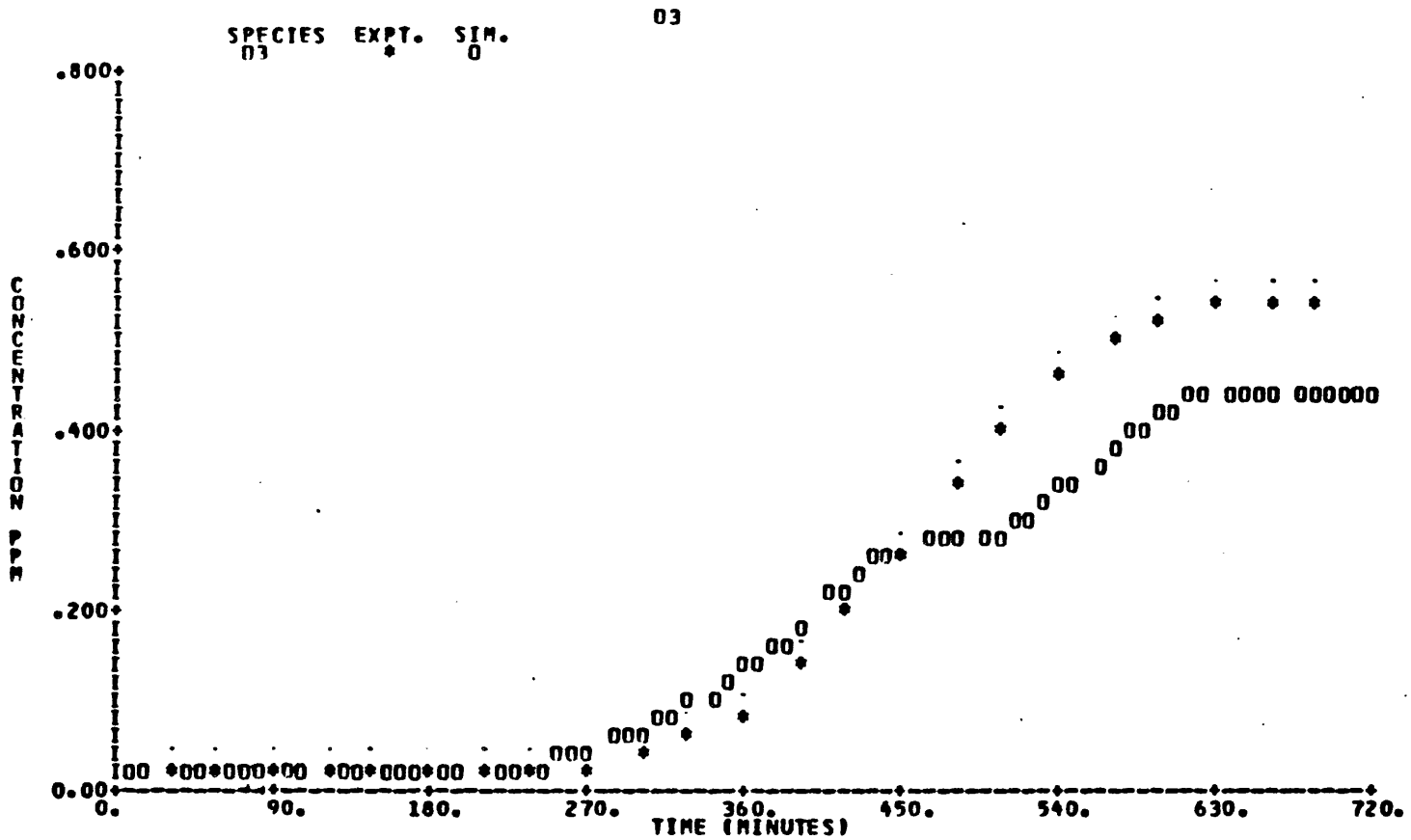

Figure A.21.b. Comparison of Concentration-Time Profiles Predicted by the SUR2 Mechanism with Experimental Data from the Red Side of the UNC Experiment of August 26, 1981.

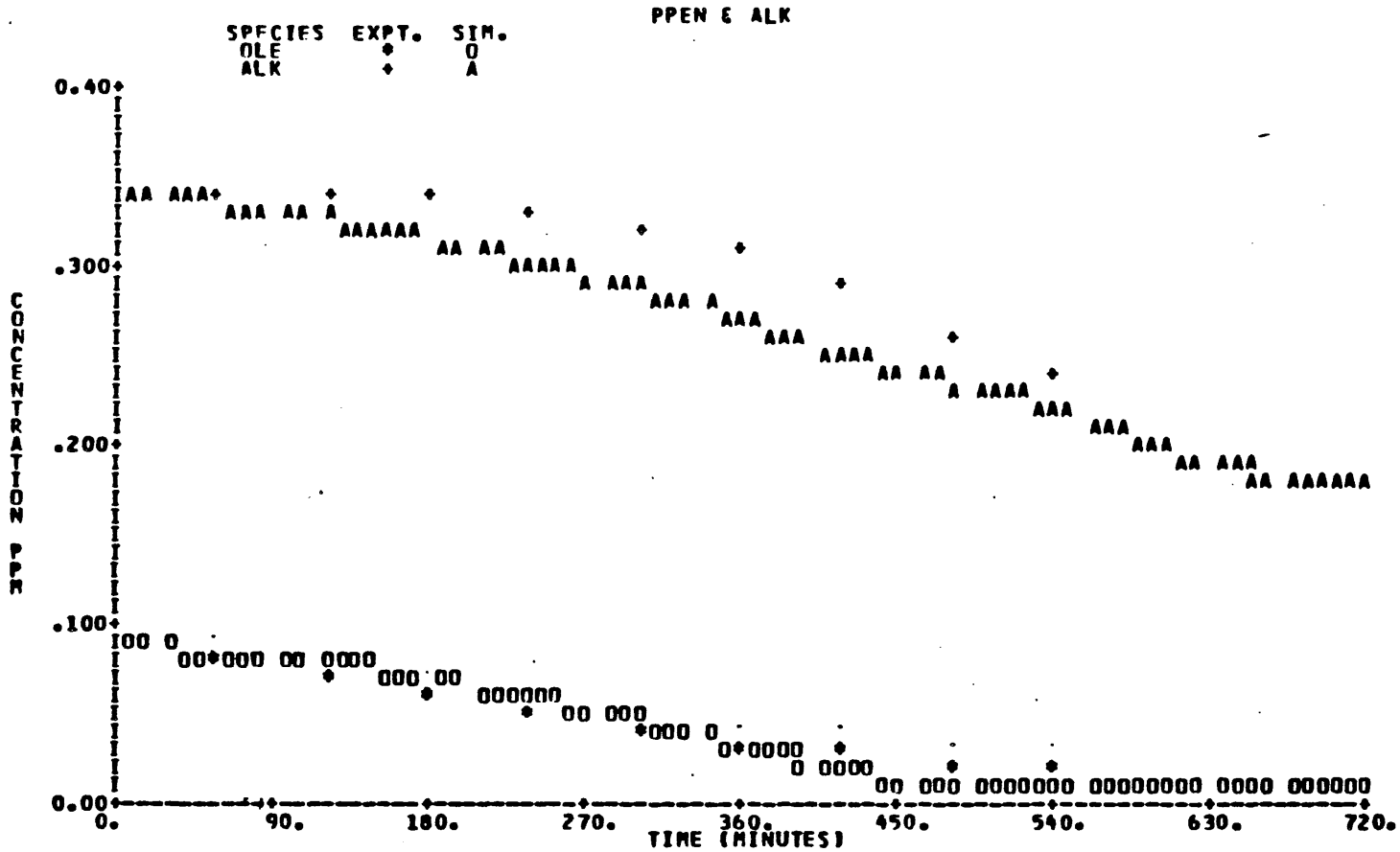

Figure A.21.c. Comparison of Concentration-Time Profiles Predicted by the SUR2 Mechanism with Experimental Data from the Red Side of the UNC Experiment of August 26, 1981.

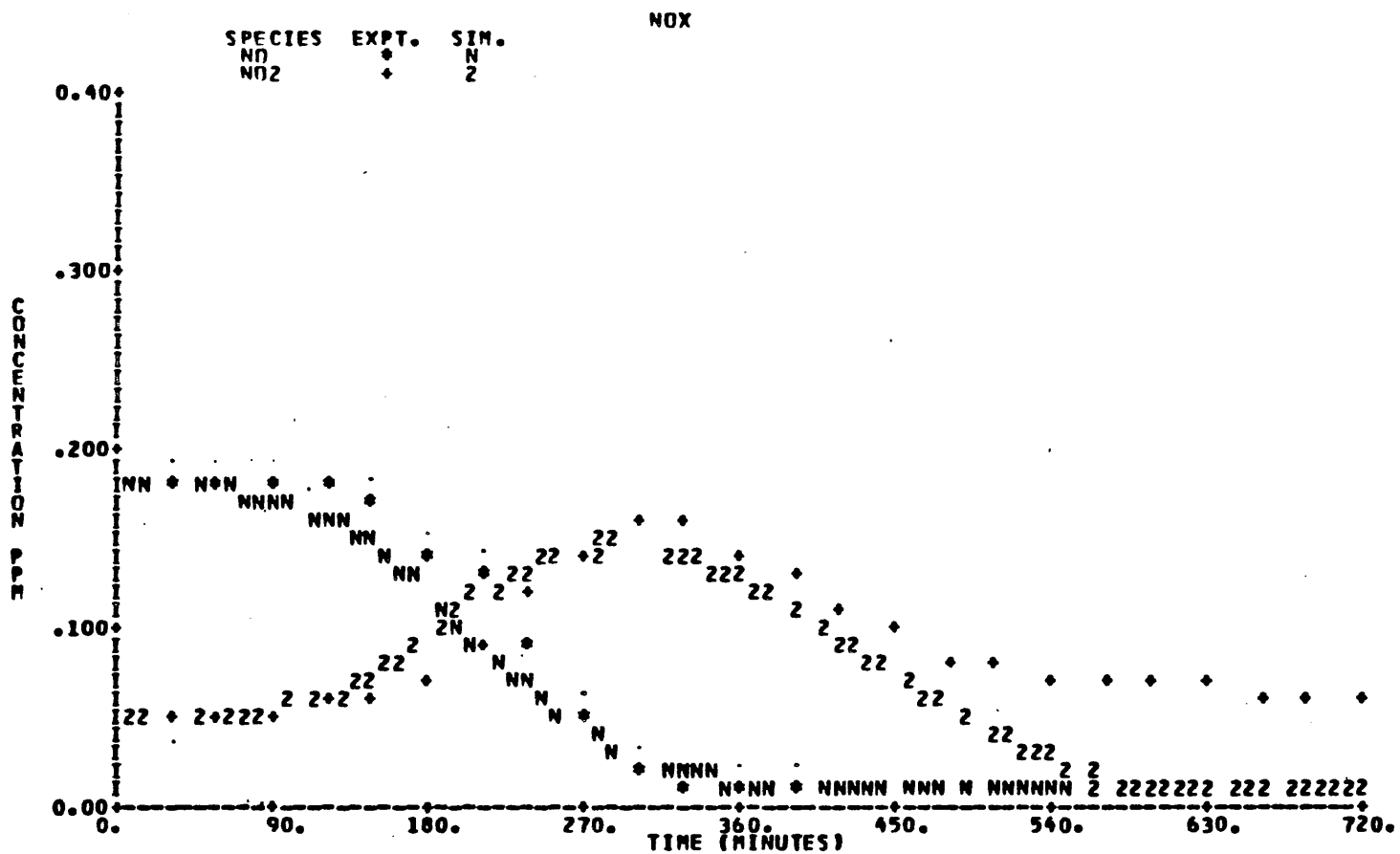

Figure A.22.a. Comparison of Concentration-Time Profiles Predicted by the SUR2 Mechanism with Experimental Data from the Blue Side of the UNC Experiment of August 26, 1981.

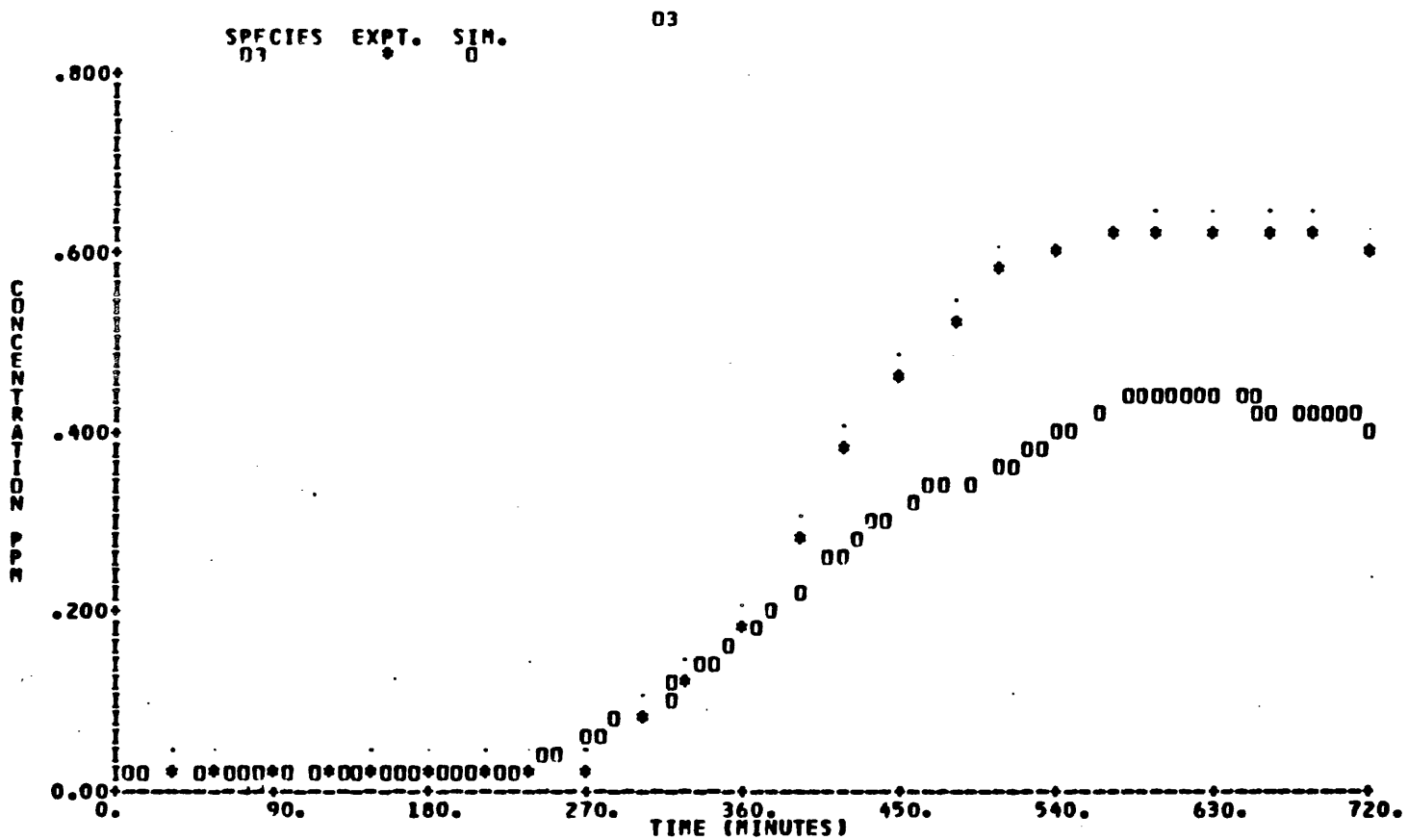

Figure A.22.b. Comparison of Concentration-Time Profiles Predicted by the SUR2 Mechanism with Experimental Data from the Blue Side of the UNC Experiment of August 26, 1981.

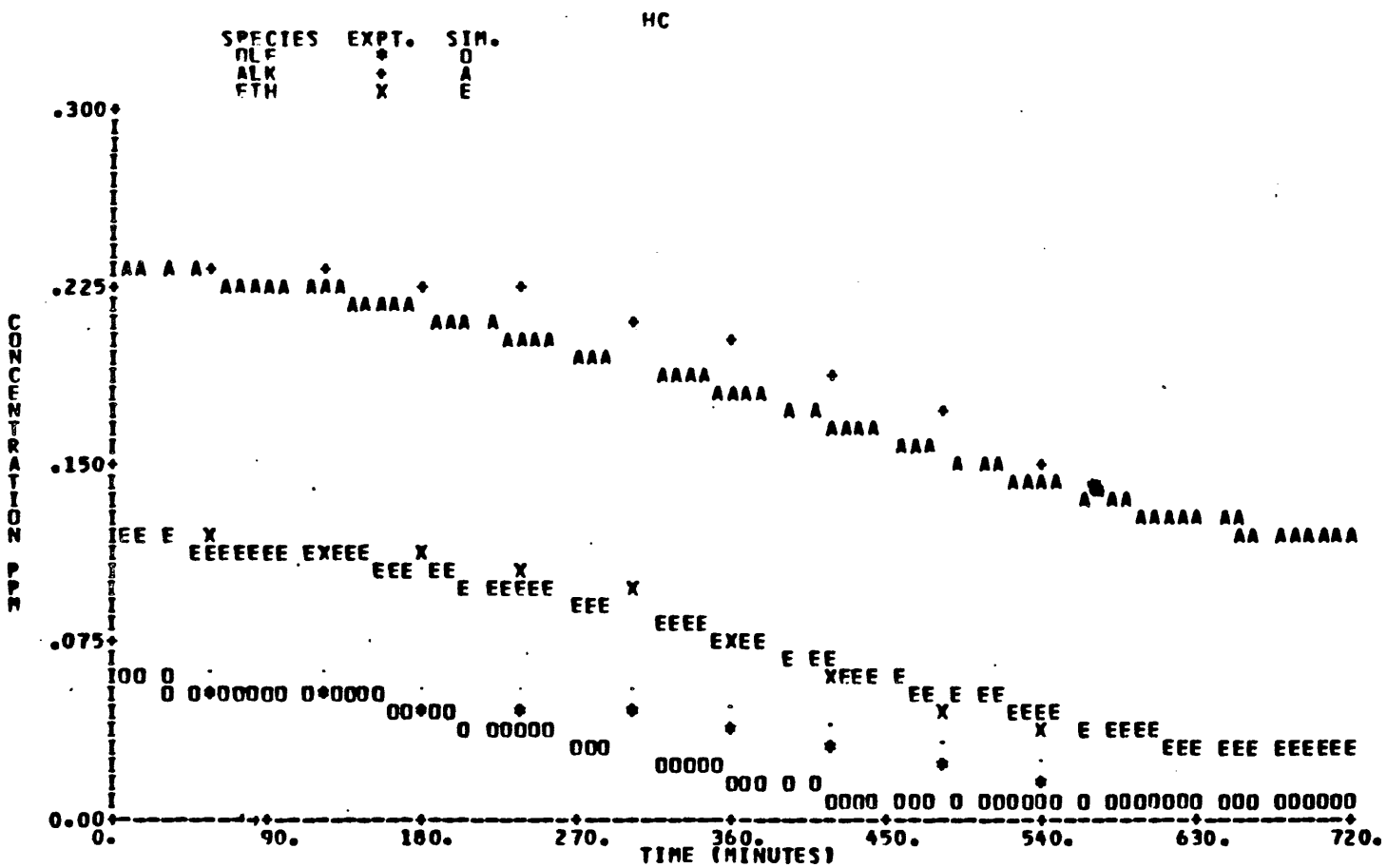

Figure A.22.c. Comparison of Concentration-Time Profiles Predicted by the SUR2 Mechanism with Experimental Data from the Blue Side of the UNC Experiment of August 26, 1981.

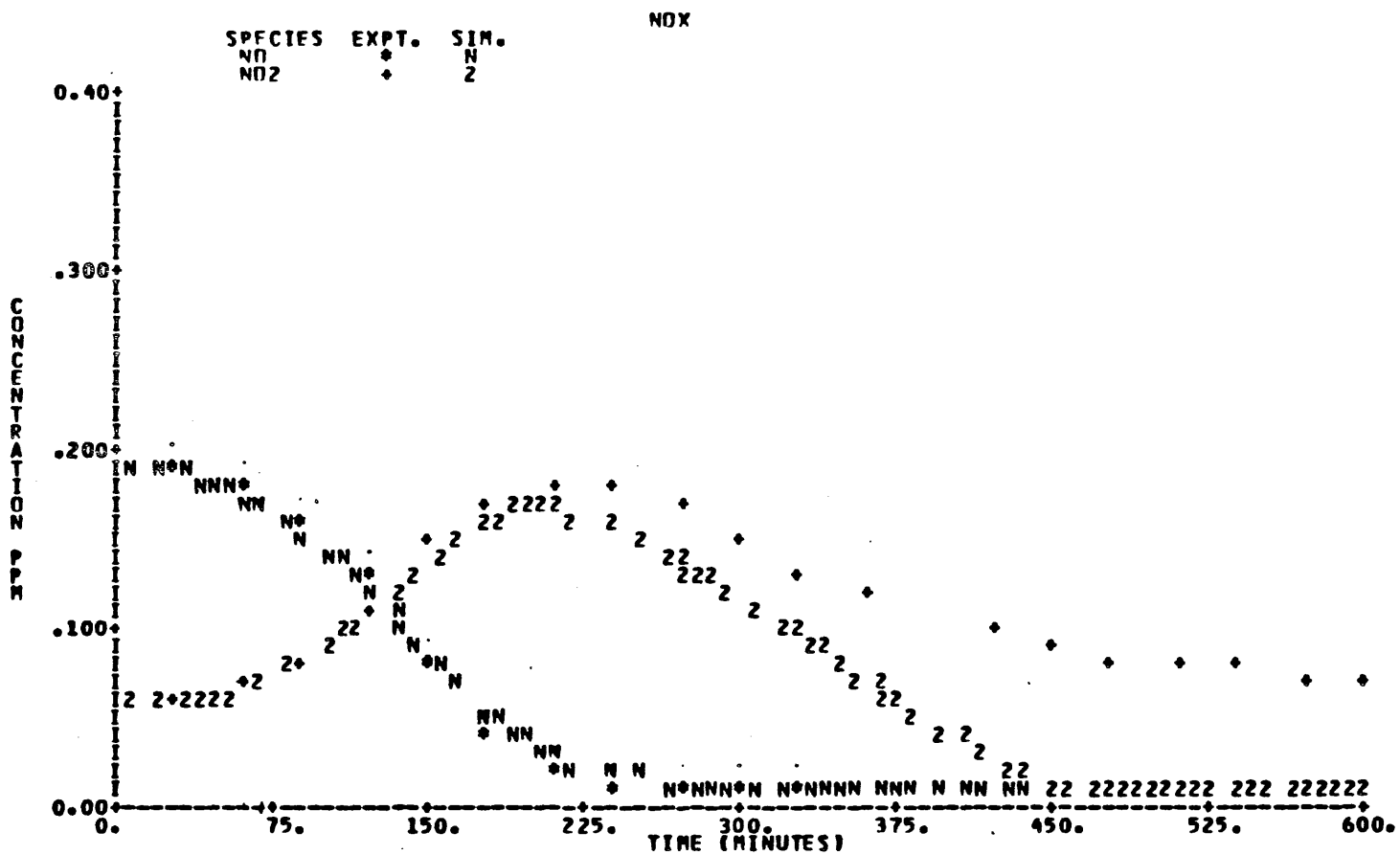

Figure A.23.a. Comparison of Concentration-Time Profiles Predicted by the SUR2 Mechanism with Experimental Data from the Red Side of the UNC Experiment of September 2, 1981.

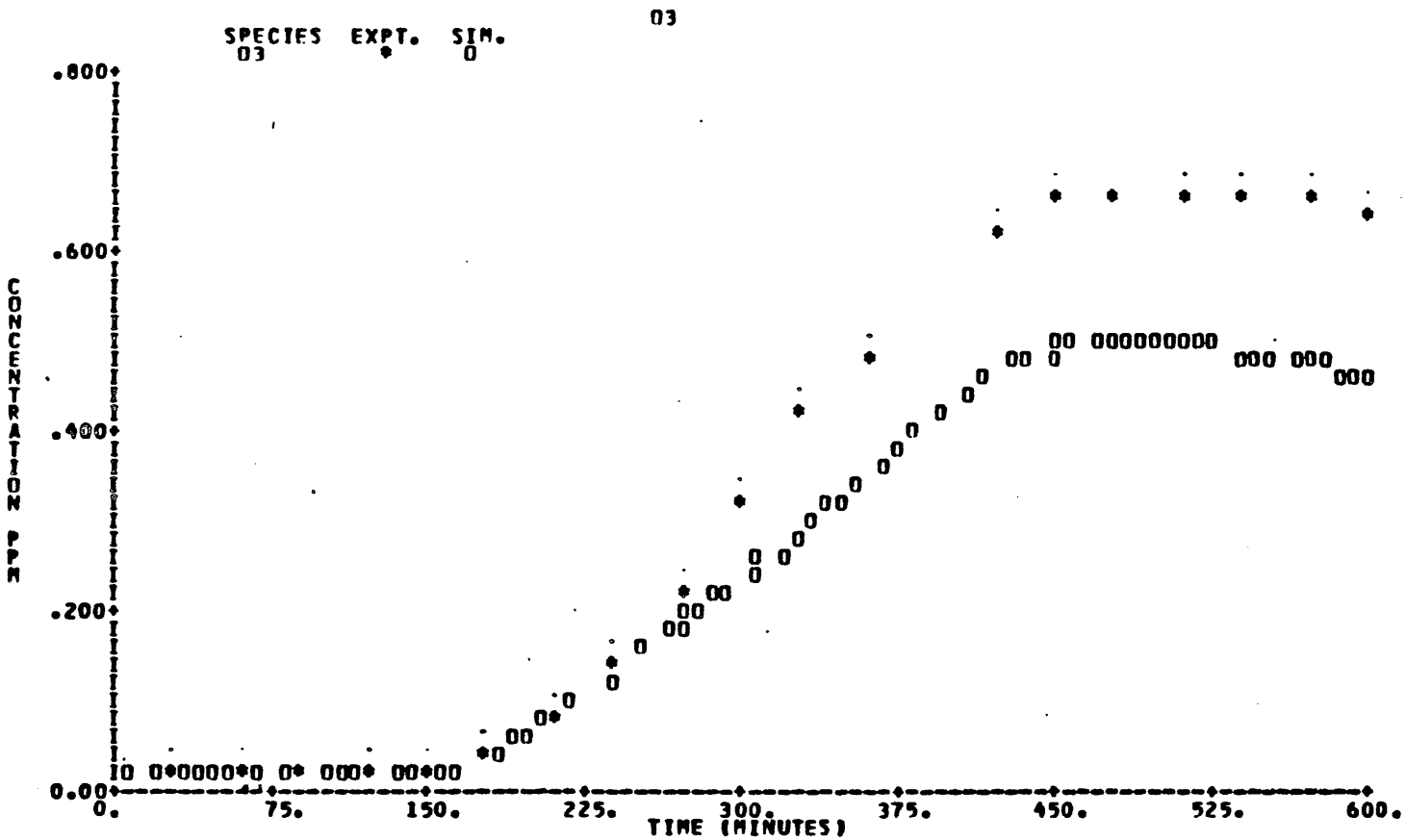

Figure A.23.b. Comparison of Concentration-Time Profiles Predicted by the SUR2 Mechanism with Experimental Data from the Red Side of the UNC Experiment of September 2, 1981.

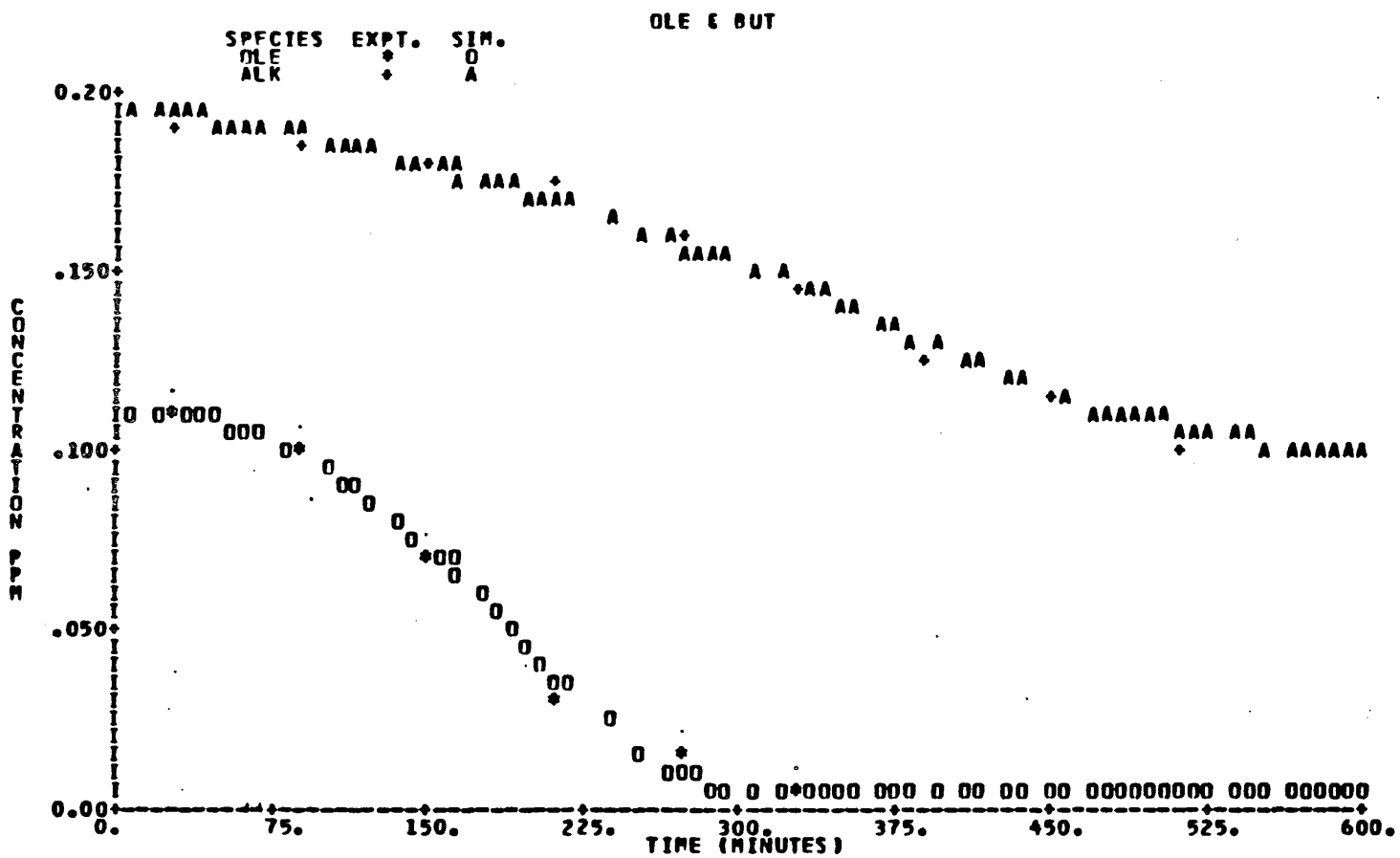

Figure A.23.c. Comparison of Concentration-Time Profiles Predicted by the SUR2 Mechanism with Experimental Data from the Red Side of the UNC Experiment of September 2, 1981.

CARB LIBRARY
07426

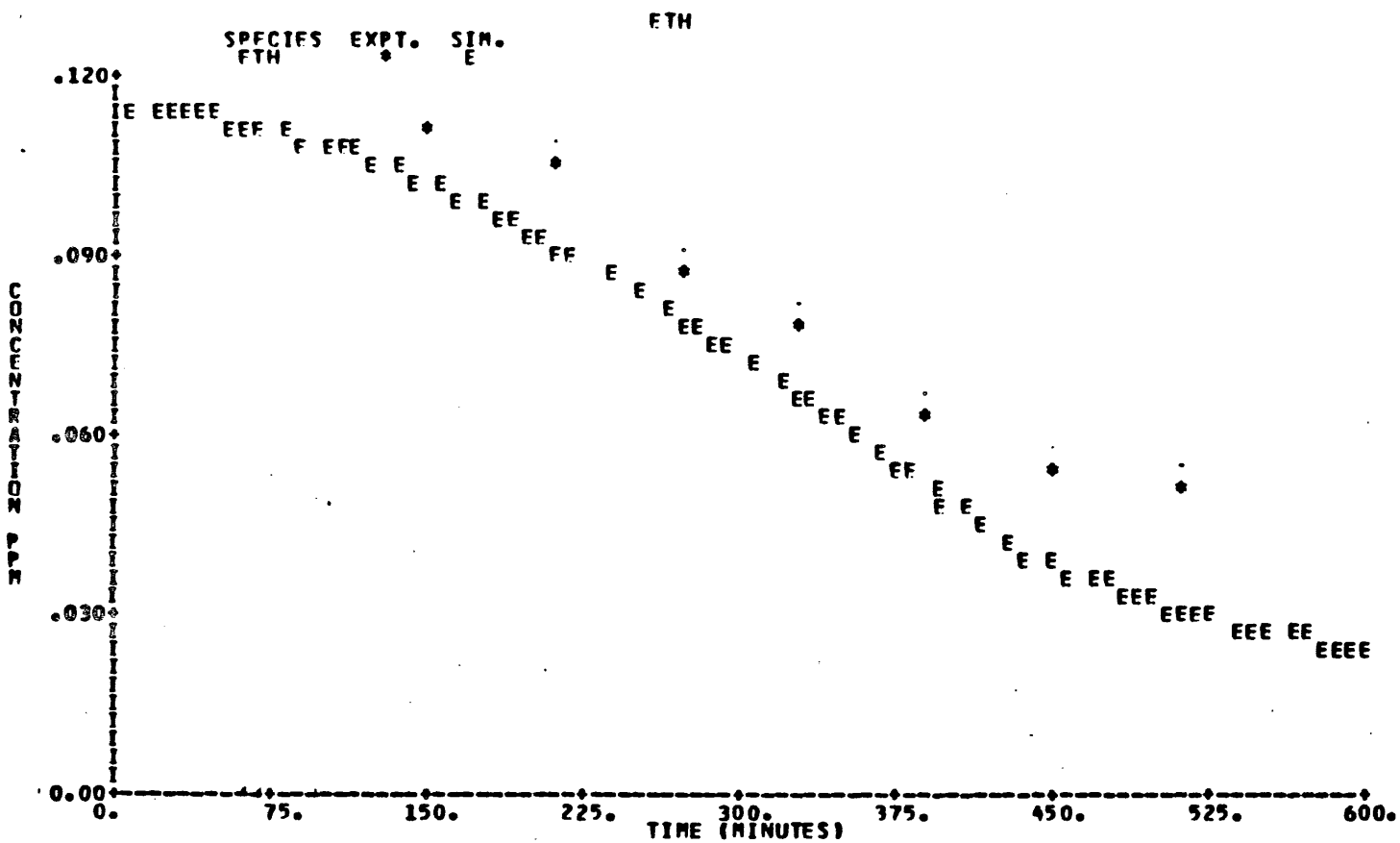

Figure A.23.d. Comparison of Concentration-Time Profiles Predicted by the SUR2 Mechanism with Experimental Data from the Red Side of the UNC Experiment of September 2, 1981.